The Influence of the Benguela Low-Level Coastal Jet on the Architecture and Dynamics of Aeolian Transport Corridors in the Sperrgebiet, Namibia

Ian CORBETT

8, Well Way, Hout Bay 7806, Cape Town, South Africa
(ian.corbett@knoco.co.za)

Abstract: Exploration for aeolian diamond placers within the southern Sperrgebiet requires a thorough understanding of aeolian transport across a broad range of scales from a systemic regional level to a micro-topographic-scale at the individual particle level. Within this arid zone the transport of coarse-grained aeolian bedload, including diamonds, is driven by the impact of saltating sandflow, which produces a uniquely characteristic diamond dispersal pattern as well as a variety of coarse-grained bedload features, textures and fabrics.

For the first time the Namibian Aeolian System (NAS : see Annex 1 for abbreviations) which runs along the entire continental margin from the Orange River in the south to southern Angola in the north can be studied within the context of the recently discovered Benguela Low-Level Coastal Jet (BLLCJ). The structures produced in response to the hydraulic behaviour of the BLLCJ flow are shown to influence strongly the location of zones of high-energy erosion and aeolian sand accumulation throughout the system.

The boundary conditions of the Namib Aeolian Erosion Basin are redefined to include the influence of the BLLCJ on the architecture and dynamics of sandflow pathways through this high-energy aeolian erosion landscape. Empirical sandflow measurements were previously used to identify narrow, linearly extensive Aeolian Transport Corridors characterised by high sandflow conditions. The corridors are commonly marked by the development of mono-trains of large barchan dunes along their length. The advent of Google Earth Engine time-lapse video provides an observational platform enabling spatial and temporal changes in sandflow and bedforms to be examined over a 32 year period. It thus provides many new insights into sandflow-dune and dune-dune interaction throughout this large-scale system down to the resolution of individual protobarchan genesis.

The influence of the hydraulic behaviour of the BLLCJ flow together with localised effects of topography on surface wind flow structure is examined through analysis of a unique 10 km wide regional Airborne Laser Scanner (ALS) dataset stretching 170 km from Chameis Bay in the south to Schmidtfeld, to the north of Lüderitz.

Aeolian bedforms and erosional features and patterns of coarse-grained aeolian bedload textural features and fabrics are mapped in detail throughout the Sperrgebiet. Changes in bedform interaction are shown to reflect variation in the pattern of surface flow created by localised topographic blocking and steering effects. The new system-wide perspective on the pattern of sandflow that feeds into, and maintains, the present-day Namib Sand Sea shows clear evidence of the influence of the BLLCJ as well as a variety of different types of vortices, which is a newly recognised element in the boundary conditions of this high-energy system.

It is concluded that favourable conditions exist for the formation of horizontal rolls and vortex structures of varying length-scales within the Marine Boundary Layer (MBL) associated with the BLLCJ. It is proposed that these strongly influence both the development of the erosional aeolian landscape and the pattern of bedforms that develop within Aeolian Transport Corridors in response to surface wind flow over complex topography.

Key Words: Namib Aeolian System; Low-Level Coastal Jet; Sandflow; Barchan Dune; Bedload Dynamics; Turbulent Flow.

To cite this article: Corbett, I. 2018. The Influence of the Benguela Low-Level Coastal Jet on the Architecture and Dynamics of Aeolian Transport Corridors in the Sperrgebiet, Namibia. *Communications of the Geological Survey of Namibia*, **20**, 9-58.

Introduction

The presence of diamonds in the Namib Aeolian System within a region known as the Sperrgebiet (Forbidden Area) between Oranjemund and Lüderitz is just one of many unique aspects that characterise this remarkable desert (Fig. 1).

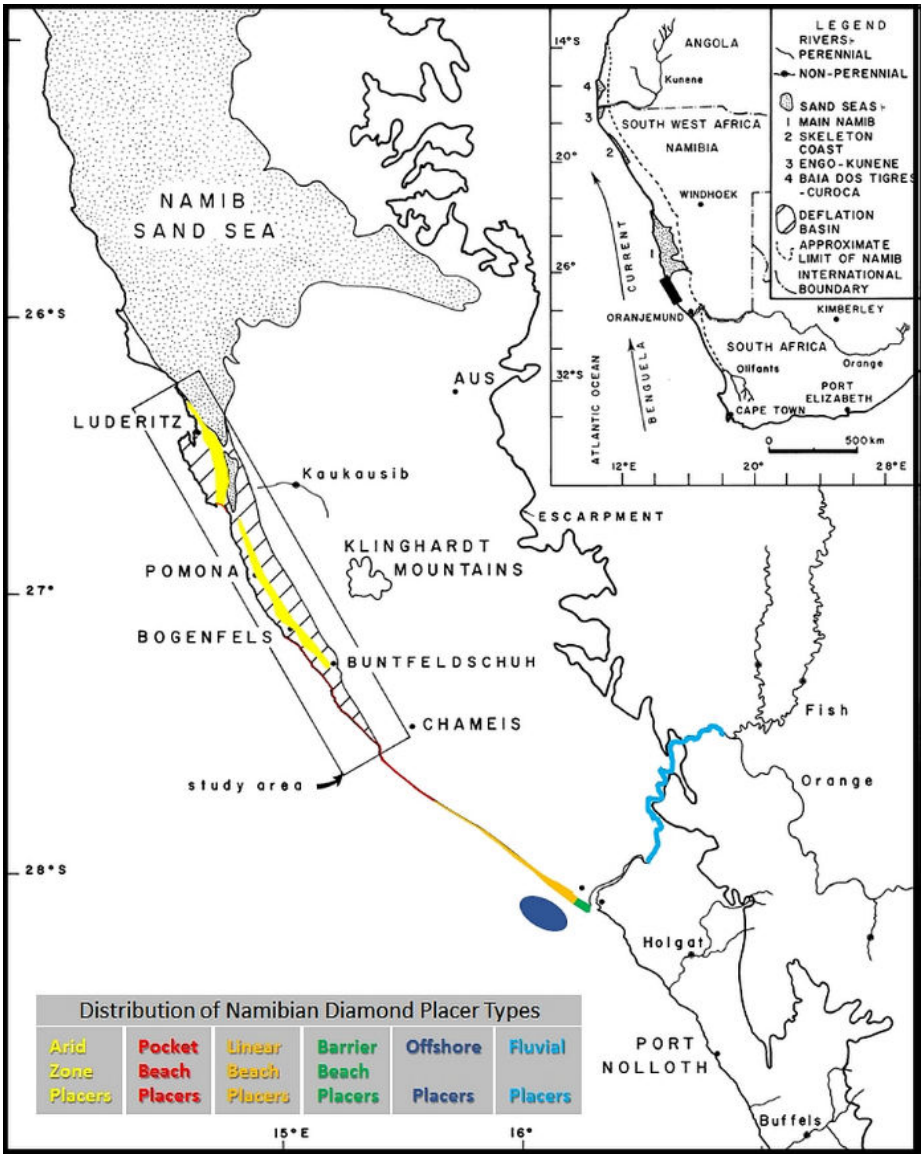

Figure 1. Spatial relationship of the placer types comprising the major components of the Namibian Diamond Placer System with respect to the portion of the Namibian Aeolian System that lies within the Sperrgebiet, which is the main focus of this paper.

The research on which this paper is based was originally motivated to support diamond exploration within the Sperrgebiet to locate areas with remaining economic mineral potential. Commencing in 1984, defining the sandflow pattern through the Namib Aeolian Erosion Basin (NAEB) was a prerequisite to understanding aeolian bedload transport in order to predict the location of economic arid zone diamond placers. These spectacularly rich diamond deposits are situated at the distal end of the Namibian diamond placer system (Fig. 1), which is arguably one of the greatest sources of gem diamonds to have ever been discovered (Hallam, 1964; Corbett, 1996; Bluck *et al.* 2005, 2007).

The objectives of this paper are to:

1. Contextualise the coastal Namibian Aeolian System (NAS) with respect to the new understanding of the meso-scale circulation system following discovery of the Benguela Low-Level Coastal Jet (BLLCJ);
2. Revisit the pattern of sandflow through the southern Namib and more specifically to re-examine, in detail, the nature and dynamics of

Aeolian Transport Corridors (ATCs) (Corbett, 1989, 1993) and;

3. Review the implications of the BLLCJ and explore the possibility that helical longitudinal vortices with different length-scales play a role in maintaining the narrow, linear nature of these high-energy sandflow pathways.

To achieve these objectives it is necessary first to summarise key developments which have taken place in terms of understanding the nature of turbulence which are pertinent to this study.

Recent Advances in Understanding Rolls, Vortices and Turbulence

The challenge of scale has come to the fore in research seeking to understand the structure of turbulent flow at a laboratory and atmospheric scale. It is now evident that some structures generated at a laboratory scale by turbulent flow are larger than the experimental systems being used to study them (e.g. (Hutchins & Marusic, 2007a, 2007b). At the atmospheric scale, the challenge of measurement is equally, if not more difficult to overcome. Despite this, significant insights into the structure of flow within the Atmospheric Surface Layer (ASL) of the Planetary Boundary Layer (PBL) are beginning to emerge with implications for the study of sediment transport.

The possibility that horizontal rolls / counter-rotating helical vortices account for the development of some aeolian erosion features and bedforms has been a subject of some debate since Hanna (1969) proposed their involvement in developing and maintaining longitudinal aeolian dune forms. Corbett (1989, 1993) advocated that the narrow, high sandflow pathways that he termed Aeolian Transport Corridors might be due to the presence of counter-rotating helical secondary vortices (rolls) within the Planetary Boundary Layer (PBL) above the NAEB. Based on empirical sandflow monitoring the wavelength of the vortices was estimated to be between 500 m to 1 km, with mono-trains of barchan dunes migrating along pathways where the counter-rotating flows converge on the bed (wall) along paths aligned with the mean flow direction. Conversely, Lancaster (1995) questioned whether rolls could significantly influence depositional patterns on the basis of a lack of empirical evidence, arguing that longitudinal rolls would wander through time, erasing linear dune patterns.

An in-depth review of more recent literature on rolls and turbulent flow structure is beyond the scope of this paper, but it is important to outline some key merging insights that have been made to establish a framework for the discussion on how the observations presented here might relate to:

1. Interaction of flow within the Planetary Boundary Layer (PBL) with the bed and;
2. The generation of coherent structures in the Atmospheric Surface Layer (ASL) over the NAEB.

The existence of well-ordered meso-scale flows within the PBL had been documented through observation of cloud streets and anecdotal glider pilot experiences (e.g. Kuettner, 1959), but a full appreciation of the extent to which roll vortices exist naturally within the PBL has only become apparent later through radar observations, astronaut observation from Earth orbit and especially through satellite radar data (Brown, 1970, 2000). The resulting evidence base has confirmed beyond doubt the widespread existence of meso-scale (e.g. 2-3 km high, 500 km long), well-ordered roll vortices. They are now known to prevail for more than 60% of the time in some areas of the world (Brown, 2000) where conditions of high shear flow and a small vertical heat flux (for discussion see Salesky *et al.* 2017) are conducive to their preferential development. Research on hurricane landfall and the patterns of destruction left by these extreme events has also led to the realisation that roll vortices are commonly generated where high shear flows traverse the ocean-land boundary where they strongly modulate surface wind speed (Wurman & Winslow, 1998; Morrison *et al.* 2005; Svensson *et al.* 2017). Rolls have been observed with wavelengths ranging from sub-kilometre to 2 to 4 km wavelengths between counter-rotating convect-ive bands and they account for damage swaths extending for several hundred metres in the mean wind direction (Wakimoto & Black, 1994).

Many new insights into the structure of turbulent flow have emerged, and continue to emerge, raising new possibilities to explain how erosional and depositional patterns observed within the NAEB might relate to the formation of coherent structures (sensu Cantwell, 1981). A selection of some of the

developments most pertinent to this study include:

1. Forward-facing steps provide important sites for the generation of flow structures (typically longitudinal vortices and horseshoe vortices) which lead to the formation of wind-aligned erosional grooves (Pollard *et al*. 1996)

2. Particle Image Velocimetry measurements by Adrian *et al*. (2000) have visualised coherent ordering of hairpin-like structures into larger-scale structural entities termed hairpin vortex packets;

3. The development of vortex packets induces the formation of Low-Momentum Regions (LMRs) that are elongated in the streamwise direction. LMRs have been shown to be adjacent to High Momentum Regions (HMRs). LMRs form very long, streamwise features in the Log Layer (Hutchins & Marusic, 2007a, 2007b) and meander in the spanwise plane. These have been termed "Superstructures" which have been shown to extend at least several times the depth of the Boundary Layer. They are sites of intense sweep and ejection-like events where Turbulent Kinetic Energy flux is highest.

4. Coherent hairpin structures provide a mechanism by which near-wall features can grow into structures (large-scale motions (LSM) and very large-scale motions (VLSM/ Superstructures) that scale with boundary layer depth to produce a hierarchy of coherent structures (for a review see Dennis, 2015);

5. The hairpin, large-scale motion (LSM) and very large scale motion (VLSM) structures observed in smooth wall turbulent boundary layers at the laboratory scale appear to be closely mimicked by a set of coherent structures of much greater length-scale within the Surface Layer of the PBL (Marusic & Hutchins, 2008; Zeng *et al.* 2010; Wang *et al.* 2017) although the mode of formation is quite different (Hutchins *et al.* 2012);

6. Turbulent "Superstructures" (sensu Hutchins & Marusic, 2007a, 2007b) within the PBL appear to modulate the amplitude of smaller-scale structures within the PBL (Mathis *et al.* 2009);

7. Mejia-Alvarez *et al*. (2013) have shown that during turbulent flow over complex topography:

a. Equivalent features to LMRs and HMRs develop;

b. Counter-rotating wall-normal vortex cores located along the spanwise boundaries of LMRs is consistent with slices through the legs/necks of individual streamwise-aligned hairpin-like vortices or packets;

c. The overall structure in the Log Layer over complex topography is consistent with that found in smooth-wall turbulence;

d. Smaller-scale LMR and HMR regions bounded by streamwise vortex cores appear to coexist beneath larger-scale LMR and HMR features;

e. Complex roughness elements induce a "channelling effect" in the flow or persistent wakes related to dominant roughness features in the case of the Low-Momentum Pathway;

f. A distinction is made between the Low-Momentum Pathways and High-Momentum Pathways (LMPs and HMPs) on the one hand, and Low-Momentum Regions and High-Momentum Regions (LMRs and HMRs) on the other: while LMRs and HMRs are not persistent in space, LMPs and HMPs are persistent in the sense that bed roughness appears to generate large-scale heterogeneity in the mean streamwise velocity in the form of preferential pathways for low-and high-momentum events;

g. The flow channelling persists despite the complex nature of surface topography present;

h. Bed roughness may promote generation of Turbulent Kinetic Energy in preferential regions within the roughness sublayer;

i. Preferential alignment of clockwise and counter-rotating wall-normal vortex cores are found to be preferentially aligned along the upper and lower boundaries of Low-Momentum Pathways respectively

j. The Low-Momentum Pathways tend to be streamwise aligned. Trails of wall-normal vortices are observed to be preferentially aligned with the Low-Momentum Pathways' spanwise boundaries. The direction of rotation of the vortices within each vortex trail coincides with the direction of the dominant vorticity of the Low-Momentum Pathways' boundaries. Of interest, is the observation that vortices on opposite boundaries of the same Low-Momentum Pathway tend to form counter-rotating vortex pairs.

Based on Mejia-Alvarez *et al.* (2013) it is plausible that local regions of enhanced turbulence production/dissipation due to variably scaled roughness have the potential to produce spatially distinctive sedimentary patterns in both streamwise and spanwise planes relative to the bed (wall) across a spectrum of scales.

This paper integrates recent advances in understanding the meso-scale, coastal Namibian wind system with detailed observations of the erosional aeolian landscape, bedforms and sediments that are influenced by it.

The first section examines the Namibian Aeolian System (NAS) located on the coastal plain beneath the Great Escarpment within the context of the recently discovered Benguela Low-Level Coastal Jet (BLLCJ). The bedform architecture and sandflow dynamics of the southern part of the system which includes the Namib Aeolian Erosion Basin (NAEB) and the Namib Sand Sea (NSS) are then discussed in detail. The paper concludes with a summary of new insights into the influence of the BLLCJ on sandflow dynamics of the southern part of the NAS and briefly considers the palaeogeographic implications that the BLLCJ could have for palaeo-reconstruction of the Namib Aeolian System in response to sea-level movement and/or climate change.

The Influence of the Benguela Low-Level Coastal Jet on the Macro-Architecture and Dynamics of the Namibian Aeolian System

The discovery of the Benguela Low-Level Coastal Jet (BLLCJ) by Nicholson (2010) has far-reaching implications for understanding the nature and structure of meso-scale circulation patterns controlling the development and maintenance of the Namibian Aeolian System. Although a low-level jet has previously been identified to control the erosion and transport of dust aerosols in the Bodélé Depression in Chad (Washington *et al*. 2006) this is the first time the dynamic behaviour of a coastal low-level jet is applied to understanding the architecture and dynamics of one of the world's major aeolian systems. The presence of the BLLCJ highlights structural similarities between the meso-scale Namib circulation system, and that of the hyper-arid Peruvian coastal desert (Munoz & Garreaud, 2005), and the Californian coast. The latter provides an example of an intensively researched coastal low-level jet which serves as the basis to consider the hydraulic behaviour of the BLLCJ to predict the pattern of smaller-scale variations in jet flow along the Namibian coast.

Although Nicholson (2010) interpreted the BLLCJ to consist of a single wind maxima, the analysis of higher-resolution satellite data by Patricola & Chang (2016) has shown that at a meso-scale it consists of two well-defined nearshore surface wind maxima. The maxima show marked seasonal variation in both location and intensity linked to changes in the position of the South Atlantic Anticyclone. The southern maxima peaks annually during the austral summer from December to February and the northern one from June to August. The northern maxima is located near the Angola-Benguela Front at 17.5°S and the other is situated to the south between 25-27.5°S (Fig. 2).

The loci of the BLLCJ maxima are strikingly juxtaposed to key elements of the Namibian Aeolian System including the NAEB and Namib Sand Sea in the south, and the Cunene and Bahia dos Tigres Dunefields in the north. This is the first time that the architecture and dynamics of the Namibian Aeolian System has been linked to the structure and dynamics of the meso-scale BLLCJ.

The persistent and unusually stable capping inversion which characterises the South Atlantic Ocean offshore from the Namib Desert was well-known prior to the identification of the BLLCJ (for summary see Van Heerden, 1999). However, the base of the inversion was believed to be lowest (less than 500 m) on the coast of the Central Namib near Walvis Bay. Satellite data now reveals that the height of the cool, well-mixed, stable Marine Boundary Layer (MBL) is substantially lower at the coast. In response to warmer sea-surface temperatures well offshore and weakening thermal subsidence, the strongly developed capping inversion above the MBL dips steeply eastwards as the coastline is approached. Consequently, the MBL height along the Namibian coast is 200 m or less to the south of Lüderitz (see Fig. 2), and between 200 m to 300 m from Lüderitz into southernmost Angola (Patricola & Chang, 2016).

Detailed studies of the Californian LLCJ have shown that wind speed along the jet varies abruptly due to the effect of changes in the orientation of the coastline with respect to the coast-parallel jet flow (e.g. Winant *et al.* 1988). Hydraulic expansion fans have been shown to form downwind of convex promontories formed by capes and points and hydraulic jumps have been observed to form upstream of topography blocking the flow of the jet and at sites where concave bends occur in the

coastline (e.g. Burk & Thompson, 1995; Edwards *et al.* 2001).

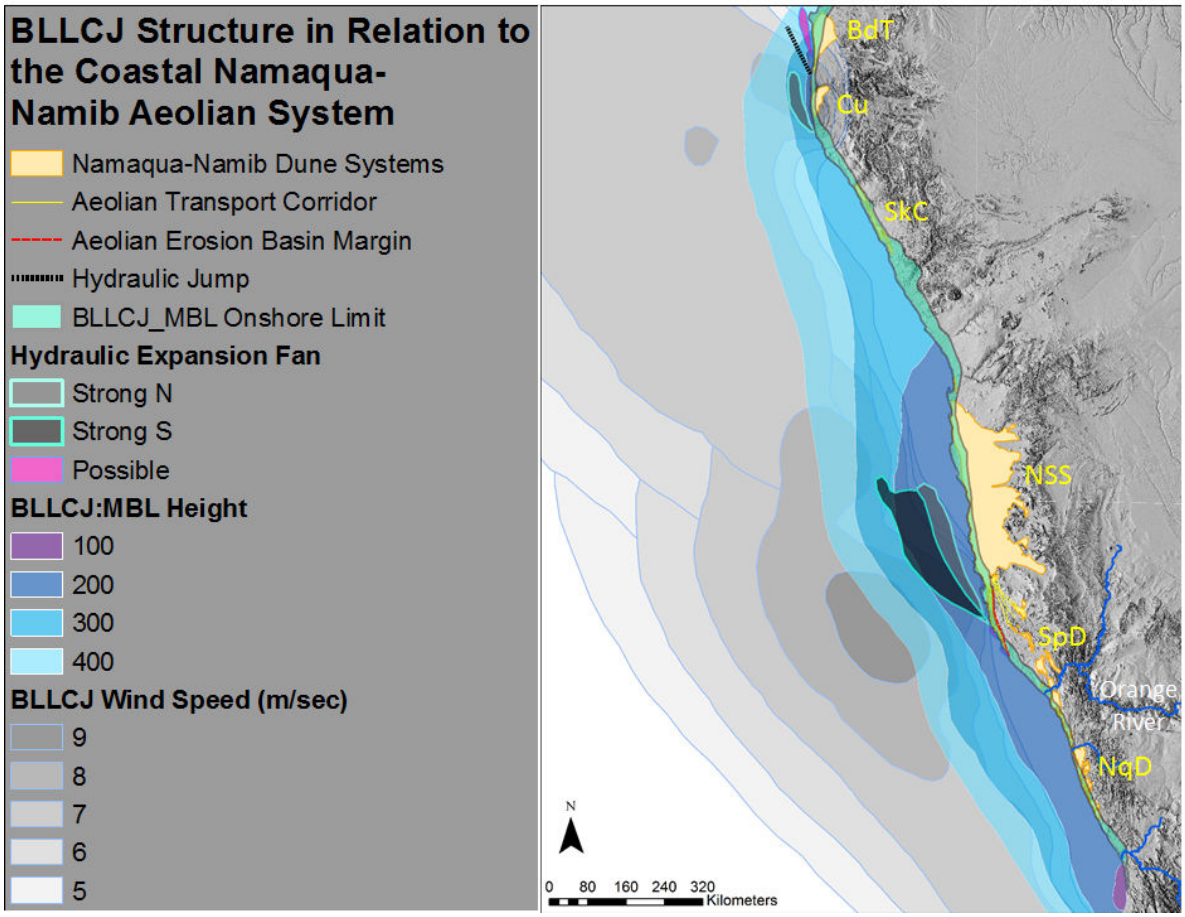

Figure 2. The location of the two wind maxima of the Benguela Low-Level Coastal Jet identified by Patricola & Chang (2016) in relation to the Namibian Aeolian System along the coastal margin. Note the juxtaposition of the large hydraulic expansion fans with the NAEB immediately south of the Namib Sand Sea (NSS) and the smaller expansion fans associated with the Cunene (Cu) and Bahia dos Tigres (BdT) Dunefields. SkC = Skeleton Coast Dunefield, SpD = Sperrgebiet Dunefields, NqD = Namaqua Dunefields.

Hydraulic expansion fans cause thinning of the MBL, which lowers the base of the capping inversion, creating fixed, well-defined zones through which surface wind flow is accelerated and often becomes supercritical. Hydraulic jumps, on the other hand, result in deepening of the MBL leading to fixed zones through which rapid deceleration of surface wind flow occurs. The hydraulic analogy for flow only applies where a jet such as the BLLCJ effectively behaves like flow through a pipe. In the case of the Californian LLCJ the ocean surface bounds the base of the jet, the capping inversion the top, and the onshore margin is bounded along the coast by a mountain barrier that rises above the height of the MBL. The seaward boundary offshore is provided by the pressure gradient directed onshore to prevent flow away from the coastal channel, completing the pipe-like constraint (Samelson, 1992). In the case of the BLLCJ, the analysis of backscattered data shows that the northern BLLCJ maxima migrates as much as 100 km inland where it is bounded by the topographic barrier provided by the Great Escarpment. Hence a similar hydraulic pipe flow condition is likely to explain the structure and behaviour of the BLLCJ (Fig. 3). Consequently, Patricola & Chang (2016) concluded that the occurrence and location of the northern maxima is controlled by the meso-scale convex curvature of the present-day Namibian coastline. Evidence of a hydraulic jump is also found upwind of the northern convexity in the coastline.

.

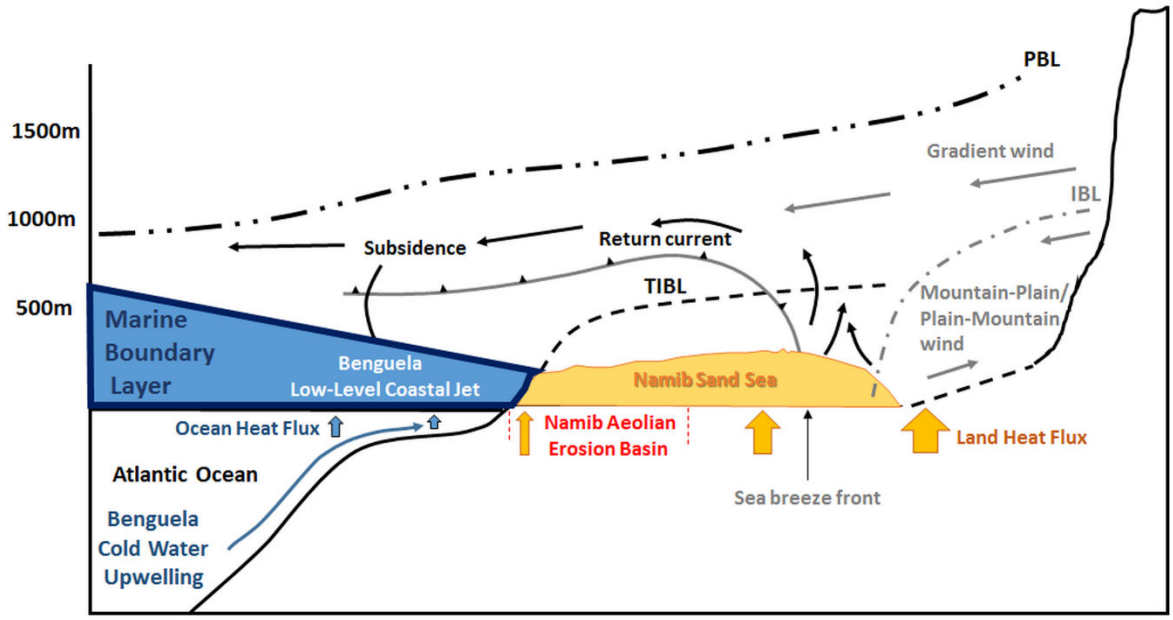

Figure 3. Summary of the key elements of the Namib circulation system and PBL structure over the coastal tract of the aeolian system. The author witnessed the presence of a BLLCJ / sea breeze front during a sandstorm event driven by an extreme easterly Berg (gradient) wind. Fine-grained sand and dust climbed up and over the sea breeze front heading out to sea across the NAEB to form a series of plumes out into the Atlantic.

Patricola & Chang (2016) have also shown that the eastern boundary of the southern BLLCJ wind maxima crosses the Namib coastline and impinges on the NAEB south of Lüderitz (see Fig. 2). The BLLCJ is intimately linked to the development of the Lüderitz upwelling cell (Nicholson, 2010), which influences the thermal contrast between the sea surface temperature and the adjacent land surface, further intensifying the jet flow. Ranjha *et al*. (2013) show the southern maxima extending onshore between the coast and the topographic barrier provided by the Great Escarpment.

While the thermo-topographically induced nature of the airflow over the Namib was previously recognised, it was interpreted to be due to the diurnal development of a sea-breeze (Lindesay & Tyson, 1990). In the light of new evidence from satellite data, the unimodal southerly winds which play such a vital role in driving the high-energy NAS are likely to be driven primarily by the BLLCJ. However, the extent to which the MBL migrates eastwards onshore has not been measured in the field as yet.

Based on an analysis of weather station data from Alexander Bay airport, on the south bank of the Orange River 10.75 km inland from the coast, Swart (2016) showed that a thermal internal boundary layer (TIBL) frequently develops and reaches equilibrium 10 km to 16 km inland during the day, confirming the prediction of Jackson (1954) cited by Lindesay & Tyson (1990). According to Swart (2016) during winter months the base of the TIBL at 0900h is at approximately 200 m about 5 km inland and reaches a height of about 500 m by 1700h. In the summer the TIBL is at about 300 m some 8 km inland at 0900h and reaches 900 m to 1000 m by 1700h. These results are consistent with earlier measurements of the depth of the sea breeze in the Central Namib by Lindesay & Tyson (1990) based on data from Gobabeb which is situated 53.5 km inland from the coast. Swart (2016) has shown that the sea breeze develops when the difference between the land and sea temperatures is 3°C or more. How the BLLCJ and sea breeze interact is as yet not known. However it is clear that the sea breeze front pushes inland some distance which would create a broader coast-parallel linear band influenced by southerly unimodal surface winds.

The onshore boundary of the Californian LLCJ is located where the steeply dipping MBL intercepts the mountain barrier. A similar situation probably prevails along the Namibian margin. Extrapolating the MBL height mapped by Patricola & Chang (2016) onshore, a narrow linear zone of varying width immediately inshore of the coastline is dominated by the unimodal surface flow of the BLLCJ (see Figs 2, 4, 5). The width of the transitional zone between the MBL and the TIBL along the

Namibian coast and its diurnal behaviour is currently unknown.

Whilst the analysis of the 20 year record of wind data from Alexander Bay highlights the dominance of the south-westerly sea breeze (52.9%), it also shows the influence of westerly winds which Corbett (1989) recorded little evidence of at Bogenfels. This is possibly due to the fact that westerly winds leaving the South Atlantic anticyclone have generally been deflected north by the Coriolis force when the BLLCJ hits the coast at Bogenfels located about 250 km north of Alexander Bay producing strongly unimodal and persistent southerly to south-south-easterly surface wind flow which is a precursor required to develop the BLLCJ along the Namibian coastline.

The Influence of the Benguela Low-Level Coastal Jet on the Architecture of the Northern Dunefields of the Namibian Aeolian System (NAS)

The northern BLLCJ maxima is fixed by the convexity in the modern coastline to the north of Cape Fria, as the Cunene River is approached.

The contours of surface wind flow produced by Patricola & Chang (2016) for the BLLCJ run coast parallel along the Skeleton Coast, but as the northern maxima is approached they veer sharply in towards the coast from Cape Fria, with the maxima located directly offshore of the Cunene Dunefield (Fig. 4).

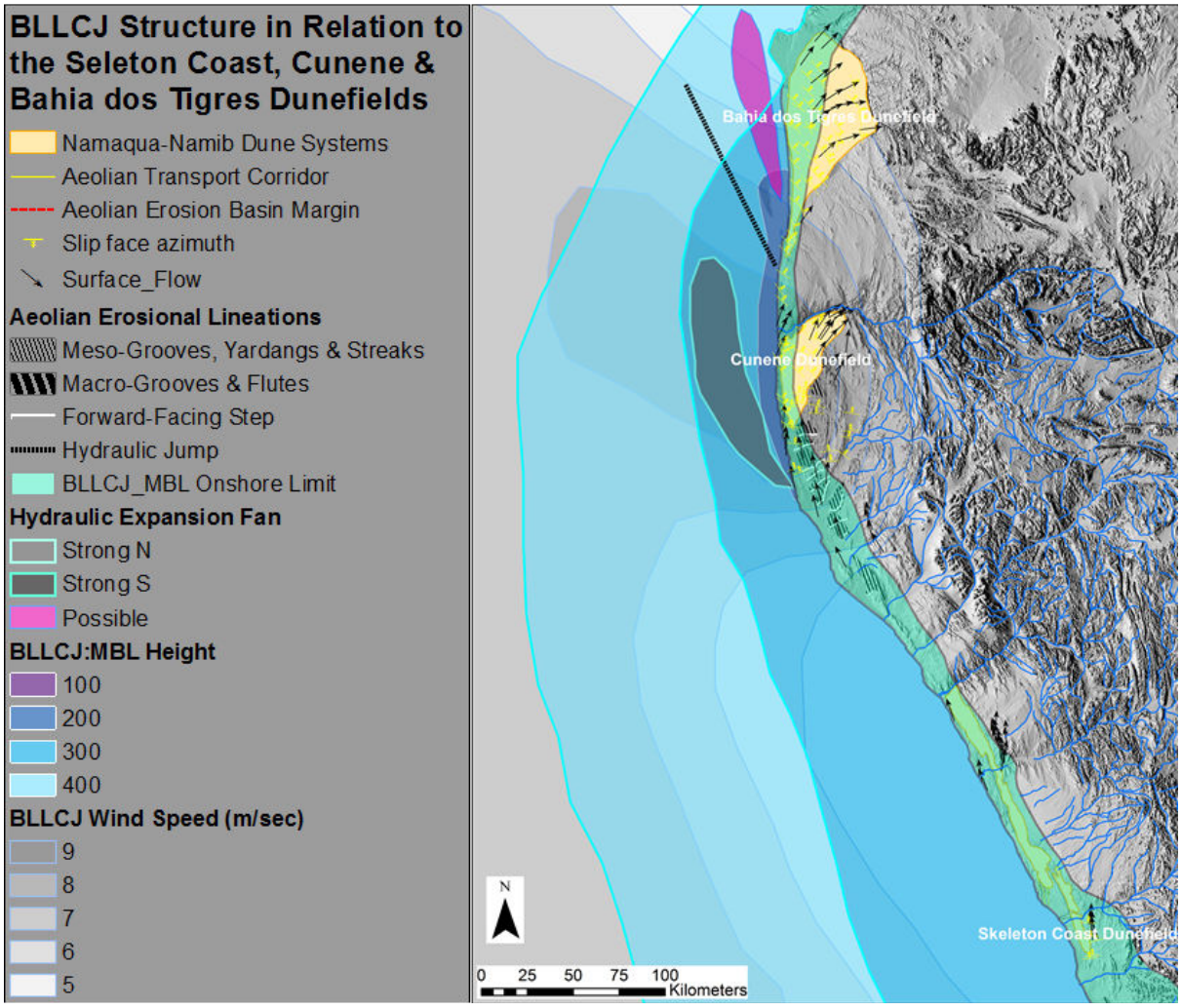

Figure 4. Structure of the BLLCJ associated with the northern wind maxima and the pattern of surface windflow associated with the Skeleton Coast, Cunene and Bahia dos Tigres Dunefields which are the key northern elements of the NAS. Note the location of the aeolian erosional lineations which form a prominent feature of the aeolian erosional landscape between the Skeleton Coast and Cunene Dunefields in relation to the hydraulic expansion fan identified by Patricola & Chang (2016) associated with the northern BLLCJ wind maxima. The hydraulic jump and northern expansion fan are predicted to be present based on this study.

The pattern of surface wind mapped using aeolian erosion features and bedforms along the coast confirms the coast-parallel flow along the straight section of the Skeleton Coast coastline. In the absence of changes in wind speed the Skeleton Coast Dunefield is found to consist of a set of juxtaposed barchan corridors. The large-scale aeolian erosional lineations which Goudie (2007) referred to as mega-yardangs are located precisely at the point at which the surface winds rapidly accelerate as the coastal convexity is approached, which leads to erosion of the Skeleton Coast barchans and a resurgence of high-energy sandflow. Note that immediately north of the aeolian lineations the MBL height is abruptly reduced north of the convexity in the coastline. The change in coastal geometry results in the development of a hydraulic expansion fan (Patricola & Chang, 2016).

As noted by Lancaster (1985, 2014) sand movement in both the Cunene and Bahia dos Tigres Dunefields leads to transport from high-energy to lower-energy surface winds. The accelerated flow associated with the expansion fan detaches from the coast creating a situation which closely resembles the hydraulic behaviour of the Californian LLCJ described by Samelson (1992). It is possible that a hydraulic jump formed at the concavity in the coastline separates the initial expansion fan from a second feature which develops north of it at the next convexity in the coastline opposite the Bahia dos Tigres Dunefield. The presence of a jump is potentially indicated by the change in the geometry of the MBL to the north of the Cunene River. Such a jump would result in the abrupt deceleration of flow within the jet. The pattern of acceleration and deceleration of surface wind flow produced by the presence of the hydraulic expansion fan and the associated hydraulic jump control the location of sand accumulation and the development of both dunefields. The orientation of slip faces of the transverse dunes which characterise both the Cunene and Bahia dos Tigres Dunefields together with the vectors of surface wind flow derived from aeolian streaks and the orientation of linear ridges delineate a pattern of surface wind flow curving inland from the coastline into an area in which the Great Escarpment steps back from the coast. Based on Samelson's (1992) Californian study it is suggested that this pattern, which is a characteristic surface flow pattern associated with hydraulic expansion fans, results from the effect of surface friction slowing wind flow away from the coast and causing the curvature of streamlines of the jet flow. It is highly probable that this pattern exerts significant control on the smaller-scale architecture of both dunefields, and that it strongly influences the spatial distribution of the different dune forms found in them.

The location of the Cunene Dunefield well to the south of the Cunene River is interesting. Garzanti *et al*. (2012, 2015) have determined that the Orange River is the provenance of the sands in the dunefield. It thus confirms the vital role that longshore drift and coastal geometry play in controlling sand supply to the NAS, and highlights the interdependencies between the dynamic behaviour of the BLLCJ, the distribution of coastal aeolian sediment supply points, and the location of sand accumulation zones in this high-energy aeolian system. In terms of sand supply it also reinforces the critical role that major rivers supplied by rainfall (and sediment) from outside the hyper-arid core can play in creating and maintaining arid zone aeolian systems.

The Influence of the Benguela Low-Level Coastal Jet on the Architecture of the Namib Aeolian Erosion Basin and the Namib Sand Sea

The southern wind maxima associated with the BLLCJ are located directly offshore of the highest-energy section of the NAS (see Fig. 2). The wind speed contours swing east and impinge onshore directly at the location of the NAEB, which lies immediately downwind of the first convexity in the coastline at Chameis, approximately 100 km north of the Orange River.

Patricola & Chang (2016) show a major hydraulic expansion fan lying directly offshore of the NAEB, with the southern end of the fan anchored to the coastline between Bogenfels and Baker's Bay (Fig. 5). The expansion fan extends north up to Meob Bay, and wind speeds associated with the expansion fan reach 12 m/second or more. A similar expansion fan lying closer to shore develops during strong winter events. The maximum height of the MBL along the southern Namibian coast to north of Walvis Bay is 200 m. Consequently a narrow linear zone exists along the coastline within which aeolian processes are dominated by the unimodal southerly BLLCJ flow.

.

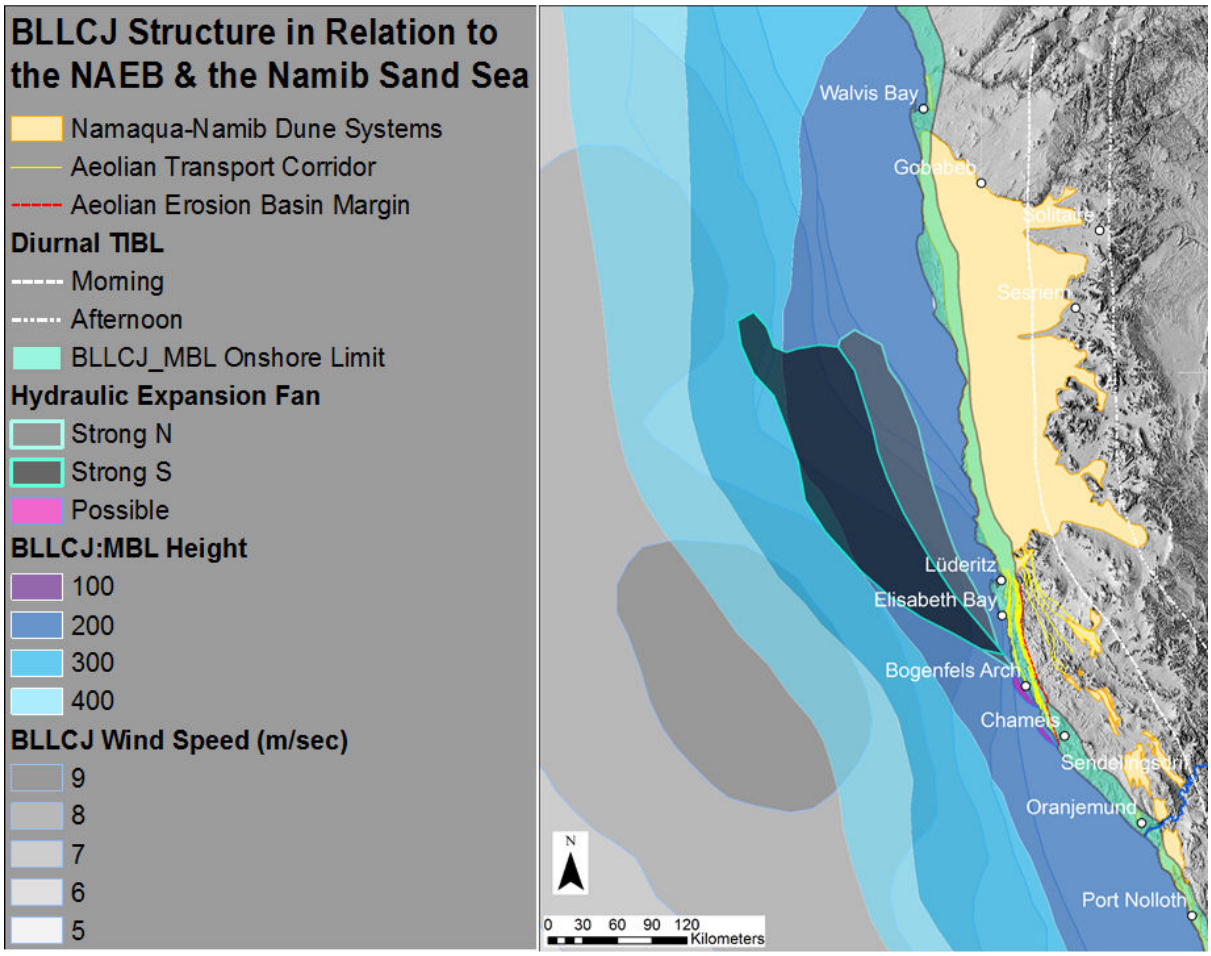

Figure 5. The structure of the BLLCJ between the Orange River mouth and Walvis Bay. Note that the NAEB and Namib Sand Sea are located directly inshore of the hydraulic expansion fan shown by Patricola & Chang (2016) for strong BLLCJ events for southern and northern surface wind maxima emanating from the first convexity in the coastline at Chameis Bay. Smaller expansion fans possibly exist, influencing wind flow at a more localised scale. A sea breeze develops diurnally immediately inland of the narrow strip which is dominated by the southerly unimodal BLLCJ flow.

Using the 200 m height of the MBL determined by Patricola & Chang (2016), the onshore limit of the BLLCJ aligns perfectly with the eastern margin of the Namib Aeolian Erosion Basin. This may explain the observation by the author of an easterly gradient wind dust storm which abruptly flowed up and over the NAEB, where a southerly surface wind continued to flow.

The resolution of satellite data used for the Patricola & Chang (2016) study currently does not permit sub-meso-scale hydraulic structures to be identified. However, it is conceivable that smaller hydraulic expansion fans and jumps are created at sites of subsequent convexities and concavities in the coastline to the north of Chameis along the coastal margin of the NAEB and the Namib Sand Sea. If this does occur, it is possible that the height of the MBL could be less than 200 m above some parts of the NAEB which would create a very thin, high-speed jet flow beneath the strongly developed capping inversion. In California, hydraulic conditions such as these lead to the development of fully turbulent supercritical flow within the low-level jet (Haack *et al*. 2000). This potentially has important implications in terms of understanding flow within the Atmospheric Surface Layer (ASL) through the NAEB which is discussed in a later section of this paper.

In terms of sandflow dynamics it is again significant that within the NAEB, headlands at which the convexities in coastline geometry occur are also sites at which log-spiral embayments form in their lee, providing point sources supplying sand to the aeolian system. These point sources supplying sand for transport through Aeolian Transport Corridors (sensu Corbett, 1993) are then exactly located at sites where the highest-energy winds associated with the BLLCJ occur.

It is interesting to re-examine the pattern of sandflow that Lancaster (1985) first mapped covering the entire Namib (Fig. 6) in the light of the discovery of the BLLCJ and the pattern of surface wind flow that characterises the dunefields in the far north of Namibia and southern Angola. The pattern from south to north through the NAEB clearly shows the increased sand transport capacity of the BLLCJ as flow accelerates in response to the development of the hydraulic expansion fan, and the reduction in capacity that occurs as the surface wind flow decelerates once again. The presence of the hydraulic expansion fan also accounts for the observation by Rogers (1977) that the unimodal southerly wind flow peaks in the vicinity of Pomona, to the south of Lüderitz.

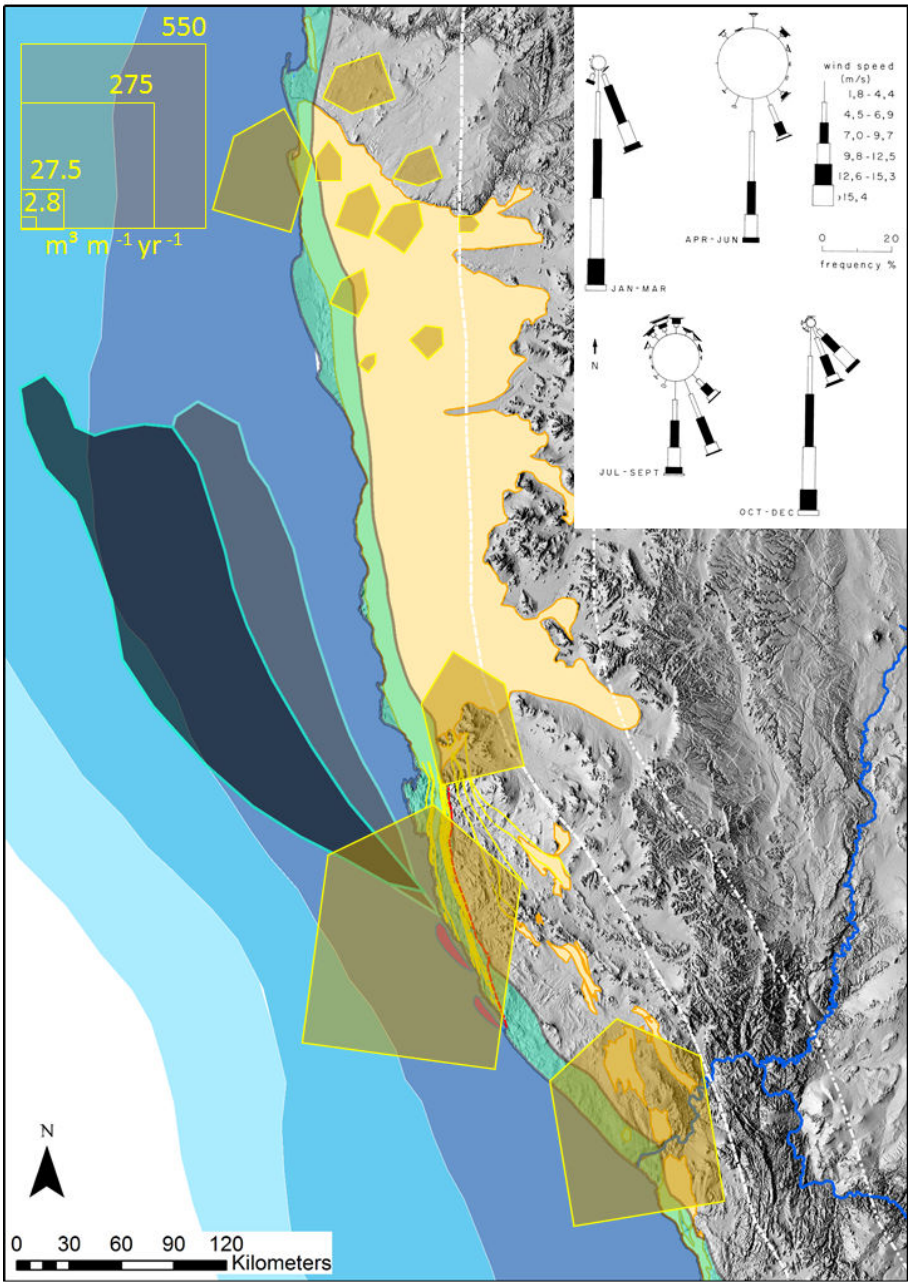

Figure 6. Wind and sand movement within the Namib Sand Sea System based on Lancaster (1985). Detailed wind roses (inset) from Corbett (1989, 1993) show the wind pattern inland of Bogenfels, where southerly to south-south-easterly surface winds prevail. Note the marked increase in sand transport capacity through the NAEB, which provides evidence of the influence of flow associated with the hydraulic expansion fan from south to north. While the transport capacity remains comparatively high in the narrow coastal tract dominated by BLLCJ flow throughout the length of the Namib Sand Sea, the transport capacity declines from west to east. Towards the northern end of the sand sea the pattern of diminishing sandflow hints that the surface wind flow may curve inwards to the east, in a similar manner to the pattern observed in the considerably smaller Cunene and Bahia dos Tigres Dunefields.

There is also a hint of curvature of the surface wind flow in the set of sandflow data provided by Lancaster (1985) at the northern end of the Namib Sand Sea, which shows some resemblance to the more clearly-defined pattern of curvature which prevails in both the Cunene and Bahia dos Tigres Dunefields.

The Boundary Conditions of the Southern Namib Sandflow System

The aeolian erosional landscape is an important feature of the region covered by this paper, and it influences the boundary conditions of the aeolian transport system in two ways:

1. Firstly, the complex topography exerts a strong influence on the nature of the coastal morphology (Corbett, 1989, 1993) which controls the physical nature of beaches supplying sand to the aeolian system;
2. Secondly, interaction of the southerly unimodal BLLCJ with coastal topography results in hydraulic behaviour of the flow;
3. Surface wind flow interaction with the surface topography can generate coherent turbulent flow structures and produce local-scale variation in both the magnitude and direction of the surface wind flow due to topographic steering.

Kaiser (1926) broadly subdivided the Sperrgebiet into two geomorphic domains which he termed the Trough Namib and the Plain Namib. This study is centred on the aptly named Trough Namib which, due to the underlying tectonic and geological fabric is characterised by numerous south-south-east to north-north-west trending troughs that are aligned with the predominant unimodal BLLCJ wind regime. The Plain Namib lies immediately east of the Namib Aeolian Erosional Basin margin. It is characterised by spatially extensive vegetated sand sheets, fields of linear dunes and extensive alluvial plains fed by ephemeral streams draining the Great Escarpment.

The boundary conditions for the Namib Aeolian System are summarised in Fig. 7. The description of the components characterising the boundary conditions of the aeolian transport system and the dynamics of this system form the basis of the rest of this paper.

Sand Supply and Source Geometry

The nature of the sediment supply for material entering the aeolian system can be sub-divided into two fundamentally different sub-categories (Fig. 7 and 8). This paper focuses on the aeolian transport system that is primarily fed and maintained by sediment deflated off coastal beaches supplied by northbound longshore transport of sediment supplied to the margin by the Orange River, together with material eroded from sedimentary sequences exposed within the Namib Aeolian Erosion Basin.

Two different source geometries can be identified along the coast:

- Point sources are confined to log-spiral and south-facing re-entrant embayments of differing size (Fig. 4). Beaches that are sufficiently fine-grained for deflation to take place occur mostly within the southern part of the study area which is characterised by log-spiral embayments to the south of Bogenfels (Corbett, 1993).
- From Prinzenbucht (Fig. 4) on the coast west of Pomona northwards, sand is supplied to the aeolian system at a number of coastal localities including the south-western end of the largest south-facing re-entrant on the present-day coast at Elisabeth Bay. These localities are characterised as line sources from which sand is actively deflated.

The difference in the source geometry and consequently the quantity of sand flux generated by the deflation of the beaches fundamentally influences the nature of the aeolian transport system that develops downwind, and in particular, the nature of barchan dune interaction that occurs. The discussion of the pattern of sand flow that follows reflects this basic sub-division.

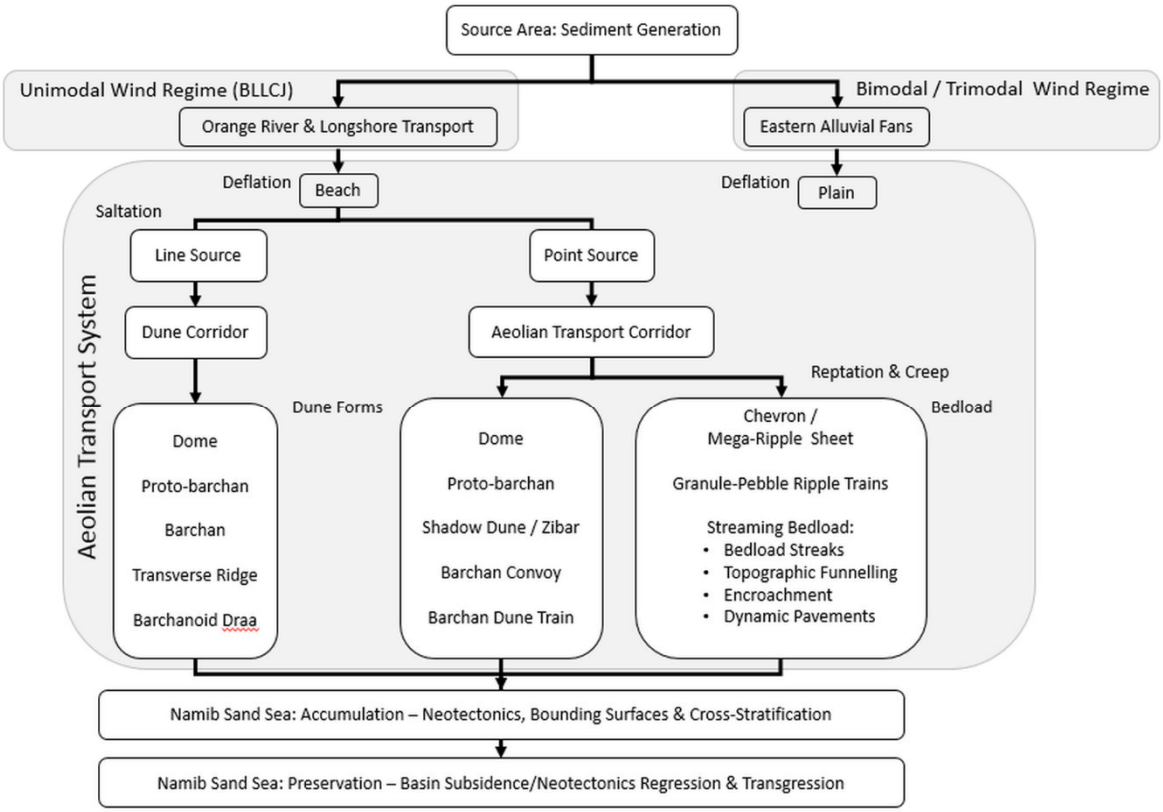

Figure 7. The Boundary Conditions for the erosional part of the Namib Aeolian System feeding the Namib Sand Sea accumulation zone.

Approach to Mapping Sandflow Dynamics

An overview of the southern Namib aeolian sandflow system and the variation in sediment source is shown in Fig. 7. Within the aeolian erosion basin from Chameis Bay northwards, sandflow primarily occurs within Aeolian Transport Corridors (Corbett, 1989, 1993) which are characterised by mono-trains of barchan dunes. On the coast from Prinzenbucht northwards, sandflow occurs within broader barchan corridors forming linearly extensive fields of size-regulated interacting barchan dunes, barchanoid ridges and transverse dunes. In contrast to Aeolian Transport Corridors (ATCs), barchan corridors commonly develop from a "V"-shaped inception point which flares out to form a pattern resembling birds flying in formation. The streamwise linearity of both Aeolian Transport Corridors and barchan corridors is a characteristic feature of aeolian systems governed by strongly unimodal wind regimes. However, whereas barchan corridors attain widths of several kilometres with many uniformly-sized barchans present within them (such as the southern Morocco example described by Sauermann *et al*. (2000), which is 8 km wide and 300 km in length) the 1 km-wide ATCs represent extreme examples of streamwise linearity.

Corbett (2016) divided the aeolian landscape of the erosional basin into seven geomorphic domains. Six are characterised by relief and landforms aligned with the prevailing unimodal southerly winds. One has a variable orientation that is directly linked to the regional geological and tectonic fabric that promotes the formation of depressions. In places this results in shallow trough-shaped features as well as positive and negative steps which cut east-west across the southerly wind flow.

In order to examine the sediment dynamics along ATCs in more detail five localities in differing erosional landscapes were selected for detailed analysis of the sandflow system using Google Earth Engine (Fig. 8a). Google Earth Engine (GEE) time-lapse video presents a fascinating opportunity to observe sandflow patterns over a 32 year period. Viewed with ALS, SRTM and Landsat coverage it is possible for the first time to discern the pattern of sandflow pathways crossing the active plinth demarcating the trailing edge of the southernmost Namib Sand Sea and follow the sandflow as it migrates 50 km into the

accumulation zone (Fig. 8b). The identified pathways demonstrate that most of the sandflow supplied by the modern system to the Namib Sand Sea is derived from the Orange River and/or the erosion of older depositional sequences to which it contributed sediment. Eastern alluvial plain sand sources are restricted to the easternmost pathways and lie outside the scope of this study.

Careful georeferencing of GEE coverage for time slices from 1984 and 2016 show that over this period, the trailing edge of the southernmost barchanoid draa located on the south-facing slope rising from the Grillental valley has migrated northwards some 200 m to 300 m. This raises interesting questions about the dynamic stability of the southern accumulation zone.

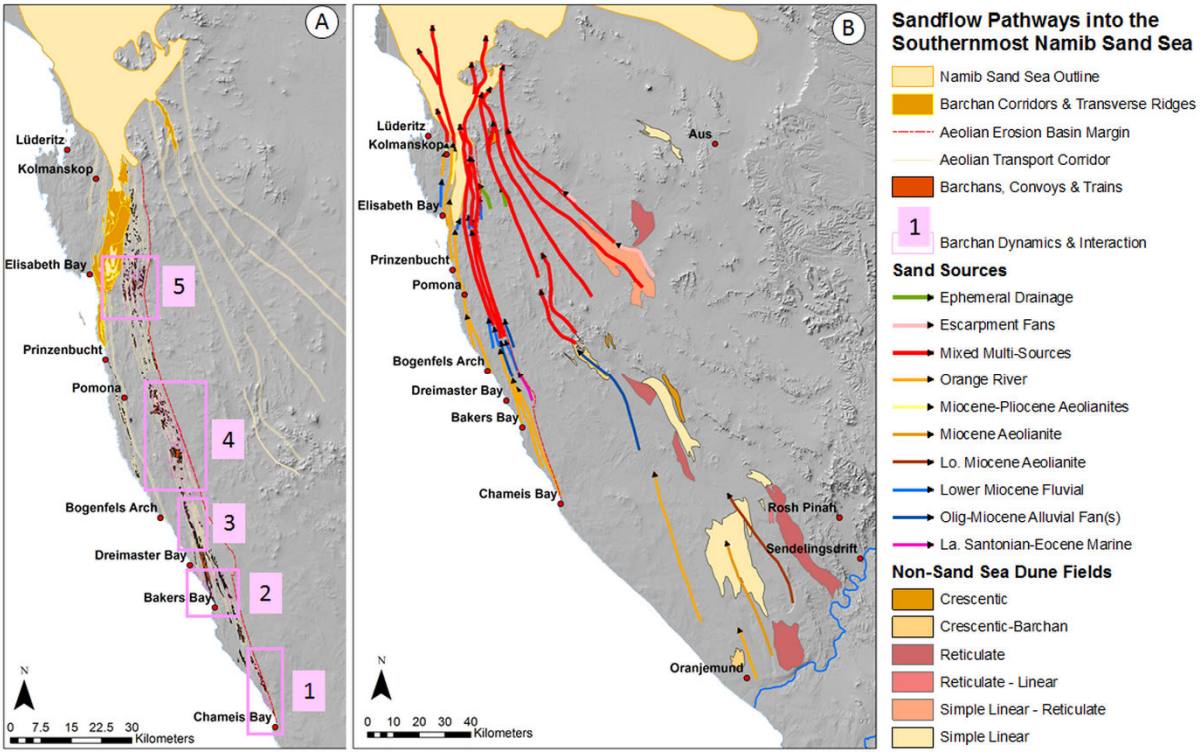

Figure 8. A) The distribution of Aeolian Transport Corridors and Barchan Dune Corridors supplying sand to the southernmost end of the Namib Sand Sea. B) Variation in sand sources influencing sandflow for the boundary conditions of the southernmost Namib Sand Sea (Corbett, 2016) covered by this paper. The eastern pathways have been defined using Scheidt (2012), Scheidt & Lancaster (2013) and Lancaster (2014) and GEE time-lapse video coverage to identify the most active transmission pathways.

The challenge that scale presents to successful mineral exploration was recognised by McCuaig *et al*. (2010). In reviewing scale-dependent perspectives on the geomorphology and evolution of beach-dune systems Walker *et al*. (2017) drew attention to the challenge presented by a lack of suitable data to enable detail to be investigated at the "plot scale". Fortunately Namdeb (Pty) Ltd acquired a unique Airborne Laser Scanner (ALS) dataset that is integrated with high-resolution low-level aerial photography covering almost the entire 170 km length of the high-energy unimodal aeolian system within the coastal zone from Chameis Bay in the south to Schmidtfeld, north of Lüderitz. Detailed mapping using the ALS dataset enables the identification of macro- and meso-scale aeolian bedforms and features which have previously not been identifiable through ground-based fieldwork. As a result, spatial patterns of aeolian sandflow and bedload transport have been identified and mapped at a level of detail that has not previously been possible at such a large scale.

Sediment Dynamics within Aeolian Transport Corridors

Corbett (1989, 1993) coined the term Aeolian Transport Corridors (ATC) for 1 km-wide sandflow conduits that became apparent through empirical measurement of sandflow in the vicinity of Bogenfels from 1984 to 1987. ATCs can be traced for over 170 km from their

coastal inception points to the position at which they enter the southern margin of the Namib Sand Sea (see Fig. 8b). Unlike barchan corridors, ATCs are characterised by mono-trains of large barchan dunes.

Modelling studies have investigated flow-bedform interaction for isolated and paired interacting barchan dunes (Endo *et al*. 2004; Palmer *et al*. 2010, 2012). Some modelling studies have also investigated the development and maintenance of linearly extensive chains of dunes (Katsuki & Kikuchi, 2011; Worman *et al*. 2013) and sand transport (Charru & Laval, 2013) has also been modelled at a laboratory scale. Computational Fluid Dynamics (CFD) has been applied to model the structure of Large Eddies produced by turbulent flow over three-dimensional dunes (Omidyeganeh & Pomelli, 2013) and barchan dunes (Omidyeganeh, 2011, 2013; Omidyeganeh *et al*. 2013).

Collectively these studies provide many new insights into the nature of flow associated with barchan dunes, its effect on sediment transport within their immediate vicinity, the way in which barchans interact physically, and the importance of variations in sandflux. However, the complete pattern of wind flow or sandflow produced by a barchan dune from immediately upwind of the stoss slope skirt to the downstream extremity of the sand leakage traces produced by near-saturated sandflow emanating from the dune's horns has yet to be modelled.

The mechanism by which mono-trains of dunes can be maintained over tens of kilometres also remains to be found. Corbett (1989) suggested the possibility that counter-rotating helical vortices in the Atmospheric Boundary Layer (ABL) might play a role in the genesis of these narrow sandflow conduits. At that time, meteorologists were just beginning to use newly emergent technologies such as Synthetic Aperture Radar to look for these macro-scale coherent structures in the ABL. Much too has therefore also been learnt since 1989 about the turbulent structure of flow in ABL (1 km to 2 km above the Earth's surface), and the Surface Layer (i.e. the first 100 m to 200 m immediately above the Earth's surface).

Detailed mapping of dune forms within ATCs using ALS data reveals the discontinuous nature of the mono-trains of barchan dunes and associated bedforms. The longest section of mono-train barchans and associated bedforms identified in this study can be traced some 55 km. The patches or chains of dunes are separated by zones of thin sand sheet accumulations on the floor of the aeolian erosion basin. These sand repositories appear to form where sandflow within converging Aeolian Transport Corridors merges and/or barchan instability leads to their erosion and the reintroduction of sand into the sandflow system. The largest sand sheet repositories extend for 12 to 15 km downwind. They represent laterally extensive planar sand sources within the active sandflow system which were not previously recognised by Corbett (1989). GEE coverage provides interesting insights into the effect that barchans migrating across these sands sheets have on the sandflow system in response to changes in flow pattern within the ASL.

The next section documents observations of barchan dune dynamics at the selected sites within the system shown in Fig. 8a as well as features related to sandflow.

Site 1 and 2: Sandflow & Barchan Dynamics at the Inception of Aeolian Transport Corridors

The chains of barchans which feed into the southern end of the Namib depositional system emanate from tightly constrained (<200 m long) coastal point sources of sand within widely separated, coastal log-spiral embay-ments (see Fig. 8a, barchan dynamics and interaction sites 1 and 2). The zone of active deflation within the log-spiral embayments is marked by the development of low, fast-moving sand domes 5 m to 10 m in width and up to 1m in height and small fast-moving embryonic protobarchan dunes 10 m to 15 m in width and 1 m to 2 m in height. Periodically, storm waves erode the beach, cutting back into the embryonic aeolian dune forms which temporarily reduces the active area of deflation.

Initially, sandflow streaming off the deflating beach accumulates immediately downwind in large, undulating sheet-like sand repositories and aeolian shadow dunes in the lee of topographic obstacles. The sheets are elongated to the north in response to the prevailing southerly unimodal surface windflow and they have clearly defined margins (Fig. 9). Downwind of the sheets narrow, south-north oriented valleys sculpted in the Precambrian bedrock funnel the chevron-shaped bedforms into narrow pathways within which the southerly surface winds are topographically steered.

ALS digital elevation models reveal that the undulating sheet-like bodies exhibit a large-

scale chevron-like geometry resembling those described from the Selima Sand Sheet by Maxwell & Haynes (1989, 1992, 2001). However, unlike Selima, where the vertical relief of the macro-scale chevron bedforms is negligible, the Namib examples vary from 5 m to 15 m in height. The absence of a slip-face leads to the classification of these sand bedforms as zibar dunes (sensu Biswas *et al.* 2015; Cooke & Warren, 1973). The surface of the zibar dunes downwind of Chameis Bay is characterised by regimented linear streets of coarse-grained sand and granule ripples which extend downwind across their surface.

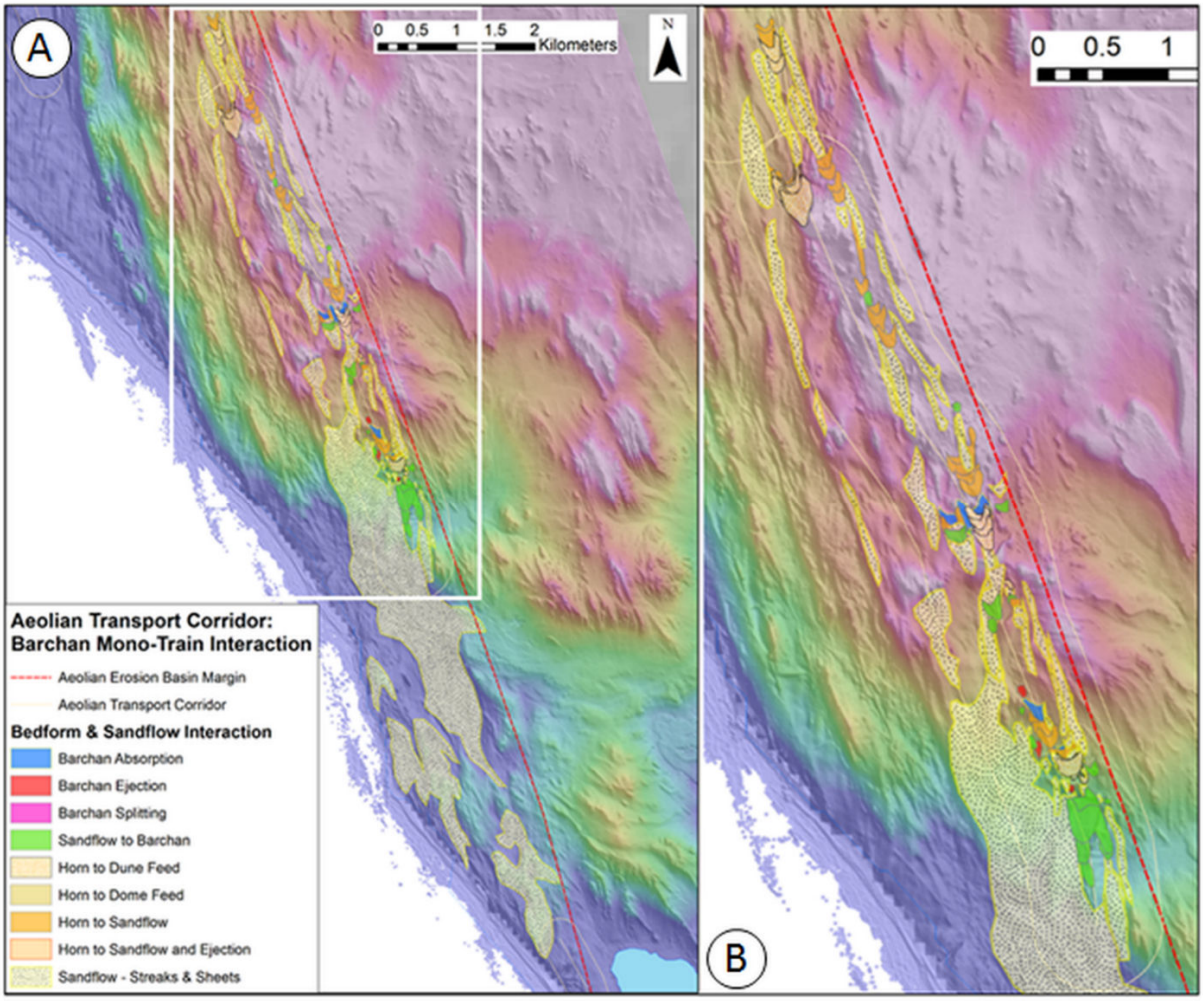

Figure 9. A) Overview of Chameis Bay ATC initiation site. The large area characterised by sandflow immediately backshore of the beach is a field of large zibar dunes. B) Close-up of insert showing pattern of sandflow-dune and dune-dune interaction downwind of the zibar field at the ATC inception point. Observation with GEE time-lapse shows sandflow migrating north in ribbon-shaped sheets or low mounds and there is a suggestion that changes in the geometry of the sand sheets occur as the sand flux entering the system varies.

The initiation of bedforms at the inception of the Chameis ATC occurs in one of two ways:

1) Firstly, shadow dunes develop in the lee of bedrock obstacles as fast-moving ribbons of sand migrate northwards, leading to the shedding of fast sand domes and/or protobarchans.

2) Sand ribbons extend from the tips of north-oriented zibar dune extensions and change rapidly into chains of fast sand domes and protobarchans which interact leading to the development of barchan dunes.

Shedding of sandflow from zibars in the form of fast sand ribbons also leads to the development of larger sand domes, some of which evolve horns and adopt a barchanoid shape but there is no clear slipface developed. Instead, topographic steering leads to the asymmetric extension of one of the horns through sand leakage. Near saturation of sand flux leaving the zibar field at these sites then plays a key role in the initiation of smaller, fast-moving bedforms which rapidly evolve into barchan dunes.

The alternation between streaming sand ribbons and fast sand domes and/or protobarchans is commonly observed as bedforms emerge and disperse back into the streaming sandflow. Despite the rapid streamwise growth in barchan size, ribbons of streaming sand continue to migrate northwards and there is clear evidence of barchan size changes, with the periodic shedding of narrow, elongate sand leakage traces from the horns of barchans as they reduce in size. In some instances leakage traces extend almost 2 km from barchan horns. Once developed, the leakage traces are observed to remain in place for periods of 2 to 3 years before their erosion leads to the sand being resorbed back into the sandflow. The traces are extremely narrow, between 50 m to 100 m wide, with little evidence of lateral dispersion in the downwind direction. Once leakage traces erode, sand mounds appear in the downwind direction, with some having barchanoid geometries but no clear slipface. Leakage traces extend from the horns of these bedforms mimicking the behaviour of barchan dunes.

Barchan interaction is commonly observed between fast protobarchans and barchans and their larger, slower moving counterparts. Sequences of absorption, ejection and splitting take place as chains of barchan dunes develop until the sandflow emanating from the horns of the lead dune is reincorporated into the streaming sandflow.

The complex topography produced by the intricate network of narrow valleys and bedrock highs leads to topographic steering of wind flow in the Surface Layer. Rapid, localised variations in surface wind velocity results in the dispersion of fast sand domes, protobarchans and barchans as the sand is resorbed into the sandflux streaming through the valleys. In other instances the convergence of valleys leads to localised increases in sandflux. Where the sand streams coalesce, saturation of the sandflow presumably initiates the rapid growth of barchan dunes.

Ultimately, as the train of barchans is traced downwind the sandflux maintaining them is reduced to the point that the barchan dunes are eroded. When this occurs, the dune form is progressively (but rather quickly) resorbed back into the streaming sandflow. During this process the main body of the dune reduces in size and the released sand migrates to the horns from which sand leakage traces extend rapidly downwind. In the case of the Chameis ATC the initial cycle of sand capture by bedform evolution and its resorption back into saltation sandflow takes place over a streamwise distance of approximately 15.8 km.

A second ATC inception site (Site 2, Fig. 8a) was examined in detail at Marmora Pan, to the north of Chameis Bay (Fig. 10).

Site 2 was selected because of the development of a large zibar dune field and the recognition of extensive fields of previously unidentified giant megaripple bedforms. Based on mapping of bedforms and observation of the area in the field and using GEE, the sandflux generated here is probably much lower than that generated at either Chameis or Baker's Bay due to the straight coastline and coarse-grained nature of the beach.

The zibar dune field is one of the best developed along the entire coast with a clearly defined chevron pattern. The high-resolution ALS video coverage shows that the sandy zibars are migrating across an underlying surface comprised of giant megaripples. Like the Selima examples, the chevron-shaped bedforms are identifiable due to contrasting sediment colour, especially where they occur on the surface of dark-coloured pan sediments at Marmora Pan.

In contrast to the Selima examples which exhibit negligible relief, the Namib examples are characterised by a windward-facing stoss slope which is steeper than the gently inclined lee slope. The light-coloured mega-ripple sheets consist of large, quartz granule dominated low amplitude (1 to 2 metres) bedforms with a wavelength ranging from 250 m to 580 m. The mega-ripples forming the chevron fields and the regimented streets of granule ripples characterising their surfaces appear to mark important coarse bedload entry points into the Namib Aeolian Erosion Basin.

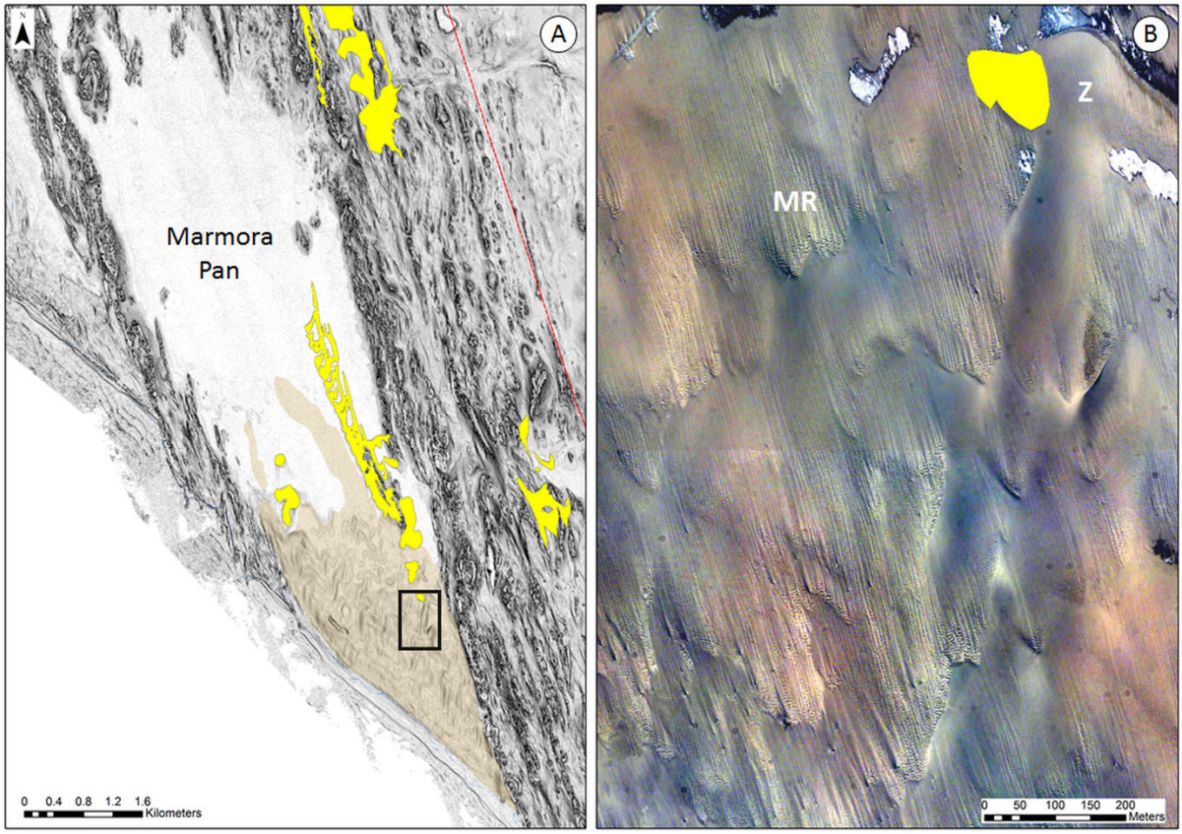

Figure 10. A) Zibar development on Marmora Pan (light brown). The straight coastal configuration and coarse-grained nature of the high-energy beach reduce deflation of sandflux. Aeolian dune generation is triggered by topographic obstacles and/or changes in surface roughness. Shadow dunes and barchan convoys grow in the lee of Precambrian bedrock highs. B) Chevron fields of megaripples forming sheets on the Marmora Pan with zibar dunes migrating across them.

Similar megaripple fields have been identified at Chameis, Marmora and Dreimaster Bay. Within the Sperrgebiet coarse bedload accumulations such as these potentially include diamonds in an assemblage dominated by quartzitic components. It is clear that the rippled surfaces of the mega-ripple bedforms are currently undergoing active transport. At least some of the bedload is probably being derived from the modern beach. However, a number of other possibilities exists:

- The megaripple bedforms could be the product of aeolian reworking of subaerially exposed marine inner shelf sediments during regressive events, or;
- Aeolian reworking of latest Pleistocene/Holocene nearshore facies related to the most recent transgressive events known within the area.

Either scenario has interesting implications for the development of arid zone diamond placers in the Sperrgebiet. At Elisabeth Bay, an analysis of sampling and production data has confirmed that the size and grade of the diamonds within the associated marine placer is larger than that of the low-grade aeolian sheet placers. (Head, 2014; Burger, 2015). The study by Head (2014) showed that the marine influence could be traced 400 m downwind from the source as the subaerially exposed nearshore to inner-shelf marine gravels were progressively reworked by aeolian processes, introducing diamonds into the aeolian bedload transport system. Observations using the Jago submersible to support offshore diamond mining operations have recorded the presence of gravel waves migrating northwards along the inner shelf to depths of 70 m (Spaggiari, 2011). These gravel bodies are presumably driven shoreward by nearshore currents generated during storm events.

Based on the sheet-like geometry of the low-grade aeolian diamond placer at Elisabeth Bay, and the sedimentary structures preserved within the aeolian sequences being mined, it is probable that similar megaripple bedforms and zibars might have contributed to, or even account for, the development of that orebody. Unfortunately, surface evidence to confirm this is no longer visible due to disturbance by mining. However, aeolian sequences within the Elisabeth Bay placer are characterised by wind-

ripple lamination in which thin (1 to 5 cm thick), lense-shaped concentrations of extremely well-rounded granules of siliceous particles occur. Low-angle, planar erosional surfaces are marked by lag concentrations of quartz granules. The stacked, sheet-like geometry of the placer developed over the last 5 myr according to Burger (2015) who identified a number of aeolian sequences of different ages separated by erosional bounding surfaces. Some of the older aeolian sequences are diagenetically cemented. During this time period the continental margin is known to have been subjected to transgression to 50 masl and numerous regressions occurred based on evidence from diamond mining operations on the inner-shelf. Diamond exploration recently led to the discovery of a marine beach placer in the south-eastern corner of Elisabeth Bay approximately 20 mbsl. The dynamic nature of the marine-aeolian interface along this margin thus has the potential to create diamond placers with complex histories.

Site 2, 3 and 4: Sandflow Dynamics Downwind of Coastal ATC Inception Points

Two geomorphic domains are broadly recognised downwind of ATC inception points along the coast:

1) Aeolian Erosion has exploited the regional geological structure to produce complex and rugged topography dominated by wind-aligned endorheic basins and bedrock highs, some of which form positive and/or negative steps. As a result surface windflow is topographically constrained and steered;

2) Alluvial plain/duricrust inversion landscape in which positive and negative steps are present but surface windflow on extensive planar surfaces is comparatively unconstrained topographically.

Site 2: Topographically constrained ATC sandflow dynamics

Wind-aligned endorheic basins form one of the most widespread geomorphic domains within the aeolian erosion basin (Kaiser 1926; Corbett, 2016). Surface windflow within this domain is topographically constrained. Topographic steering of Surface Layer wind flow characterises these areas. As a result, localised compression and expansion of flow within the Surface Layer occurs where valleys converge/diverge and surface wind flow patterns are complicated by the presence of cross-wind oriented topographic barriers (Fig. 11).

Barchan dunes generated along the Chameis ATC reach a finite point of growth downwind at which the sand flux is no longer sufficient to maintain barchan dunes. At these locations the growth and maintenance of the furthermost barchan downwind is observed to be punctuated periodically by erosion of the dune resulting in the streamwise extension of linear, narrow sand leakage traces. Sand leakage traces show minimal evidence of lateral diffusion and they commonly extend from one particular barchan horn. Bilaterally symmetric dunes and leakage traces are also observed in some instances, when leakage traces extend more evenly from both horns.

Inland of Baker's Bay the rugged aeolian erosion landscape is bounded to the east by the 120 m high Buntfeldschuh escarpment which creates a major topographic boundary constraining wind flow in the Surface Layer. GEE time slices enable mapping of temporal and spatial changes in the pattern of sandflow and the growth, interaction and decay of barchan dunes.

Starting in 1984, two large barchan dunes coalesced immediately south of site 2 (see Fig. 8a for location map). The eastern dune maintained a barchan geometry but the western dune went through a complex sequence of evolutionary events culminating in the development of a set of five interacting barchans. The sequence of changes was triggered by the passage of streaming sandflow across a topographic depression. On exiting the depression, the sandflow arrives at the base of a positive south-facing ramp leading in to an area of complex, positive relief controlled by the underlying geological structure.

The eastern upwind barchan is influenced by accelerated surface windflow due to the compression of flow up a south-facing spur, whilst the western sand flux is topographically steered into a depression leading up a gently inclined south-facing slope. This led to sandflow saturation and the evolution of a large sand mound which transformed into a barchanoid sheet and ultimately a large barchan dune from which four smaller, faster-moving barchans were ejected. Ejection was triggered by the initial dune capturing streaming sandflow resulting in its progressive growth until it migrated upslope onto the raised relief, at which point smaller barchan dunes were progressively ejected. The ejection process was initiated by the development of fast sand

patches and sand domes immediately downwind of the horns of the upstream barchan. The sand patches/domes progressively assumed a barchanoid geometry, with well-developed sand leakage traces extending from their horns. As the sequence of events progressed the sand deposited in leakage traces from the lead barchans was resorbed into the streaming sandflow. This process was potentially aided by the migration of the dunes and leakage traces towards a series of transverse ridges.

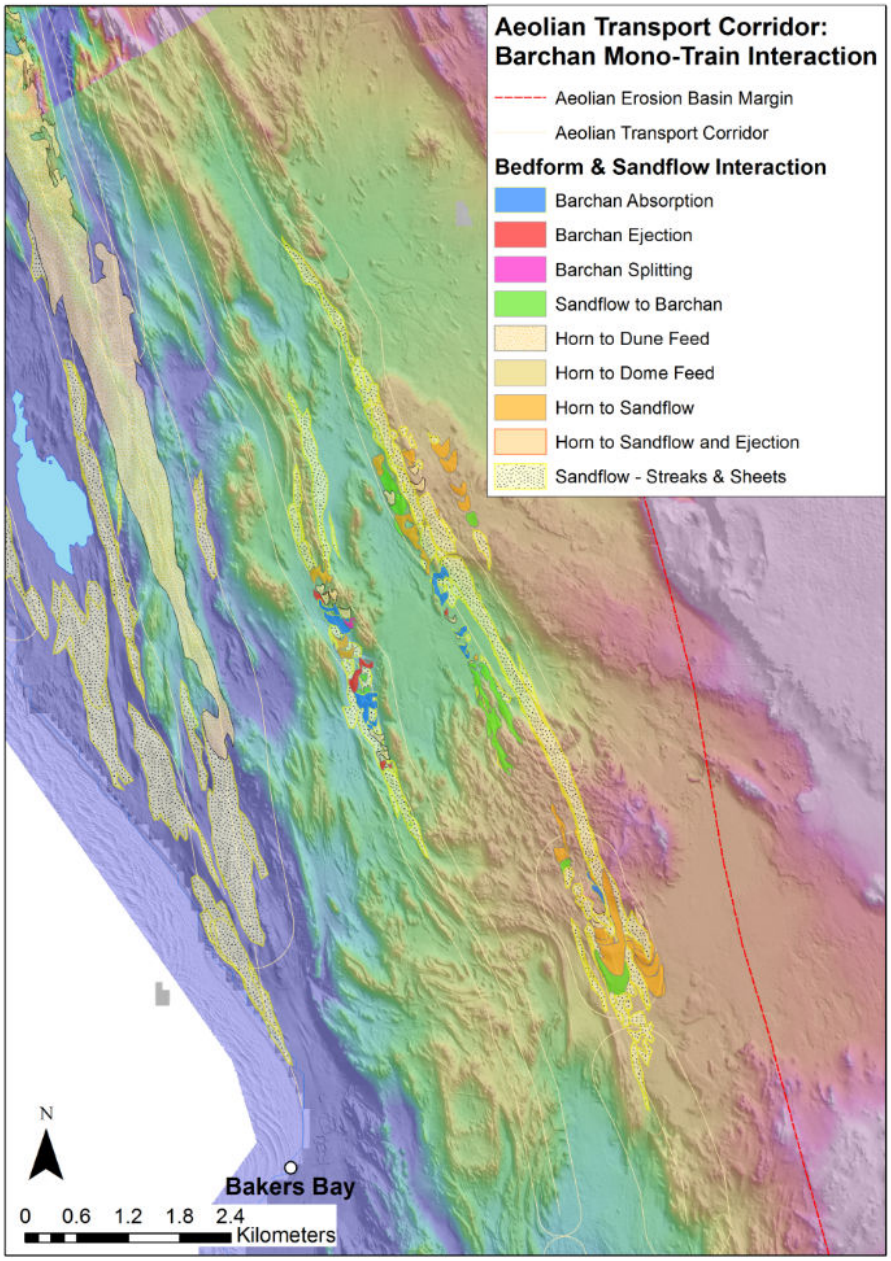

Figure 11. Sandflow dynamics within the Chameis (far right) and Marmora (middle) ATC showing the regeneration of barchan dunes downwind of sandflow and the sand sheets and zibars immediately landward of the coastline at the inception of the major Baker's Bay ATC.

Towards the northern limit of the area analysed, the streaming sandflow crosses a topographic high and descends down into a depression. As the sandflow crosses the negative step at the northern end of the topographic high, sand streaks/ribbons evolve into shadow dunes. On the surface of the sand ribbons/shadow dunes fast sand domes and protobarchans form into convoys migrating downwind. Barchan dunes are ejected from the leading edge of the convoy/sand stream. Initially bedform nucleation occurs as sand patches or mounds which rapidly grow into barchan dunes migrating across the topographic depression.

At the northern edge of the depression a bedrock promontory forms an abrupt positive step. As the dunes migrate up and over the step the barchan form changes rapidly as a result of dune erosion leading to the formation of fast, interacting sand patches and mounds. Although they have no slipface, some retain a barchanoid form. Absorption, splitting and ejection is observed as the barchan dunes reform and begin to migrate downwind to the north. The presence of complex, rugged relief spawns more interactions until the sandflow stream and barchan dunes approach a south-facing bedrock buttress which splits the sand flux into two streams either side of a ridge. The majority of the sandflow migrates along the western margin of the ridge producing a shadow dune which evolved downwind into a protobarchan convoy. Isolated fast barchan dunes migrate down the eastern margin of the ridge before being funnelled towards a slower dune which absorbs them causing it to grow until local wind flow increases due to topographic steering causing the dune to be eroded. At this point small, fast barchans are ejected as saturated sandflow leaks from its horns.

Sites 3 and 4: Topographically unconstrained ATC Sandflow Dynamics

To the east of Bogenfels the Baker's Bay ATC crosses an area of less rugged topography (Fig. 12). Wind flow within the Surface Layer here is less topographically constrained than it is within areas floored by endorheic basins. Corbett (1989) deployed sand traps at this locality to measure sandflow and dune migration rates were monitored here from 1984 to 1987. This section of ATC contains some of the largest isolated barchan dunes forming a mono-train within the Namib sandflow system within one of the main ATCs that are currently active within the southern Namib sandflow system.

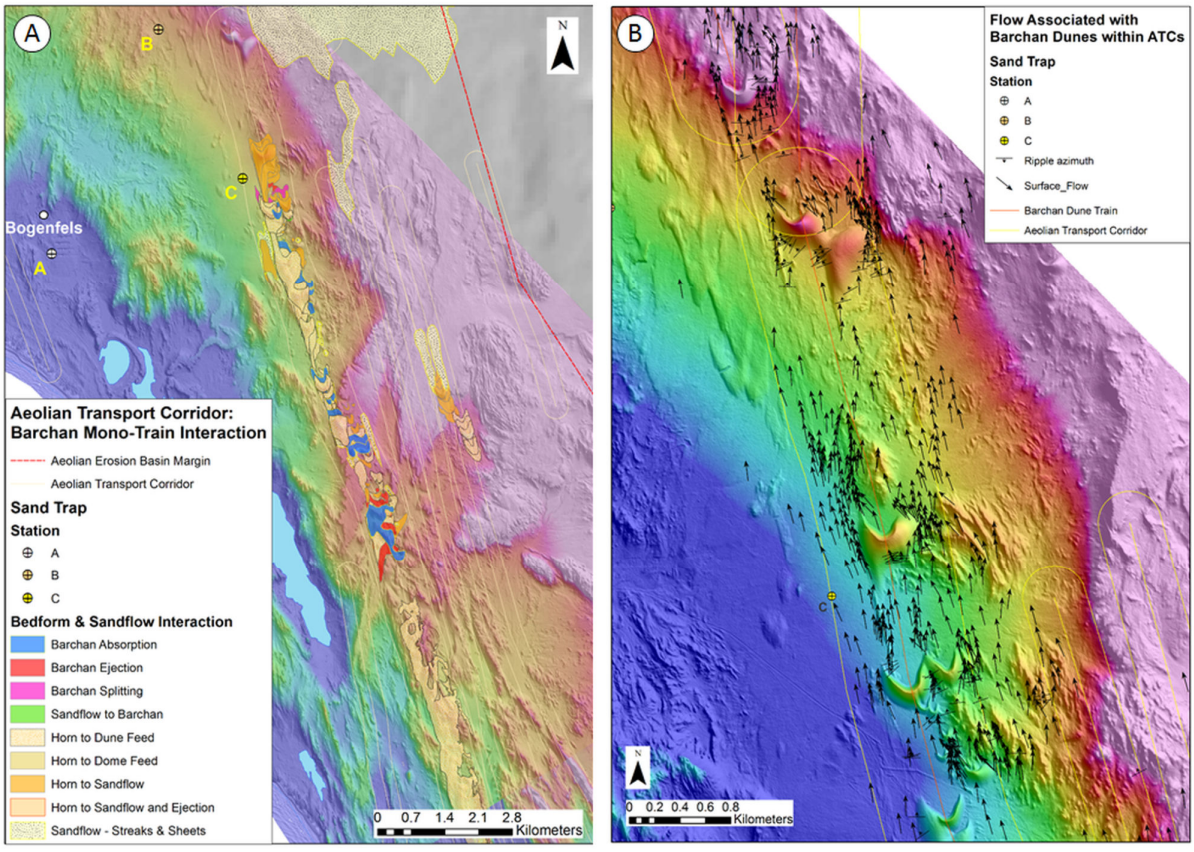

Figure 12. A) Map of barchan dune migration and interaction to the east of Bogenfels. The western ATC is fed from Baker's Bay and the eastern one from Marmora Pan. The relative difference in bedform development reflects the variation in sandflux. The distribution of sites at which absorption occurs is closely linked to changes in topography which modify the flow lines in the Surface Layer to cause acceleration and deceleration of wind flow. B) Detailed mapping of aeolian current shadows and sand streaks reveals that surface flow downstream of the barchan horns is directed back towards the centre-line of the dune migration path.

Although no endorheic basins are present to steer the surface windflow, the main barchan dune train traverses a series of topographic highs produced by erosion of the underlying Precambrian geology and topographic inversion of an extensive Miocene alluvial fan sequence (Corbett, 2016). This creates a positive and negative step either side of a plateau surface.

The Baker's Bay ATC is one of the main conduits within the southern Namib sandflow system. The large barchan dunes which form the mono-train are located downwind of an extensive sand repository that extends for 12.5 km from its inception point. The repository consists of a continuous series of shadow dunes and protobarchan-barchan convoys that form in the lee of bedrock highs. Towards its northern end, the sandflow dynamics are complex and varied as a result of the ejection of sand patches and fast sand domes, chains of fast barchans and barchans coupled with the episodic passage of streaming sand ribbons. Some ribbons and streaks are observed to be directed from the outer margin of the repository back in towards the centre-line of the ATC by the surface wind flow.

At the downwind end of shadow dunes, fast sand domes and proto-barchan convoys evolve into embryonic barchan dunes. Normal barchan dunes (terminology of Bourke & Goudie (2009) developed from Sharp's original classification) then progressively break away and migrate northwards as part of a discrete barchan dune mono-train. The barchans forming the chains or trains progressively increase in size downwind to the north, until they reach 400 m to 500 m in width and length, with crest heights of between 30 m to 35 m. Corbett (1989) recorded one of these large dunes migrating north at a rate of 30 to 50 m/year (Corbett, 1989). At Elisabeth Bay smaller barchans typically migrate 70 m to 100 m per year (Burger, 2015) and observation of GEE time series suggest that embryonic forms such as fast sand domes and protobarchans migrate significantly faster than 100 m/year.

Downwind along the Baker's Bay corridor, where wind and sand flow are topographically less constrained, the separation distance between large barchan dunes in a single train progressively increases until the leading barchan becomes unstable and sand leakage from the horns is no longer balanced by the incoming sand flux from upwind. The separation distance between dunes reaches 1100 m to 1250 m at this point. Field measurement of wind flow associated with barchan dunes at Torra Bay further north in Namibia by Baddock *et al*. (2011) showed that the dunes act as isolated bedforms once separation distance reaches 17 times the dune height. In the Sperrgebiet separation distance is about 30 times the height, or approximately 3 times the dune length. Hence the treatment of the barchans as isolated bedforms is consistent with modelling studies as well (e.g Palmer, 2010; Palmer *et al*. 2012; Omidyeganeh, 2011, 2013; Omidyeganeh & Piomelli, 2013; Omidyeganeh *et al*. 2013). In terms of turbulent wake generation, the upwind dune therefore theoretically has no direct influence on the wind flow pattern associated with the dune located downwind of it.

GEE reveals a remarkably complex sequence of events taking place along the mono-train of large barchans during which fast barchans are absorbed and ejected and larger dunes coalesce and split.

Changes in topography produced by positive (forward-facing) and negative (backward facing) steps transverse to the surface wind flow trigger changes in the dynamics of dune forms migrating along the ATC. Barchan dunes capturing incoming sand flux grow until they approach the crest of the positive step where a marked change in dynamics is observed. The compression of flowlines up the positive step leads to the erosion of sand from the barchan as it approaches the crest, resulting in the rapid generation of sand leakage traces from the dune's horns.

The leakage traces take the form of thin, elongate sand patches which detach from the remnant of the source barchan. The sand leakage traces subsequently erode and either become resorbed into the streaming sandflow or they migrate northwards evolving into discrete fast sand patches and/or sand domes which rapidly evolve into small fast barchans that migrate across the plateau. The migration rate of the fast barchans is orders of magnitude greater than their larger counterparts, so that they collide with, and are absorbed by the larger dunes. This triggers the ejection of barchans downwind of the barchan by which they are absorbed.

While some of the larger barchans maintain their geometry as they migrate up and over the positive step, in other instances the passage of sandflow over it leads to the formation of large, slipface-less sand mounds with a barchan form. Moving in parallel, the barchanoid sand mounds and barchan dunes merge and coalesce as they migrate across the plateau and split as

they descend the negative step on the northern side of the plateau. As the dunes and sandflow descend the negative ramp produced by the topographically inverted relief, barchan interactions take place with smaller, faster-moving barchans being absorbed by the downwind dune resulting in its growth prior to splitting taking place. These interactions lead to changes in sandflux and long sand leakage traces develop forming wind-aligned sand ribbons from dune horns and/or bedrock highs. The leakage traces/sand ribbons eject fast protobarchans and small barchan dunes from their downwind margin. In some instances large barchan dunes develop as the sand ribbons grow, but they are rapidly eroded as the output sandflux from their horns is resorbed into the streaming sandflow.

Within the Baker's Bay ATC it is difficult visually to identify the sand leakage traces emanating from barchan horns. However, the geometry of downwind barchans and the time series mapping of the dune forms reveals that the long trailing spur which characterises some of the larger barchans is maintained directly by the sand leakage trace from the western horn of the barchan located upwind. This conclusion is consistent with the wind flow pattern mapped from high-resolution ALS photo-coverage which delineates flow lines from the horns angled inwards towards the centreline of the migrating barchan (Fig. 12b). Although the flow pattern is undoubtedly influenced by subtle topographic steering of the surface wind flow as well, analysis of many dunes in other ATCs as part of this study show that this is a consistent flow pattern associated with large barchan dunes within the southern Namib system. Within the Baker's Bay ATC aerial photographs looking south down the centreline of the barchan mono-train confirm the presence of this flow pattern (Fig. 13a).

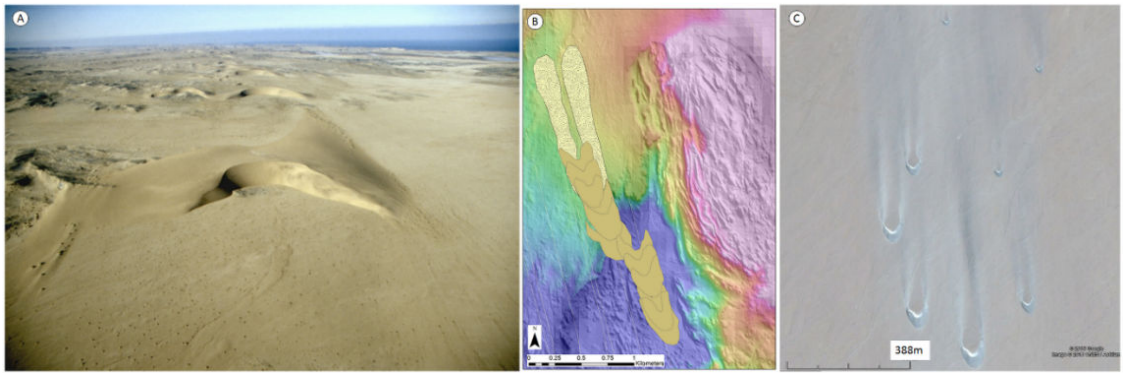

Figure 13. A) Low-level oblique aerial photograph to the south looking directly upwind along the mono-train of large barchans mapped in the section of the Baker's Bay ATC in Fig. 8a and Fig. 12a. Note the aeolian current shadows on the stone pavement which show that surface, flow back towards the migration path centre-line. B) Map of two migrating barchan dunes shown in Fig. 12b with long sand leakage traces extending symmetrically downwind of both horns reflecting the topographically unconstrained nature of the surface flow associated with the dune forms. C) Examples of sand leakage traces produced under topographically unconstrained flow conditions at La Joya, Peru. Note the downwind extension of the sand leakage traces from the barchan horns. The shape of the proximal leakage traces indicate flow back towards the centreline of the dune migration path and they show minimal lateral dispersion downwind over a distance of 2.5 km.

The separation distance of the large, slow barchan dunes within the Baker's Bay ATC increases rapidly northwards and the dunes become completely isolated along its length in terms of wake effects in the Surface Layer. However, GEE observation shows that the dune interaction continues due to the passage of sandflow from the horns of upstream barchans. This form of interaction is initiated by the extension of a sand leakage trace from a horn of an upwind dune, which detaches and migrates northwards over a distance of 4 km to 5 km before it is absorbed by the downwind barchan. The receiving barchan subsequently develops an elongate sand leakage trace.

The observation that the leakage traces downwind of barchan horns periodically expand in size and downwind extent implies that the traces from barchan horns are either responding to:

- The arrival of discrete "packets" or pulses of sandflow streaming along the corridor which temporarily destabilise the incoming and outgoing sandflux and/or;
- The natural cycle of dune growth and erosion/decay as sandflow is captured and released by individual dunes.

To the east of the Baker's Bay ATC a number of less easily traced ATCs converge. Two barchan dunes define the presence of one of the eastern ATCs. They are sufficiently separated to behave as isolated dune forms (Fig. 13b), but the leading dune receives sand from the western horn of the upwind barchan. The sand leakage trace that has developed from the downwind barchan is one of the best developed in the study area. The sand leakage traces are almost bilaterally symmetrical indicating that wind flow is topographically unconstrained, and they extend downwind for a distance of about 1.5 km. The lateral dispersion of sandflow within the leakage trace is minimal. The width of the best developed leakage trace varies from 150 m proximal to the horn and expands to 230 m approaching the lobate, distal end. Comparison with sand leakage traces emanating from barchans in La Joya, Peru (Fig. 13C) suggest that lateral dispersion of sand leakage traces is less marked in the Namib system.

Large-Scale Rhomboid Mixed Sand and Bedload Sheets

Large, *en echelon*, rhomboid-shaped sheets of mixed sand and coarse-grained bedload have been identified using the ALS data (see top left in Fig. 12b) towards the northern end of the first barchan dune train within the Baker's Bay Aeolian Transport Corridor (Corbett, 2016). These large bedforms are 1 to 2 metres thick, 200 m to 300 m wide and 200 m to 600 m long. Exploration sampling of isolated mixed sand and coarse bedload sheets on the stone pavement bordering the western side of the corridor contain surprisingly high-grade concentrations of diamonds, and these bedforms have been mined economically in places. The internal structure of these sheets contains wind ripple laminae (sensu Kocurek & Nielson, 1986) well-defined lense-shaped laminae of well-sorted and well-rounded granule to small pebble sized quartz clasts indicating that coarse aeolian ripples were associated with them during their formation.

The origin of the bedforms is not certain, but the presence of significant concentrations of diamonds within them may give a clue. There is no known evidence of features such as these migrating north within the present-day Baker's Bay ATC, although bedload transport is definitely taking place as discussed in the next section. The possibility exists that they are relict features. During marine transgression, the coastline at Bogenfels forms a large, south-facing, re-entrant bay similar to that of Elisabeth Bay today. The rhomboid bedforms occur predominantly above the 90 m contour, with a few isolated and rhomboid en echelon bedforms located between the 50 m to 90 m contour. From the packing of the rhomboid sheets it is likely that they migrated northwards until they encountered and packed up against a south-facing bedrock slope. These large bedforms could thus represent the reworked remnants of modified mega-ripple sheets and zibars deposited by aeolian transport within the Bogenfels embayment. This might either have been in response to one or more transgressive fronts driving inner shelf gravel and grit upslope within the embayment or perhaps occurred as sea-level dropped during later regression(s) leaving marine sediments containing diamonds subaerially exposed on the floor of the embayment.

Macro-scale Bedload Patterns within ATCs

The aeolian erosional landscape within the Sperrgebiet is topographically complex, and it results in localised flow patterns which topographically steer the sandflow. The resulting distribution of saltation load drives the transport of the bedload.

Detailed field mapping during diamond exploration led to the identification of a variety of different types of aeolian bedload deposits, some of which display a clear relationship to topographic relief. Applying this knowledge to the interpretation of the high-resolution ALS dataset has enabled concentrations of uniformly coloured patches formed by coarse quartz granules on the desert floor to be mapped. One of the best areas in which these deposits can be observed lies south south-east of Bogenfels where diamond mining has been confined to relatively small, isolated areas and the desert floor is largely unmodified (Fig. 14). Funnelled by the relief of the erosional aeolian landscape, the paths of the presently active ATCs merge along the eastern side of the Bogenfels Salt Pan, funnelling sandflow through a narrow tract in which active bedload transport creates a suite of depositional patterns as the particles stream through the landscape (Fig. 14).

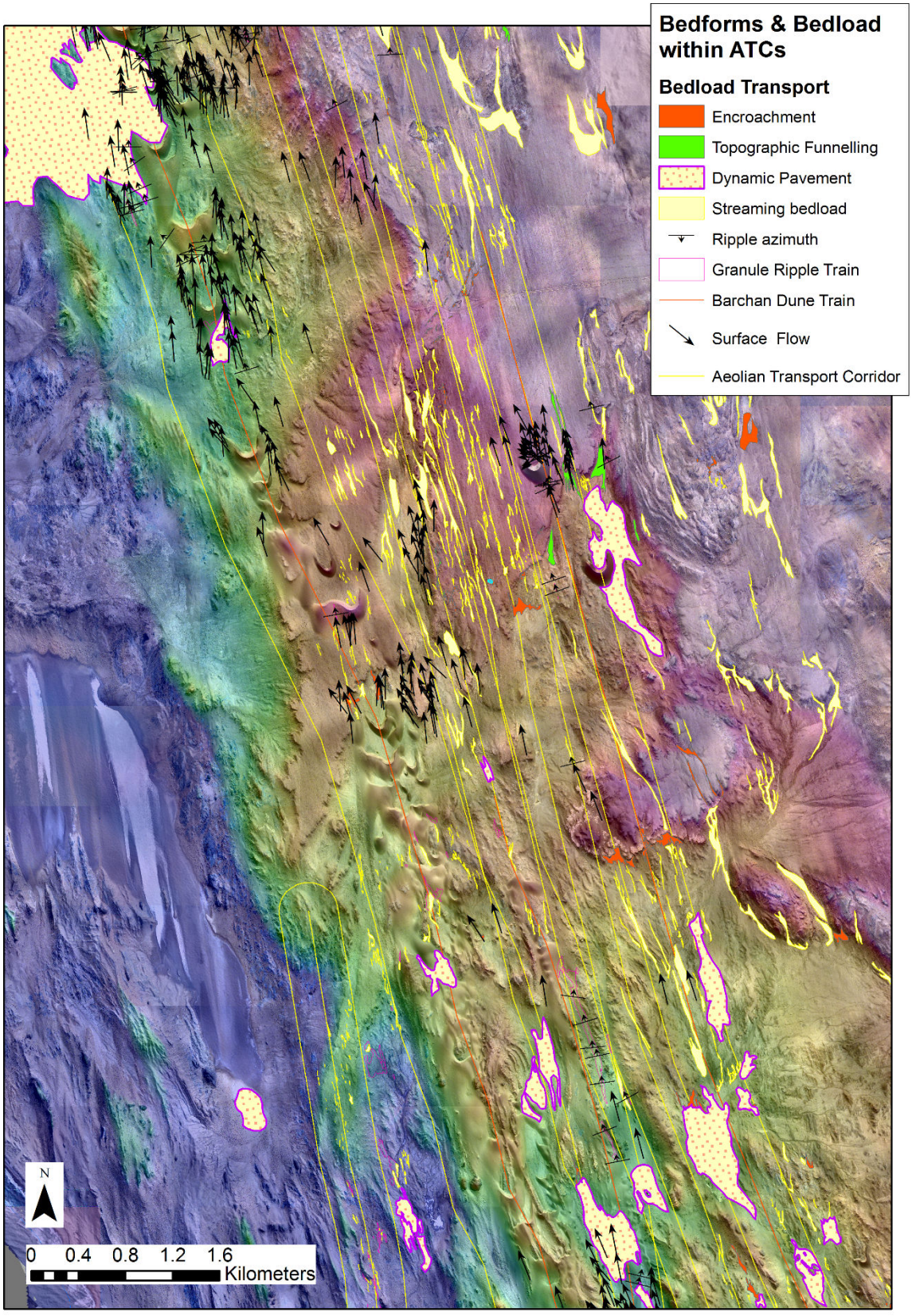

Figure 14. A variety of different types of aeolian bedload transport deposits shown in relation to the topography of the erosional aeolian landscape. The pale blue-white, south-north oriented streaks above the scale bar consist of salt on the surface of the southern end of the Bogenfels Pan.

Streaming Bedload (Streaks, Ribbons, Topographic Funnelling and Encroachment)

Concentrations of coarse bedload particles forming narrow ribbon-shaped streaks aligned with the prevailing unimodal windflow are a common feature on the desert floor throughout the Namib Aeolian Erosion Basin (Fig. 14). The granule/small pebble assemblage is usually dominated by quartz and other resistant siliceous particles but in some cases particles of locally eroded freshwater carbonate dominate the assemblage.

Evidence of streaming bedload in the form of coarse-bedload streaks is seen both in areas where surface wind flow is topographically constrained and unconstrained. While some characteristics are common in both contexts, bedload transport produces quite distinctive patterns depending upon the setting.

As shown in the southern part of Fig. 14, areas of complex topography, such as the endorheic basin topographic domain in the south of the picture, streaks of streaming bedload are commonly associated with and/or transition into trains of coarse granule ripples. This transition frequently occurs along the sides of the south-facing ramps at the northern end of endorheic basins. These ramps form localised catchments for ephemeral streams which erode aeolian sediments on their surfaces and transport it towards the base-level of each basin where deposition commonly occurs in close proximity to ponded water bodies. Subsequent aeolian deflation aided by salt crust formation develops and maintains stone pavements on the floors of the endorheic basins (Corbett, 1989, 2016), many of which have been mined for diamonds.

The endorheic basins in Fig. 14 to the south-south east of Bogenfels were sub-economic, so their surfaces have not been disturbed by mining activity. These basins experience extremely high sandflow conditions because a number of ATCs converge in this area due to topographic steering of the surface flow. Consequently, the stone pavement surfaces are dynamic sites of aeolian bedload transport. The ALS photo-coverage reveals that their surfaces are characterised by narrow linear streaks/ ribbons of coarse bedload that are aligned with the surface wind flow. While some of the striping is produced by the deposition of aeolian sandflow, streaming bedload can be seen migrating up south-facing ramps and across watersheds into successive endorheic basins. The surfaces of the dynamic stone pavements are also characterised by subtle, narrow, linear white streaks/ribbons which represent concentrations of coarse quartz bedload particles. The streaks/ribbons of streaming bedload are aligned with the prevailing unimodal surface wind flow. In many instances the bedload streaks with a spanwise spacing of 8 m to 15 m and streamwise lengths of 40 m to 200 m cut across the channelised ephemeral stream networks and display bifurcating paths at both the north and south ends.

The pattern of quartz bedload migrating across planar, topographically unconstrained surfaces is more pronounced. These surfaces are actively being created by topographic inversion of a coarse gravel alluvial sequence cemented by a calcareous crust (Kaiser, 1926). The surface windflow ascends a positive step cutting obliquely across the southerly surface wind direction along the leading edge of the alluvial terrace (see central part of Fig. 14). Streaming bedload is constrained to discrete streak/ribbon-shaped pathways aligned with the prevailing unimodal wind direction. More prominent streaks/ribbons are, in places, up to 20 m wide (generally 5 m to 10 m). A hierarchy of streak/ribbon development can be discerned. The better developed, larger streaks/ribbons can be traced in a streamwise direction for as much as 1.5 km and they have a regular spanwise spacing of 150 m to 175 m (Fig. 15A). In between the largest-scale features the bed is also characterised by bedload streaks with a spanwise separation of 30 m to 40 m, and these too have less-prominent streaks between them which are 2 m to 3 m wide and typically 10 m to 70 m long. Irrespective of scale, the bedload streaks/ribbons cut across the ephemeral stream networks crossing the plain formed by the inverted relief, illustrating that they are not simply infilling random depressions in the surface - they are spatially organised and flow-aligned and at all scales evidence is seen of branches bifurcating in a northerly direction and coalescing at their northern end to form nodes.

Closer examination of Fig. 15A shows light patches of bedload banked up against a forward-facing step facing south into the prevailing wind direction with streaks/ribbons streaming northwards above the step on the planar topographic inversion surface. This confirms the mobile nature of the bedload. The high-resolution DEM in Fig. 12B shows that some of the more prominent bedload streaks/ribbons above the step are located

within shallow grooves in the surface that are aligned with the unimodal southerly surface wind flow (Fig. 15B). These features closely resemble those described by Pollard *et al*. (1996) in both aeolian and glacial environments. The most spectacular aeolian examples of grooving are those described in the Western Desert of Egypt by Embabi (1999) and Brookes (2001), which occur on a far larger scale than those observed in the Namib.

.

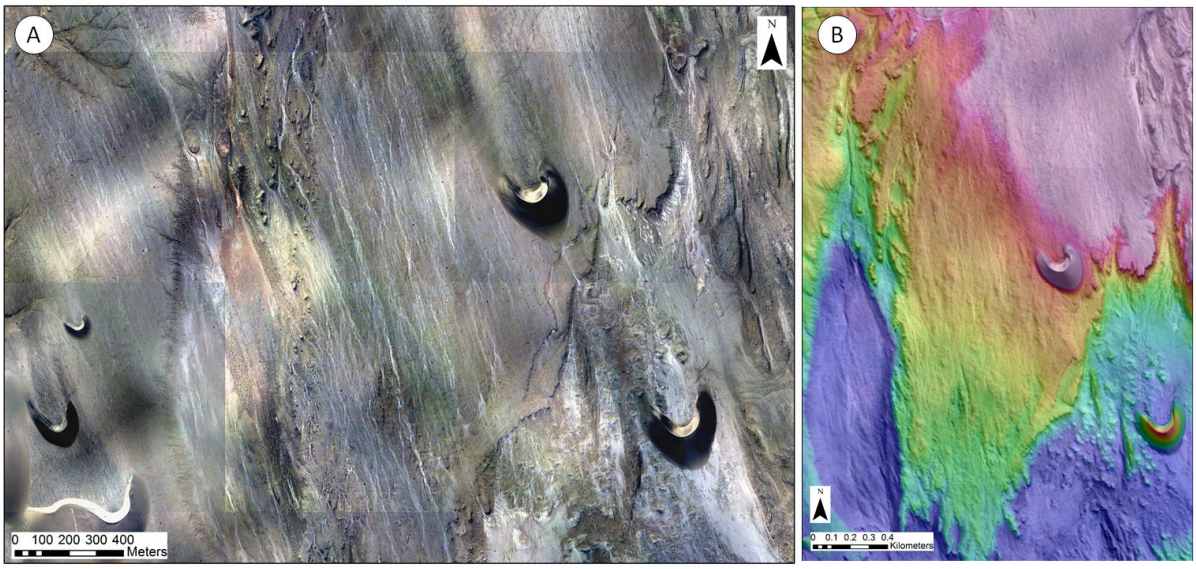

Figure 15. Bedload streaks/ribbons on a planar low relief surface above a forward-facing step produced by topographic inversion of an alluvial sequence. A) Shows the light-coloured streaks of quartz-dominated bedload particles oriented in the prevailing direction of southerly unimodal surface wind. B) Provides a slightly enlarged view of (A) transparently draped onto the high-resolution ALS DEM to show the context of the streaks in relation to the pattern of surface flow-aligned erosional grooves on the surface on which the streaks occur.

Embabi (1999) and Brookes (2001) recognised a cycle of aeolian erosion beginning with surface grooving and ending with the development of widely separated yardangs comprised of playa sediments. Spatially, juvenile surfaces marked by grooving occur downwind of mature surfaces on which erosion has passed through the complete cycle. A similar gradation in maturity is observed in the Namib. The grooved alluvial surface is located downwind of the exposed Precambrian bedrock floor which has been completely stripped of any remnant of the alluvial sequence as topographic inversion has progressed.

Aeolian transport is highly sensitive to subtle changes in surface relief, and this is true for aeolian bedload as well as saltation based on field observations during diamond exploration. Topographic funnelling of aeolian bedload is commonly observed across a spectrum of scales within the erosional landscape of the NAEB. At the macro-scale, endorheic basins display a characteristic distribution of bedforms comprised of coarse-grained bedload particles together with streaks and ribbon features. Windward-facing slopes and ramps as well as forward-facing and backward-facing steps also influence the pattern of bedload transport and deposition at a far smaller-scale (Figs 14 and 15). The topography results from the erosion of Precambrian bedrock as well as of Cenozoic sedimentary sequences and it is strongly influenced by the geological structure.

Encroachment deposits are diagnostic of the high-energy Namib bedload transport (Corbett, 1989, 2016). They are comprised of extremely well-sorted concentrations of bedload (small pebbles and granules) that are easily identified on ALS photo-coverage due to the white, quartz-rich clast assemblage (Figs 14 and 15A). They form almost exclusively upwind of sites marked by forward-facing, positive steps and south-facing risers/ramps from meso- (sub-metre) to macro-scale (tens to hundreds of metres). The largest examples are located towards the top of the south-facing ramps at the northern exits of endorheic basins. In many cases, these were sites of fabulously rich diamond deposits. The encroachment deposits blanket windward-facing slopes with a mono-layer of densely-packed particles which is underlain by a vesicular soil horizon or fine-grained sand. Mature encroachment deposits characteristically display an imbricate fabric. In the Namib, the long-axes of grains are preferentially inclined into the prevailing

southerly wind, producing a stable surface under conditions of unimodal southerly wind flow. During major southerly wind events grains have been observed to vibrate/oscillate on encroachment surfaces. This grain motion is either indicative of reptation (sensu Anderson & Haff, 1988) or it is the effect of turbulent eddies on the surface of the bed. In either case it would appear that grains progressively orientate into position through small movements until they adopt a stable position.

Despite the stabilisation of encroachment surfaces, which probably reduces the rate of bedload transport across them, bedload streaks and ribbons are seen to extend northwards on the surface above the step shown in Fig. 15A. This confirms the continued migration of bedload to the north. Field observations of meso-scale risers and steps together with the ALS data show that migration past an obstacle often occurs through narrow gaps in the topographic barrier. The overall plan geometry of encroachment deposits and the subsequent streaks or ribbons that emanate from them is potentially important for understanding their genesis.

During extreme southerly wind events observations by the author showed that bedload particles migrate laterally in front of steps in areas where sandflux is very low. Individual bedload particles were seen vibrating and/or oscillating in position on the bed prior to jumps or hops sideways along the base of micro- to meso-scale, south-facing dolomite risers. Over time, these infrequent movements lead particles to migrate along barriers until slots or gaps are encountered, whereupon they pass through. They then either become trapped in scour pits in the lee of the barrier (Corbett, 1989) or they continue their migration northwards unabated. Fig. 15A shows meso- to macro-scale examples, with encroachment deposits at the base of successive south-facing steps on the topographic inversion surface. It is important to note that in a number of instances multiple bedload streaks or ribbons feed into an area that is occupied by an encroachment deposit beneath the step, but noticeably fewer streaks or ribbons emerge from it on the bed above the step. The bedload pattern mimics the pattern of flow visualised by Pollard *et al*. (1996) over a forward-facing step. These authors concluded that particles they observed in the experiment emerged concentrated within threads marking pathways between Taylor-Görtler-type vortices. Complex flow patterns were visualised in front of the step, where flow separation occurs. The complex nature of the flow coupled with the likelihood of near-wall vortex generation on the bed in front of the step could account for the development of the imbricate fabric of encroachment deposits described in the Namib.

Brookes (2001) recognised erosional grooves across a wide spectrum of scales from hundreds of metres down to a centimetre scale. Noting that as erosion continues grooves lengthen and deepen brought him to the conclusion that the scale of the erosional features imply the existence of spatially persistent large-scale structure in air flows over long periods of time. He considered two possible explanations which might account for groove initiation and development:

1. The generation of stable horseshoe vortices;
2. Progressive self-organised regularity of erosion by random vortices which become fixed by the evolving surface relief.
3. The third possibility is that Taylor-Görtler-type vortices generated as flow traverses forward-facing steps could account for the pattern of bedload pathways observed.

Mejia-Alvarez *et al.* (2013) also identified the existence of "preferential pathways" created by coherent turbulent structures termed Low-Momentum Regions and High-Momentum Regions which were first recognised in laboratory-scale smooth-wall turbulent flows (Adrian *et al*. 2000; Hutchins & Marusic, 2007a, 2007b). It has subsequently been determined that similar structures tend to scale to outer variables approaching the kilometre scale in the streamwise direction within the ASL (Marusic & Hutchins, 2008; Hutchins *et al.* 2012). The structures form distinctive patterns of alternating streamwise streaks or ribbons which subsequent studies have revealed to be related to the growth and concatenation of hairpin vortex packets (Adrian, 2007; Balakumar & Adrian, 2007). The large meandering structures have also been shown to be responsible for amplitude modulation of smaller coherent structures (Mathis *et al*. 2009), creating localised variation in flow velocity, vorticity and bed shear stress along their paths. Importantly, in relation to the bedload features being discussed here, studies also provide evidence for:

- Vortex organisation in the streamwise direction and different spanwise length scales have been found to vary linearly with distance from the bed (wall) to generate self-similar growth of spanwise structure (Tomkins &

Adrian, 2003). Tomkins & Adrian (2003) found that additional scale growth takes place through the merging of vortex packets on an eddy-by-eddy basis, a mechanism first put forward by (Wark & Nagib, 1991);

- Mejia-Alvarez *et al*. (2013) note that the channelling of turbulent structures continues despite variation in the topography over which the flow passes.

Whilst researchers studying sand streamers have questioned the possibility that long structures such as LMRs and HMRs influence the development of sand streamers of saltating sand grains, observations in the Namib show that bedload transport definitely exhibits features consistent with the notion of preferential pathways. Given that aeolian bedload transport is wholly driven by the impact of saltating sand particles, the organisation of bedload into streaks/ribbons displaying regularity of spanwise spacing leaves no doubt that a link between surface wind flow and bedload transport must exist. By implication, if bedload is organised, then the sandflow must be organised in the same manner as well. The bedload streaks/ribbons described here bear an uncanny resemblance to long coherent structures in turbulent flow. Their pattern suggests that spanwise vortex growth may be influencing the development of progressively better-defined bedload streaks/ ribbons downwind from the forward-facing step.

Dynamic Pavements on the bed beneath ATCs

Dynamic pavement in the context of the NAEB occurs specifically on the floor of endorheic basins and/or on the desert floor beneath the high-energy sandflow that characterises ATCs. The stone pavements are characteristically dominated by an assemblage of resistate minerals which is usually dominated by quartz. The pavements are the product of the collective interaction of weathering and pedogenic processes, aeolian erosion and transport, raindrop impact and ephemeral stream and sheetwash events. For this reason the pavements are usually located at or close to the base-level of the local ephemeral stream networks and on the lower part of south-facing ramps at the northern ends of endorheic basins.

Many of the arid zone diamond deposits mined in the NAEB within the Sperrgebiet were associated with dynamic pavements and features related to streaming bedload occurring upwind and downwind of them.

The diamonds formed part of the mobile granule and small pebble component of the stone pavement clast assemblage. The surfaces display a range of micro-topographic trapsites due to a combination of immobile roughness elements provided by footwall and obstacle clasts (>small pebble to boulder) which influence bedload transport and bedforms that develop in response to bedload migration.

Bedforms comprised of aeolian bedload are a diagnostic feature of high-energy, aeolian dynamic pavement surfaces. The bedforms take a variety of forms. Very low-amplitude (<2.5 cm) ripples with a distinct crest line oriented perpendicular to the prevailing unimodal wind direction are one of the more easily identified. The crests vary in plan shape from straight to arcuate. The low-angle lee face is typically sandy, and often has scattered granule and small pebble clasts on its surface. The ripple wavelength varies from 10 to 20 cm. The windward stoss slope of the ripples are covered with a mono-layer of granules and small pebbles. Depending on the maturity of the surface, packing density can vary but particles on the stoss slope develop an imbricate fabric as packing density increases. On mature, stable surfaces in equilibrium with sandflow driven by the southerly unimodal surface wind, the long axes of particles dip into the oncoming southerly wind.

More subtle bedforms confirming the mobility of bedload granules and small pebbles on the dynamic stone pavements develop in association with pebble clusters forming immobile roughness elements. The clusters create micro-topographic obstacles to the migration of bedload particles streaming across the pavements. As migrating particles become organised on the pavement surface they bank up against the immoveable objects to form micro-scale versions of encroachment deposits. Through time the mobile particles on their surface become organised into stable configurations and they too develop imbricate fabrics.

The presence of the bedforms on dynamic pavements has implications for the genesis of near-wall turbulence in the roughness/ logarithmic layer in response to complex micro-scale topography. Such surfaces probably stimulate the development of a complex suite of vortices, including the formation of hairpin

vortex packets. As the surfaces stabilise, flow in the roughness layer is likely to be comprised of quasi-stable coherent structures including LMRs and HMRs. Micro-scale turbulence generation linked to the distribution of bedforms and immobile roughness elements such as obstacle clasts will have played a key role in determining micro-scale sites in which diamonds would have concentrated. These processes probably account for the economic significance of dynamic stone pavement surfaces flooring endorheic basins such as the Idatal which made the region famous.

Heavy rain, which is a rare occurrence in the hyper-arid NAEB, plays a crucial role in destabilising dynamic pavement surfaces (Corbett, 1989, 2016). Raindrop impact destroys the imbricate fabrics that develop and it also creates erosional pedestals on which larger clasts perch. Once the surface begins to desiccate after rainfall saltating sand particles are able to erode sand from between the clasts on the surface, starting the process of surface reorganisation and stabilisation. The deflation of fine-grained sediment is commonly enhanced by the development of a salt crust. As desiccation progresses and salt crystallises the pressure created causes the sediment to form a veneer of hexagonal sand domes. Once exposed to saltating sand particles the domes are rapidly abraded and destroyed and the fine-grained sediments are transported away from the dynamic pavement. This destabilisation process aids progressive lowering of the surface by deflation of the finer-grained material as described by Cooke (1970) which, in the case of this system, played an important role in increasing the grade of the diamond deposits.

The rainfall destabilisation process also releases the larger pebbles and obstacle clasts which form immobile roughness elements in stable pavement surfaces. Heavy rainfall with large raindrops leads to deep impact erosion of the underlying fine-grained pedogenic layer. If rain occurs over an extended period, smaller pebbles and granules are washed away from their stable positions revealing the vesicular soil horizon. As erosion proceeds the larger clasts in the surface rest on pedestals as much as 2 cm in height as the soil around them is removed by rainsplash. Later, as the surface dries and desiccates the pedestals are abraded by saltating sand particles and the clasts reorganise initiating the development of a new dynamic pavement surface. Some clasts then align in the classic pavement orientation with their long axes perpendicular to the unimodal southerly wind flow through a process of rolling like that described by Bagnold (1941) and Sharp (1964). The smaller, mobile clast population undergoes transport and reorganisation until surface stability is restored. It is during this time that any diamonds incorporated in trapsites on the stable surface are released into the mobile bedload population to migrate northwards, until they come to rest once more in stable micro-scale trapsites on the pavement. However not all diamonds are retained in trapsites. Some become incorporated in streaming bedload migrating through endorheic basins and migrate up the south-facing ramps at their northern end where they often became incorporated into, and concentrated within, aeolian gravel/granule ripples. Although rainfall is highly episodic, these concentrations were commonly eroded by ephemeral streams which carried the diamonds back to the base-level of the system.

In some cases a combination of fluvial and aeolian processes led to remarkably high concentrations of diamonds associated with positive and negative steps from micro- to macro-scale.

Site 4: Sandflow Dynamics and ATC Generation Downwind of Thin, Planar Sand Sheet Repositories

Sandflow migration along the eastern margin of the aeolian erosion basin at Site 4 (Fig. 8a) is dominated by pulses of sandflow. GEE time-lapse reveals the episodic migration of sand streaks/ribbons over much of its length (Fig. 16). Bedforms develop along the margin where sandflow streaks/ribbons interact with topography which modifies flow within the Surface Layer. Where topography forms obstacles to flow, their blocking effect reduces upwind flow velocity and reduces pressure up the windward slope (Wiggs *et al*. 2002). Immediately downwind bedforms evolve rapidly into a mono-train of barchan dunes which can be traced over 10 km downwind.

Whilst point-sources are located at the coast, laterally extensive thin, planar sheet-like sand repositories are distributed within the NAEB throughout its length. The laterally extensive sand sheets appear to occur most frequently where ATCs converge and flow within the Surface Layer is topographically uncon-strained. The sand sheets act as internal sand sources within the system from which sand entrained into saltation can either be incorporated into streaming sandflow or

captured by barchan dunes located downwind (Fig. 16).

A number of possibilities exists to explain the presence of these "in-system" sand repositories, and it is likely that they are the product of a combination of different factors:

1. Their presence where flow is relatively topographically unconstrained may mean that the sand transport capacity of the system is reduced and/or
2. They might be marking sites where widespread sand deposition occurs during high-energy wind reversals which rapidly entrain large quantities of sand from sites that form stable sand repositories under unimodal southerly wind conditions.

GEE time-lapse shows broad sand streaks/ribbons elongating and extending downwind as sandflow streams northwards, steered in some places by the effect of topography on the prevailing unimodal southerly surface wind. Once streams of sandflow form in the lee of topographic highs and migration is triggered they move downwind. Whilst smaller ribbons represent sand leakage traces from barchan horns, the more persistent sand ribbons can be observed migrating several kilometres northwards as discrete pulses of sandflow. Little or no evidence is subsequently seen of sand ribbons regenerating at the same location for the duration of the remaining GEE record. Hence sandflow along pathways appears to be punctuated by periods during which there is minimal flux for periods of several years or more. The migrating linear ribbons of sandflow show minimal evidence of lateral diffusion as they cross the rocky desert floor over time periods of as much as 10 to 15 years. These events provide confirmatory evidence that sandflow transport occurs in discrete pulses through the aeolian erosion basin.

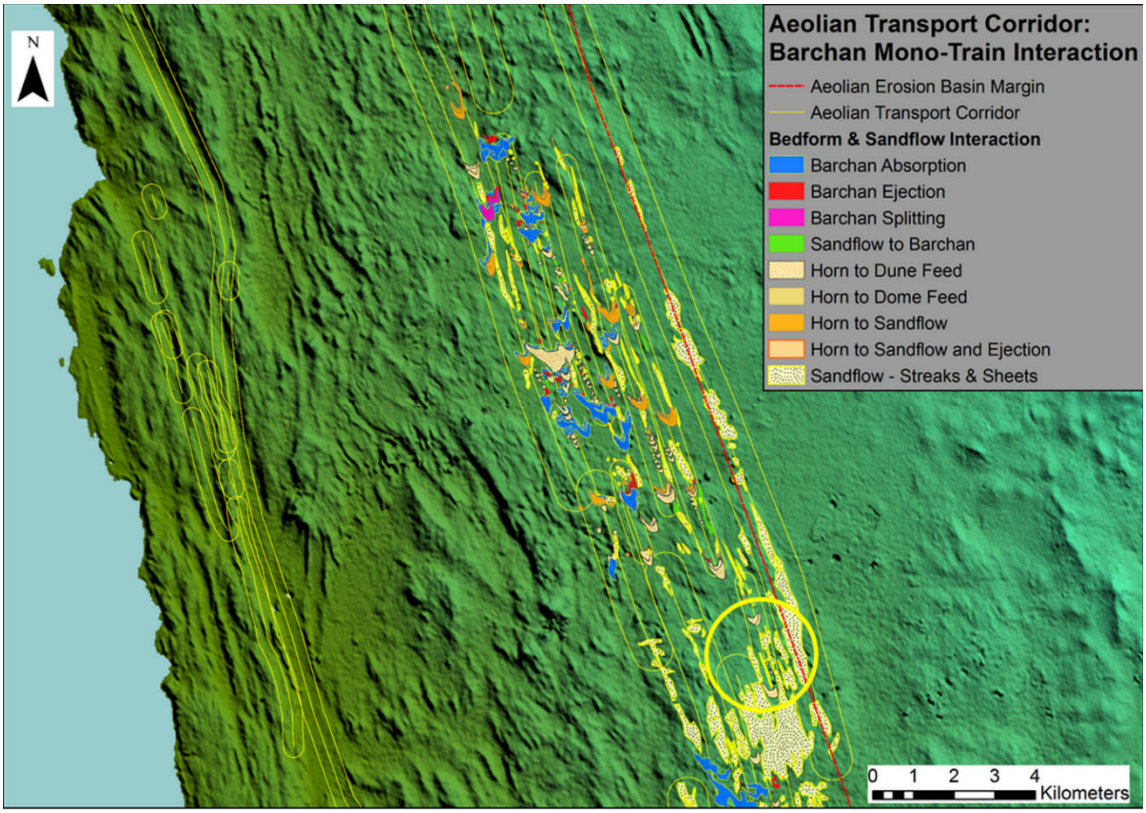

Figure 16. Barchan dune migration pathways developing downwind of a large, planar sand sheet repository north northeast of Bogenfels. A pattern of sand streak/ribbon transport leading to the development of large barchan dunes initiates the development of preferred sandflow pathways. Complex dune-dune interactions, ribbon-dune and dune-ribbon interactions progressively lead to spanwise organisation of the sandflow into a quasi-regular cross-flow spacing. As this reorganisation progresses with distance downwind, the number of preferred pathways declines and ATCs progressively emerge. The barchans in the yellow circle are shown in Fig. 17A. Background DEM JAXA (AW3D30).

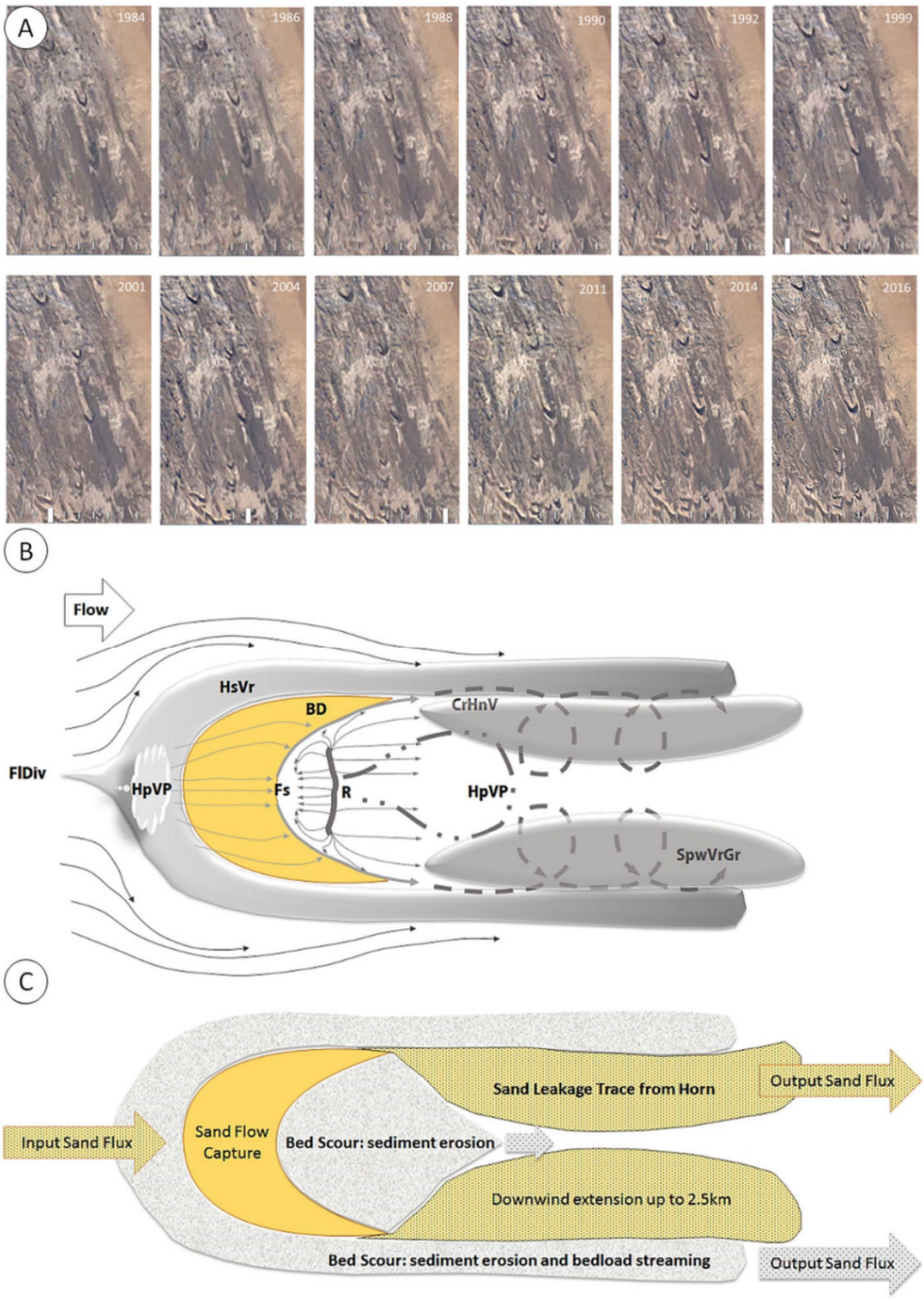

Figure 17. A) GEE Time-lapse series showing a sequence of changes in surface wind and sandflow patterns associated with a large topographically unconstrained barchan dune. Note the pattern of bed scour and sand streak/ribbon development from 2007 onwards. B) Idealised turbulent structure and vortex development associated with a large barchan dune integrating observations from laboratory-scale experiments, numerical models, field and GEE observations. The flow diverges just ahead of the upwind margin of the dune skirt (FlDiv) and a horseshoe vortex (HsVr) is generated. The possibility exists that Hairpin Vortex Packets (HpVP) are generated from the bed in the zone of divergence. In the log-layer flow up and over the dune separates (Fs) forming a recirculating flow which reattaches (R) to the bed downwind of the slipface. Downwind of the dune three coherent structures are potentially generated: An HpVP located down the centre-line of flow and two counter-rotating vortices (CrHnV) are generated from the barchan horns. Spanwise vortex growth (SpVrGr) occurs where the vortices generated from the horns interact with the downwind extensions of the horseshoe vortex arms as well as with the hairpin vortex packets generated in front of the dune's slipface. C) The pattern of bed scour and sand leakage trace deposition for the idealised case shows a characteristic pattern that is observed in natural systems where flow in the ASL is topographically unconstrained. Where dunes migrate through topographically complex terrain, any turbulent structures present in the ASL are largely masked by the complexity of the flow and the interactions of sandflow with the complex terrain forming the bed.

The complex pattern of interactions between sandflow and dune forms strongly suggests that there is spanwise organisation of the mapped migration pathways for bedforms and sandflow downwind of the sand sheet. The spanwise separation of sand streaks/ribbons and pathways of fast barchans show evidence of a regular cross-stream spacing. A separation distance of 550 m to 630 m is apparent for pathways of fast barchans and a larger one of 750 m to 900 m for sand streaks/ribbons. At the downwind limit of the sequence analysed, the separation distance increases to about 1050 m.

The emergent sandflow pattern downwind of a planar sand source suggests that progressive organisation of the sandflow takes place along preferred pathways whose spanwise (cross-flow) separation distance reflects the scale of the dune-forms from which the sandflux emanates with increasing distance downwind of the sand sheet. The migration of large barchan dunes with a width and length of 500 m or more plays a key role in modifying the pattern of flow within the ASL, which stimulates the release of sandflow from the sand sheet repository (Fig. 17). As flow within the ASL interacts with the surface topography dune-dune interactions modify the dune forms through absorption and ejection to produce more complex and larger compound dunes. The lateral separation of the sandflow pathways downwind of these dune forms changes in response to variation in the sandflow associated with them and the separation of the horns from which the output sandflux leaves the dune.

The downwind end of a sand sheet repository is shown at the southern end of the sandflow system mapped in Fig. 16. A large, isolated barchan dune is seen in the time-lapse coverage from 1984 to 2016 to be migrating northwards across the sand repository (Fig. 17). Between 1984 and 1987 several major wind reversals affected the southern Namib aeolian system (Corbett, 1989) creating widespread ferocious, but short-lived sandflow conditions from north to south. During these events the large barchan dunes were observed to reverse. Although the early time-lapse images are of a lower resolution, dune reversal may account for the apparent “smudginess” of some large dune forms, such as the one shown in Fig. 11. From 1987 onwards the dune increased in size as it migrated northwards, becoming better defined. The extension of sand streaks/ribbons at different points downwind of the dune can also be seen in the time series shown in Fig. 17.

From 1990 through to 1992, the bedrock surface along the south western edge of the stoss slope / dune skirt became exposed, either in response to the advance of the dune or erosional scour along the trailing edge. Over the next few years the area downwind of the barchan slipface was swept clear of sand until, in 2004, sand was once again deposited on the northern side of the dune in front of the advancing slipface. The source of this sand cannot be clearly observed, so it is not known whether it is related to wind reversal(s) or not.

From 2007 onwards a scour zone exposing bedrock immediately upwind of the dune skirt reappeared. Sandflow was mobilised through deflation of the sand sheet upwind of the dune. As the barchan continued to migrate northwards the length of the scour zone extended northwards too, as the sand sheet was eroded within a narrow zone along the margin of the barchan. This was incorporated into the sand leakage traces emanating from the left and right horns of the barchan. Subsequently, a series of fast sand domes and protobarchans were ejected from the right horn, and they were absorbed by the barchan some 3 km downwind. As sand leakage continued from the right horn, a linear tract ahead of the horn was scoured clean of sand ahead of the advancing barchan. Over the 9 year period, sand sheet erosion progressively released a large pulse of sediment into the streaming sandflow - either in the form of fast bedforms or as sand streaks/ribbons leaving a narrow, streamwise corridor of bedrock scoured clean of sand in the centre of the sand sheet. This process is responsible for creating the finger-like projections of sand extending from the northern edge of the sand sheet in Fig. 16.

GEE coverage reveals a similar process of erosion and sand entrainment along the southern edge of the sand sheet. As large barchan dunes migrate into the sheet, they form a linear trail marked by bed scour as sediment from the sand sheet is reintroduced into the sandflow system. Whilst the dunes might be regarded as being “isolated” in terms of the influence of turbulent wake generation due to their wide spacing, dune-dune interactions continue to occur between successive dunes through streaming/ribbons of sandflow and/or chains of fast barchans over distances exceeding 4 km in the downwind direction.

Changes in the patterns of bed scour and sandflow deposition associated with the barchan provide some key insights into the dynamics of the sandflow system where the sand source is no longer restricted to a point

source. The time series also shows how the growth of large barchan dunes can affect the pattern of flow in the ASL leading to sand entrainment within a narrow zone around the dune skirt and downwind of the advancing horns.

Fig. 17B is a conceptualisation of the flow structure associated with large, topographically unconstrained barchan dunes. The depth of the Planetary Boundary Layer generally varies between 1 km to 3 km, and within this, the Atmospheric Surface Layer can be between 60 m to 300 m deep. The impact that surface roughness has on flow within the ASL is influenced both by the height and the breadth of the body (Kaimal & Finnigan, 1994). At the scale of large barchan dunes 35 m to 40 m in height with a width of 550 m to 600 m and a length of 500 m or more in the Namib system, an isolated barchan on a planar sand bed represents a significant axisymmetric topographic obstacle to flow within the ASL.

The presence of the barchan dune in Fig. 17A triggers a variety of different flow responses over the 32 year GEE record. The observed pattern of bed scour immediately upwind of the barchan dune skirt and its progression around the windward base of the dune and subsequently downwind of the horns is particularly interesting because it closely resembles the pattern of bed scour produced by coherent structures in turbulent boundary layer flow around obstacles (Paik *et al*. 2007), called horseshoe vortices. Horseshoe vortex structures have been shown to play a key role in the formation of erosional features in glacial and aeolian environments by Shaw (1994, 1996).

Their role in creating strikingly lineated aeolian erosion landscapes sculpted in playa lake sediments has been examined in detail by Embabi (1999) and Brookes (2001) in south-central Egypt. The development of horseshoe vortices and their role in the formation of dunes in the lee of obstacles is well established (e.g. Tsoar, 2001), but their association with barchan dunes has not previously been documented to the best of the author's knowledge. This possibly relates to scale, since many barchan field studies focus on comparatively small barchan dunes. In the case of large, 30 m to 35 m high barchan dunes it is possible that the flow structure resembles the pattern modelled by Hunt *et al*. (1978) for stratified turbulent flow past a low axisymmetric hill for low Froude numbers. These authors demonstrated that under these conditions a return flow can be generated on the upwind centre-line of obstacles to flow which tend to a zero gradient. The resulting vortex takes the form of a horseshoe. The vortex structure which forms around the base of the axisymmetric hill, is similar to modelled turbulent flow around a surface mounted cube (Hussein & Martinuzzi, 1996; Martinuzzi & Tropea, 1993). The formation of a horseshoe vortex structure is conceptually applied to explain the observed pattern of scour and deposition associated with the large barchan shown in Fig. 17b. The strength and continuity of the horseshoe vortex varies with the Froude Number. Although Michelsen *et al*. (2015) pointed out that the analytical model for low hills is not valid for barchan dunes due to the presence of a flow separation bubble, the genesis of a horseshoe vortex would potentially explain the observed pattern of bedload transport around the skirt of large barchan dunes within ATCs.

The presence of horseshoe vortices may explain why sand leakage traces are better-developed for some barchan dunes than others. Where horseshoe vortices are sustained for some distance downwind, bed scour may predominate, facilitating the rapid removal of leakage trace sand. Where the vortices are absent or they dissipate rapidly downwind, the deposition of sand leakage traces may prevail.

Such a flow pattern may not be readily visible unless the substrate over which the barchan is migrating aids its recognition. This was the case for the dune shown in Fig. 17a, where the progressive and sustained erosion of the surrounding sand sheet made the flow pattern visible. In other instances within the Namib system, bedload transport in association with the barchan dunes may be the best way to identify the flow pattern as this is readily mapped with the ALS dataset. At a laboratory-scale and in the case of CFD models the region modelled shown in publicaions has often been clipped so tightly that the flow pattern upwind of the stoss slope and downstream of the horns and the area of flow separation has not been shown sufficiently completely. This has now been improved upin by Bristow *et al*. (2018, fig. 4). In other instances Particle Image Velocimetry studies of flow over an isolated barchan dune (e.g. Palmer *et al*. 2012) provide a 2D perspective of flow patterns along the streamwise centre-line flow only. It has also been shown by Michelsen *et al*. (2015) that this approach underpredicts the wind velocity over dunes. The conclusion of Palmer *et al*. (2012) that flow upstream of their isolated dune model consists of spanwise vortices adjacent to strong

Low-Momentum Regions associated with the incoming turbulent boundary layer provides an interesting context with which to look at the example in the Namib.

Bagnold (1941) observed that the output sand flux primarily emanates from the horns of barchan dunes. Downwind of the horns, the output sand flux has been shown nearly to approach the carrying capacity of the wind (Sauermann *et al*. 2000). However, relatively little research has sought to determine the pattern of sandflow within the leakage trace downwind of barchan dunes horns.

Knott (1979) presented one of the earliest attempts to predict the pattern of flow generated from barchan horns. He hypothesised a pattern of counter-rotating helical vortices directed inwards at the bed. The conceptualised flow pattern from the horns of the barchan in Fig. 17b and the flow lines associated with flow separation and reattachment are from the study of flow across a barchan by Omidyeganeh *et al*. (2013). Collectively, the proposed pattern of turbulent structures and vortices combine to produce the pattern of bed scour and sediment deposition shown in Fig. 17c. Based on observations made using Google Earth, this pattern appears to develop only when flow arriving at barchan dunes is topographically unconstrained and dunes are outside the influence of turbulent wakes generated by upwind dunes. The pattern of scour and the plan form of the sand leakage traces on the bed in particular, which are characteristically observed under these conditions (Fig. 13c) probably provides evidence of the spanwise growth of vortex structures. This appears to take place when the arms of a horseshoe vortex emanating from the upstream skirt of the dune and vortices extending downwind from the horns of the dune encounter coherent hairpin vortex packets generated downwind of the dune slip face. The geometry of the sand leakage trace produced closely resembles the structures shown by Adrian *et al*. (2001) arising from the interaction of adjacent hairpin vortex packets and is consistent with modelled flow for an isolated 3-D barchan dune (Bristow *et al*. 2018).

Another locality within site 4 provides more insight into the interaction of sandflow and dune forms downwind of planar sheet sand sources. To the east of the Baker's Bay ATC, isolated barchan dunes mark the convergence of a number of ATCs. Time-lapse video shows episodic ejections of fast sand mounds, sand domes and protobarchans from the horns of some of these large, slow-moving dunes. The ejected bedforms are short-lived because as they evolve into a barchanoid form sand leaks rapidly from the embryonic horns. The sand is resorbed into sandflow streaming north along the floor of the ATC in which the bedforms are located. Some embryonic dune forms develop and disappear over migration distances of a few hundred metres downwind. The relatively rapid changes in bedform-sandflow dynamics may be evidence of localised topographic steering and/or acceleration of surface wind flow lines due to the topography.

Further downwind of planar sand repositories barchan dunes reform, but they do not develop into mono-trains. Instead, they evolve into V-shaped fields of barchan dunes resembling the sites elsewhere within the system where the sandflux is sufficient to sustain the development of barchan corridors regulated by barchan dune interactions.

This change in bedform propagation appears to be influenced by topographic steering of surface wind flow. There is a tendency for sand deposition and the genesis of bedforms to occur where surface wind flow is either funnelled by topography or turbulent eddies are generated in the lee of topographic highs leading to deposition and bedform evolution.

Downwind within the Baker's Bay ATC sand deposition in the lee of a topographic high caused the development of an extensive sand sheet comprised of large coalesced barchanoid sheets and sand mounds. GEE time-lapse shows that over a period of 20 years slip faces formed and the entire sand body began to migrate northwards. The western sand body reverted to a slip-faceless mound/protobarchan whilst the other two mounds maintained a barchan form. These split as the smaller of the two migrated away from the larger, slower dune. Time-lapse video shows the sand mound / protobarchan and other localised sand sheets reorganising into "parabolic sand fronts" with no visible slipface. The scale of these bedforms varies, but the trailing arms can exceed a kilometre in length and the width of separation can vary from about 200 m to 500 m. A complete cycle of growth and decay could not be observed over the 32 year period, but the parabolic forms are seen to become progressively better defined as the front migrated northwards. Eventually, a burst of sandflow was ejected from one of the bedforms resulting in its instability leading to erosion and the dispersion of sandflux whereas uneroded mounds retained their parabolic form. The author has not observed these bedforms in the

field, but they appear to play a similar role to barchans, capturing sandflow as they grow and ultimately releasing sand back into the system as they erode and disperse. Coalesced examples display a chevron-like geometry, and the absence of a slipface suggests they might be best classified as zibar dunes, rather than parabolic dunes.

Within the V-shaped fields of coalesced barchans, the dunes are observed to increase in size downwind over a distance of about 4 km. A complex series of absorptions, coalescence and splitting interactions occur as the dunes migrate and fast protobarchans and barchans are ejected from the horns of the larger barchans that develop. Sand leakage traces also extend northwards from barchan horns, and the sandflow is either captured by a downwind barchan or it is resorbed into the active sandflow. Fast barchans shed from the horns of barchans furthest downwind are also rapidly resorbed into the active sandflow, vanishing from view as rapidly migrating sand streaks/ribbons.

Convergence of ATCs and the deposition of laterally extensive, planar sand sources within the sandflow system is seen to have a marked and lasting influence on sandflow dynamics downwind of them. Typically, size selection/ regulation through dune interactions occurs within barchan corridors (e.g. Hersen *et al.* 2004; Hersen & Douady, 2005; Durán *et al.* 2009). The fields of dunes selected for these studies display size uniformity, and perhaps importantly, the published examples are located in areas in which surface wind flow is topographically unconstrained. The 32 year GEE time series is still too short to observe a full cycle of dune genesis and decay at this point in the Namib system. However, it is clear that as complex topography is re-encountered downwind, localised steering of the surface wind flow probably causes variations in the sandflux carrying capacity of the wind flow. Larger dunes are seen to become unstable and reform into fast-moving smaller dune forms which are progressively eroded and the sand from them is resorbed back into streaming sandflow.

The resolution of the time-lapse does not allow the pattern of sandflow through the yardang fields south of the Grillental to be identified in detail, but it appears to reorganise downwind of sand sheet repositories. GEE coverage shows sandflow migrating through the basin to the north of the sand sheets and the progressive development of narrow linear sandflow corridors. Four evenly-spaced ATCs lead into the Grillental Valley (Site 5 in Fig. 4a). The sandflow dynamics of Site 5 are described in the next section.

Site 5: Sandflow Dynamics Associated with Depressions and East-West Oriented Valleys

The rugged nature of the aeolian erosion landscape in the NAEB virtually prohibits the existence of topographically unconstrained surface wind flow over any distance, making changes in surface roughness due to topography a key variable with potential to influence sandflow.

Downwind of the planar sand sources within the eastern half of the aeolian erosion basin topographic steering of wind flow in the Surface Layer along the south-north oriented endorheic basins effectively re-establishes point sand sources as sandflow emerges along the southern margin of the Grillental Valley. The valley is a site of active topographic inversion, with the result that a stacked sequence of Miocene fluvial and alluvial sediments forms an elevated plain. The upper unit consisting of coarse alluvial gravels is being attacked by aeolian abrasion as sandflow streams across the valley floor leading to the development of immature yardangs (see yellow arrow in Fig. 18) along the leading edge of a forward-facing step along which small-scale horseshoe vortices are generated, facilitating erosion.

Four ATCs cross the eastern half of the Grillental. They are sustained by sandflux from four point sources along the southern margin of the depression which are characterised by the rapid emergence and migration of fast sand domes, protobarchans and barchans. The process of dune formation is aided by the passage of sandflow over negative steps as flow descends into the trough and/or by turbulent eddies in the wake of positive topographic obstacles to flow. As the barchan dunes descend downslope they grow rapidly as sandflow is captured, into trains of large barchans (Fig. 18).

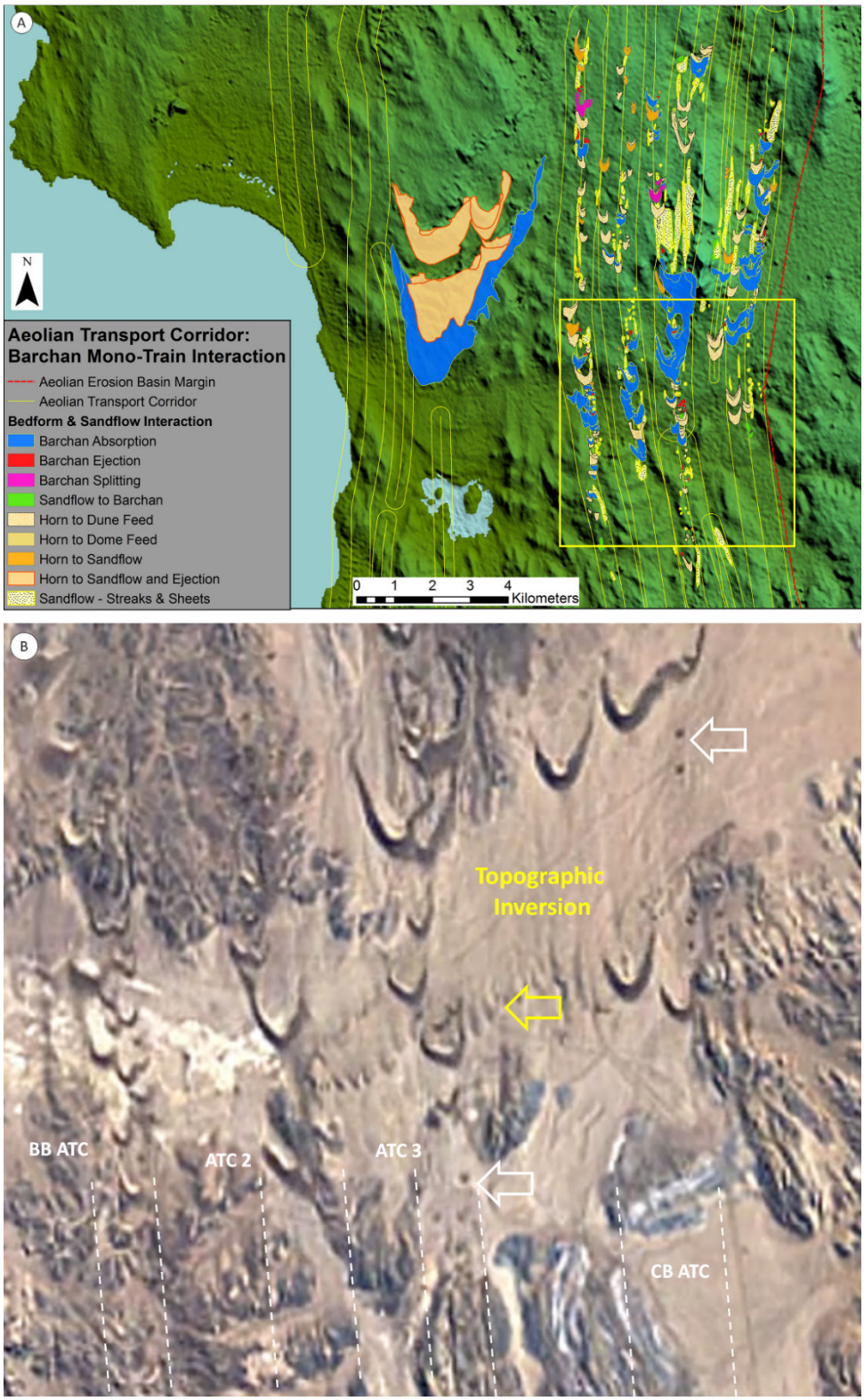

Figure 18. A) Four active ATCs enter and cross the Grillental which forms a trough perpendicular to surface wind flow. To their left, the large barchanoid draa forming the southern limit of the modern Namib Sand Sea has migrated approximately 200 to 300 m north since GEE coverage began in 1984. GEE coverage for 2013 shows the streaming of fast sand domes, protobarchans (white arrows) and barchans within 3 of the 4 ATCs. Background DEM JAXA (AW3D30). B) Two of the most persistent ATCs which begin in Chameis Bay (CB ATC) and Baker's Bay (BB ATC) border two newly developed ATCs which formed downwind of the sand sheet repositories which occur to the south of the Grillental. The high-energy sandflow through the Grillental is actively eroding the forward-facing step formed through topographic inversion due to the presence of the coarse gravel Miocene Gemsboktal Gravels. Note the embryonic development of yardangs along the windward-facing edge (yellow arrow) to form a pattern which confirms the genesis of horseshoe vortices, which control the pattern of aeolian erosion.

These slow-moving dunes absorb the smaller, faster moving protobarchans and barchans which leads to a continuous process of ejection from the horns of barchans crossing the valley floor. Absorption is also the dominant dune-dune interaction process on the northern flank of the valley where large compound barchan dunes migrate slowly up the south-facing slope. The significant role played by changes in surface topography with respect to barchan formation and migration is consistent with observations by Wiggs *et al*. (2002), Bourke & Goudie (2009) and Palmer (2010).

The pattern described above closely resembles the conceptual model of Wiggs *et al*. (2002) predicting the pattern of erosion and deposition that should result when sandflow is driven across valleys by wind flow oriented perpendicular to the valley axis. As the dunes approach the crest of the slope, streamline compression results in accelerated wind flow. Wiggs *et al*. (2002) predict that the sandflux carrying capacity increases rapidly, and the accelerated wind flow overshoots valley flanks as it ascends, reaching a maximum at the downwind valley edge. Along the northern margin of the Grillental, this effect causes a rapid switch from large compound dunes to small fast-moving dunes and sand streaming north in extended streaks/ribbons. As dune size diminishes and the migration rate increases, there is a marked change in the style of dune-dune interaction, which is characterised by splitting and the ejection of faster-moving small bedforms.

GEE time-lapse reveals that from 2007 onwards sand leakage traces extended from barchan horns as they ascended the south-facing slope and migrated either side of a north-south oriented hill named Zweikuppenberg, which rises approximately 90 m above the plateau on either side. The sand leakage traces attain maximum streamwise lengths of 2 km but very little evidence of lateral dispersion of sandflow is seen at their distal ends. From 2014 onwards sand is seen to be actively resorbed into streaming sandflow from the leakage traces, which progressively diminished in length. The sand leakage traces from the horns of the lead barchan dunes in the ATCs are also resorbed downwind into the streaming sandflow.

Wiggs *et al*. (2002) concluded that where approaching winds are perpendicular to a valley axis, the depression can act as a depositional sump for aeolian sediment. The strong influence that the Grillental exerts on flow in the Surface Layer of the southern Namib system is confirmed by the spatial pattern of barchan interaction presented by this study, which reveals that absorption, leading to the growth of very large barchan dunes is dominant within the depression. The location of the large barchanoid draa marking the start of the accumulation zone for the Namib Sand Sea on the 80 m high ramp forming the south-facing flank of the Grillental valley is therefore no coincidence. It marks the beginning of the transition from erosion and sandflow to sand accumulation.

The Transition from Sand Erosion to Sand Accumulation

The southern maxima of the BLLCJ swings onshore and pans the entire transition zone (see Figs 2, 5) and it therefore must exert a strong influence on the architecture of the accumulation zone. Unfortunately, at this point in time the effect that the complex coastal geometry between Prinzenbucht and Hottentots Bay to the north of Lüderitz has on the hydraulic behaviour of flow at this scale within the BLLCJ is unknown.

It is tempting to speculate that the combined effect of the blocking topography bounding the western and northern end of Elisabeth Bay and the marked coastline concavity could result in the formation of a series of small, rapidly changing hydraulic jumps and expansion fans. Such a configuration would cause abrupt increases and decreases in the MBL height which would translate into abrupt acceleration and deceleration of surface wind flow. This could potentially explain the location of the transition zone.

The transitional zone lies well within the section of coast that is influenced by the main expansion fan which effectively fixes the location of the NAEB. Changes in surface wind speed related to this fan as it flows northwards may well influence the location of the accumulation zone which contains the Namib Sand Sea. At the very least, the location of the blocking topography on the north western side of Elisabeth Bay probably deflects the BLLCJ flow to form a gentle arc of accelerated flow, which seems to follow the likely form of the wind speed contours which delineate the eastern edge of the southern BLLCJ maxima.

The exact location of the transition from sand erosion to accumulation is located immediately inland of Elisabeth Bay which has been, and continues to be mined for diamonds. The coastline leading into Elisabeth Bay is one of the main feeders for sand entering the aeolian system. It is a challenging high-energy aeolian environment for both man and machine. Conditions of high sandflux drive aeolian bedload transport, producing distinctive patterns of diamond dispersal and concentration which illustrate the remarkably subtle capability of wind to segregate and concentrate diamonds - a fact that was exploited during early mining operations to segregate sand from bedload.

Understanding the long-term dynamics of the transitional zone, and the south-western active plinth of the Namib Sand Sea in particular, is relevant to diamond exploration because this is the terminus for diamonds transported as aeolian bedload through the system. Consequently the area was mined extensively by the early operators using small, sophisticated bucket-wheel excavators. An understanding of how the system responds to changes in the boundary conditions of the system is therefore important from an economic perspective.

The barchan corridors that develop along the coast from Prinzenbucht northwards migrate around the eastern margin of Elisabeth Bay which is flanked by a topographic high.

This stretch of coastline provides a rare linear sand source from which sufficient sand flux is generated to create and maintain a number of corridors of barchan, barchanoid ridges and transverse dunes. Variation in the nature of the barchan corridors probably mainly reflects local changes in the sandflux but it is also influenced by the nature of the bed on which the dunes form and migrate. Barchan corridors are situated on firm, dry substrates provided by stone pavement and/or exposed Precambrian bedrock which do not have a high water table. As described in the previous section, the barchanoid draas marking the start of the sand accumulation zone are located on the south-dipping northern flank of the Grillental.

Barchanoid ridges and transverse dunes develop preferentially to the north of Prinzenbucht, where pan sediments are periodically flooded and the water-table is virtually at the surface. The scale of the corridors increases northwards and barchan dunes are superseded downwind by linear corridors of barchanoid ridges and large transverse ridges. Corridors of fast barchans migrate rapidly away from the downwind leading edge of these larger dune forms as the sandflow speeds across the last depositional gap before the plinth of the main Namib Sand Sea is encountered (Fig. 19).

The main accumulation zone begins abruptly on the northern flank of the Grillental with the development of a series of barchanoid draas which were described in the previous section. These are separated from the next accumulation zone downwind by a depositional gap separating the draa from the megabarchan dunes downwind of it which progressively decrease in size to the north. A return to accumulation is marked by the presence of larger-scale corridors characterised by the formation of barchanoid ridge and/or transverse dune forms which ascend the south-facing ramp (Fig. 20) on the northern side of the Grillental. This linear, tongue-shaped depositional tract is 5 km to 6 km wide and 26 km long. As the crest of the ramp is approached barchan dunes are ejected from the advancing front of the dune corridor marking the start of a second depositional gap through which the road to Lüderitz passes. Sandflow streaks and ribbons of sand stream northwards across the crest and down the north-facing ramp into the depression in which the main body of the Namib Sand Sea extends north.

Observation of the GEE time-lapse reveals numerous sandflow transmission pathways, starting with the horns of the first barchanoid draa. Ribbons/streaks of sandflow, fast sand domes, protobarchans and fast barchans stream from each horn in narrow corridors. The sandflow generated along the coast between Prinzenbucht and Elisabeth Bay merge with the output sandflux from the western horn of the first barchanoid draa to form a linear plinth which extends along the western margin of the accumulation zone. The plinth resembles the form of a large linear backshore foredune, but in this case it is largely unvegetated. Mapping of surface air flow using sand streaks, aeolian current shadows in the lee of vegetation and dune slip face azimuths shows that surface flow is deflected in a similar way to that described by Hesp *et al.* (2015). The sandflow is consequently deflected up the west-facing slope of the plinth to be incorporated into the accumulation zone where it is captured by barchanoid dunes and transverse dune ridges (Fig. 21).

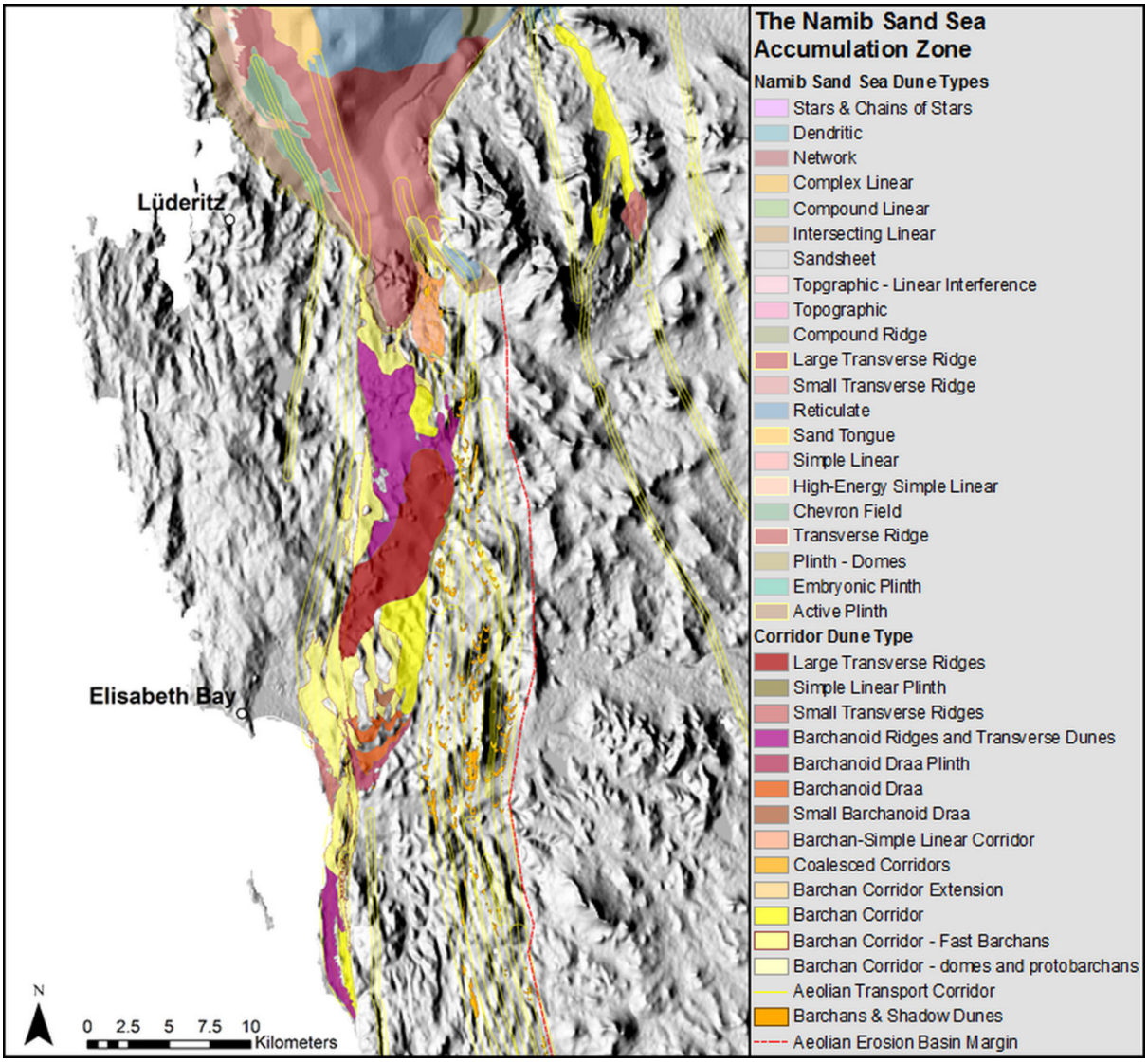

Figure 19. The transition zone from erosion and sandflow to sand accumulation at the southern end of the Namib Sand Sea. The change from point to linear sand sources along the coast from Prinzenbucht northwards supplies sufficient sandflux to maintain barchan dune corridors. Note the large barchanoid draa on the northern margin of the Grillental (see also Fig. 18) which marks the first significant switch to sand accumulation. The mono-trains of barchans within ATCs bypass well to the east of the draa before merging along the eastern flank.

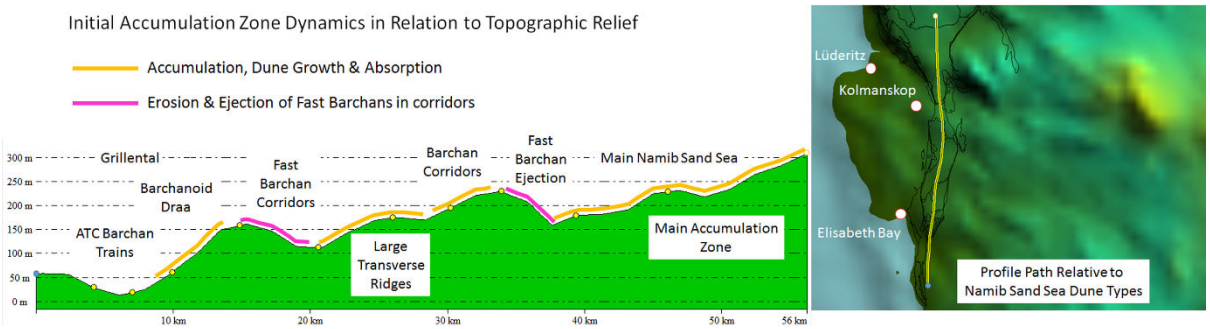

Figure 20. Longitudinal profile from the southern flank of the Grillental north into the main accumulation zone of the Namib Sand Sea showing the relationship between the topographic slope and zones of sand accumulation leading in to the main Namib Sand Sea where the main zone of accumulation begins.

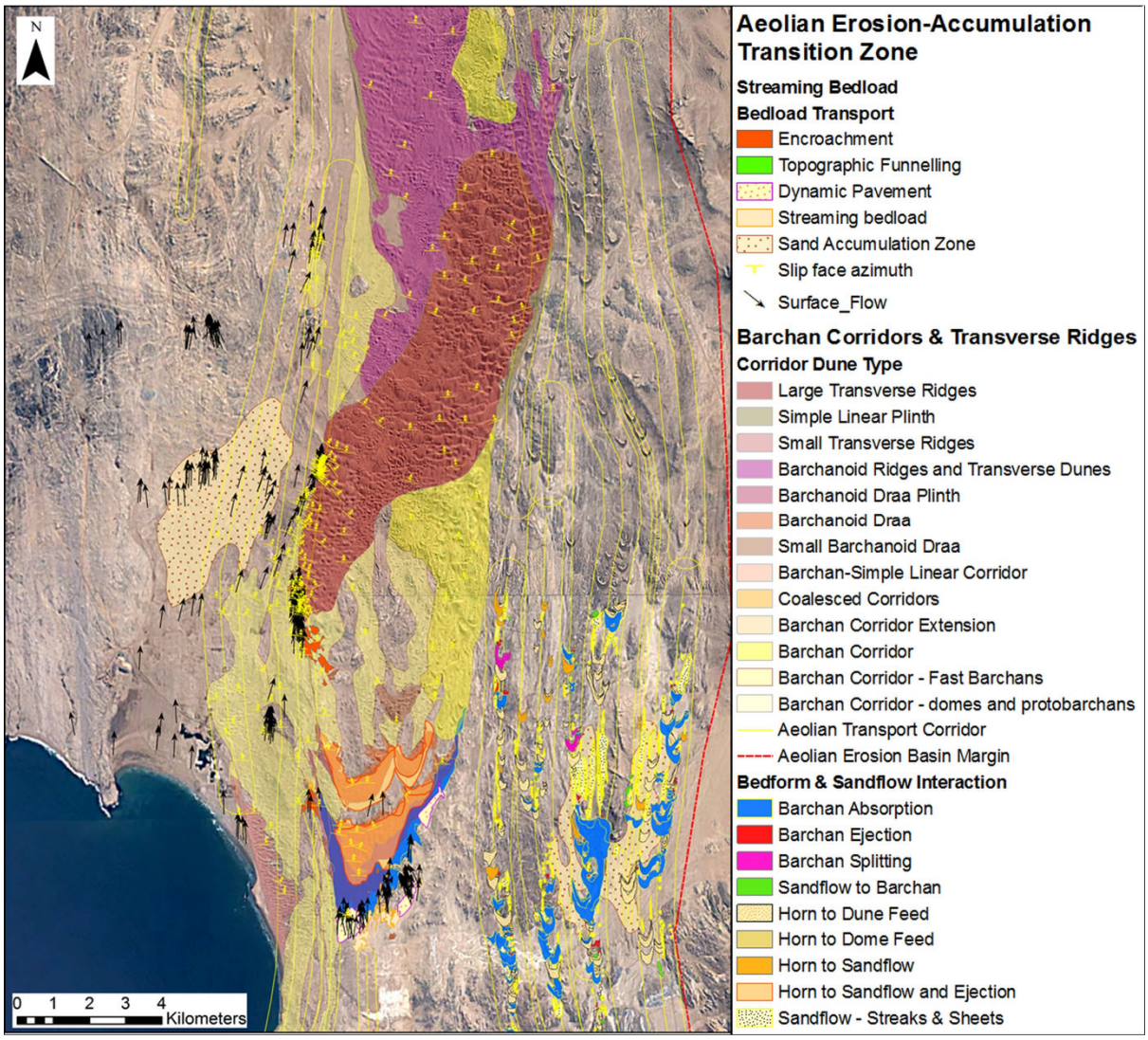

Figure 21. Surface wind flow within the transition zone from erosion and sandflow to sand accumulation. Note the steering of flow on the eastern side of Elisabeth Bay as it swings north-east before encountering the plinth along the western margin of the initial accumulation zone. This may be due to the combined effect of topography and the presence of the northern BLLCJ maxima which encroaches onshore at this point based on maps by Patricola & Chang (2016). Topographic steering of ATCs on the eastern side of the accumulation zone is also evident as the mono-trains of barchan dunes swing into towards its eastern margin. Background image Google Earth Engine.

As can be seen in Fig. 20, the depositional gaps are located immediately downwind of the crests of topographic highs along the riser leading out of the Grillental depression. A pattern consistent with the conceptual model of Wiggs *et al*. (2002) which is described in the previous section on Site 4 in the Grillental. However, in this transition zone the barchanoid draa is itself a major element of the local topographic relief. The stoss slope rises over 60 m from the skirt on the northern flank of the Grillental and the crest attains an elevation of 112 m. The length of the stoss slope to the crest is 2.4 km and the breadth of the draa at the tip of its horns is 4.13 km. The separation distance between the draa and first megabarchan is 1.4 km which increases to 1.7 km between successive megabarchans.

Wilson (1972) first suggested that transverse vortices might influence the development of large barchanoid ergs and draas. Andreotti *et al*. (2009) have shown that the development of giant dunes such as barchanoid draa and ergs begins with the superimposition of smaller dune forms and their progressive merging. The size of the draa and megabarchans at the start of the transition zone in the southern Namib places them well within the length-scale of the "giant" dunes as defined by Andreotti *et al*. (2009). Their presence in this coastal location provides some insight into their effect on the MBL and the overlying capping inversion above it. We

now know, based on the study by Patricola & Chang (2016) that the MBL spans the coastline where this transition from erosion to accumulation takes place. The base of the capping inversion above the MBL is no more than 200 m, which means that the BLLCJ may be extremely thin at this point. This potentially means that flow within the BLLCJ accelerates dramatically up the ramp, further enhancing the development of a depositional gap as the crest of the ramp is approached.

Andreotti *et al*. (2009) showed that the height of giant dunes is maximised when their wavelength is comparable to the average depth of the PBL. The giant dunes such as the draa under discussion confine BLLCJ flow to a very thin layer between the dune crest and the base of the overlying capping inversion. Based on the rule of thumb of these authors, waves generated on the interface between the MBL and the stable layer above the capping inversion should have the same wavelength as that of the dunes on the bed below. The waves create perturbations which then impinge on the bed and these control the emergent pattern of dunes and localised areas of increased bed shear stress where bed scour results in depositional gaps. These authors estimate the height of the inversion layer to be about 300 m in coastal deserts such as the Namib based on their measurement of giant dunes. The MBL over the Namib is significantly thinner, and depending on the hydraulic effect that the topography north of Elisabeth Bay exerts it could be far less than 200 m.

The acceleration of BLLCJ flow up the ramp towards the main body of the Namib Sand Sea might also account for the formation of a plume-like extension of a sand tongue northwards of the transverse ridges at the southern end of the main accumulation zone for approximately 32 km along the likely flow path of the BLLCJ (Fig. 19). This sand tongue is bounded by reticulate dunes along its eastern margin which may bear testimony to the complex pattern of surface wind that might be expected to occur within the transitional zone where the MBL and TIBL theoretically meet.

Discussion

The recent recognition of the BLLCJ underpins the importance of contextualising large-scale aeolian systems in relation to the structure of meso-scale circulation patterns in order to understand aeolian system dynamics. This paper shows that in Namibia, BLLCJ flow plays a key role in determining both the architecture and dynamics of the NAS within a narrow coastal tract along the length of the continental margin.

Detailed research on the California LLCJ has shown that coastal geometry controls the nature of the hydraulic behaviour of flow within these features. While both the strength and direction of flow in the case of California vary, the BLLCJ flow remains directionally constant, the loci of surface wind maxima it generates do vary seasonally.

In the case of the southern maxima Patricola & Chang (2016) have shown that a large expansion jet (in which 12 ms^{-1} surface winds are recorded) sits directly offshore of the NAEB and the NSS. The expansion fan develops in approximately the same location during both strong southern DJF (December-January-February) and northern JJA (June-July-August) maxima events. The presence of the topographically fixed expansion fan provides an explanation for the empirical observation that the energy of the southerly wind regime in the NAEB rises northwards from Chameis to peak in the vicinity of Pomona before declining towards Lüderitz. A transitional zone between the MBL and the diurnally developed TIBL of the PBL runs down the inland margin of the tract influenced by the BLLCJ.

The BLLCJ flow has been shown to occur within a thin MBL capped by a strong inversion capping layer. The architecture of the northern Namibian dunefields provides evidence for the effect of frictional bending of flow associated with the jet so that sandflow direction changes from coast-parallel to swing broadly north-north-easterly, as reflected in the pattern of aeolian dunes. To the south, the larger-scale NSS also shows some evidence of a similar change in sandflow direction from coast-parallel to north-easterly based on previously published data from the northern end of the NSS in the Central Namib.

Corbett (1989, 1993) estimated the wavelength of the counter-rotating vortices in the PBL to be between 500 m to 1 km, with mono-trains of barchan dunes migrating along pathways where the counter-rotating flows converge on the bed (wall) along paths aligned with the mean flow direction. This study has demonstrated that within aeolian systems such as the Namib, there is potential to generate a range of vortices, some of which are helical

counter-rotating vortices, and these occur across a wide spectrum of scale. The vortices also do not need to be generated by a single process or situation, but develop under a variety of circumstances and these are reflected in the pattern of erosion and deposition they generate.

Within the NAS the BLLCJ strongly influences sandflow dynamics. Due to the scale of the expansion jet lying offshore of the NAEB, this is especially so. It is, as yet unknown, whether flow within the jet varies from being subcritical to supercritical in nature. However, it appears to be possible that more localised development of hydraulic expansion fans and jumps could be present along the coast. The presence of a large, topographically fixed hydraulic expansion fan and the possibility that smaller fans and jumps might exist has the potential to create a complex surface wind flow pattern driven by variation in hydraulic behaviour of the flow. At a meso-scale the MBL along the entire NAEB into the southern end of the NSS has been measured to be a maximum of 200 m thick. The MBL could thus be significantly thinner in places, creating very thin, fast surficial wind flow. Detailed studies of other low-level jet flows have shown that linear counter-rotating helical vortices commonly form. The BLLCJ may therefore create ideal conditions for the development of similar vortex structures within the jet as flow crosses the temperature gradient at the ocean-land boundary.

Within the NAEB, detailed mapping of dune-dune interactions reveal that they play an important role in sandflow dynamics along ATCs which has not previously been recognised. The specific pattern of interactions which occurs reflect localised blocking effects of topography which lead to acceleration and deceleration of surface wind flow, resulting in changes in sandflow capacity. Evidence of topographic steering of flow within the BLLCJ is also found. The transition from erosion to sand accumulation is characterised by the development of very large barchan draas (termed megadunes by Andreotti *et al*. 2009), which provide evidence for the formation of transverse waves which influence the spacing of depositional gaps between the dune forms. The possibility exists that a hydraulic jump may also influence the location of the main accumulation zone of the Namib Sand Sea.

Localised steering of the thin BLLCJ by the complex NAEB topography results in linear, topographically bounded flow paths leading inland from the coast, which are reflected in the sandflow patterns described in detail in this paper. It is suggested that long linear ribbons of sandflow stretching kilometres downwind could indicate that steering is complemented by some vortex development, further constraining sandflow.

The presence of forward-facing topographic steps oriented across the unimodal BLLCJ flow produces long turbulent structures consisting of counter-rotating vortices. Their distribution is shown to control the formation of narrow, linear sandflow pathways which extend downwind for considerable distances across planar surfaces such as those formed by alluvial fan sequences cemented by calcareous crusts.

These sandflow pathways lead to the erosion of linear aeolian grooves. Their presence also enhances the development of coarse-grained aeolian bedload streaks which mark the location of the vortices. The spacing of the streaks on laterally extensive planar surfaces suggest that a regular spacing develops through time. Spanwise vortex growth as vortices merge may lead to streaks developing at different scales. The larger streaks can be traced over 1.5 km in a downwind direction.

In places within the NAEB and to the south of the Cunene Dunefield on the Skeleton Coast the development of macro-erosional grooves has led to the formation of large fields of aeolian lineations (termed mega-yardangs by Goudie, 2007) cut into the hard bedrock floor. Although the spatial stability of counter-rotating helical vortices has been questioned in the past, this study has shown that both hydraulic and coherent turbulent flow structures can be topographically fixed to create stable high-energy linear pathways through aeolian systems such as the NAS. These pathways are likely to develop at a variety of length-scales, and once initiated may become self-reinforcing.

Where energy and sand supply is sufficient linear wind-aligned features develop both erosionally in the bed and depositionally on the bed surface. It is predicted that as satellite monitoring of circulation systems continues to improve, direct evidence of such structures will be found in the circulation system across a variety of length scales, reflecting the architecture and dynamics of the aeolian system over which it flows. A summary of the predicted distribution of vorticity influencing the aeolian system within the NAEB is shown in Fig. 22.

The scale of the dunes within the NAEB, where the MBL is 200 m or less thick seems to

create flow conditions which generate somewhat different patterns of erosion and deposition than those recorded in laboratory studies. This may reflect the thin, fast nature of the flow which is likely, at times, to be of a supercritical nature. In some instances the flow pattern resembles that modelled for turbulent flow past a low axisymmetric hill for low Froude numbers.

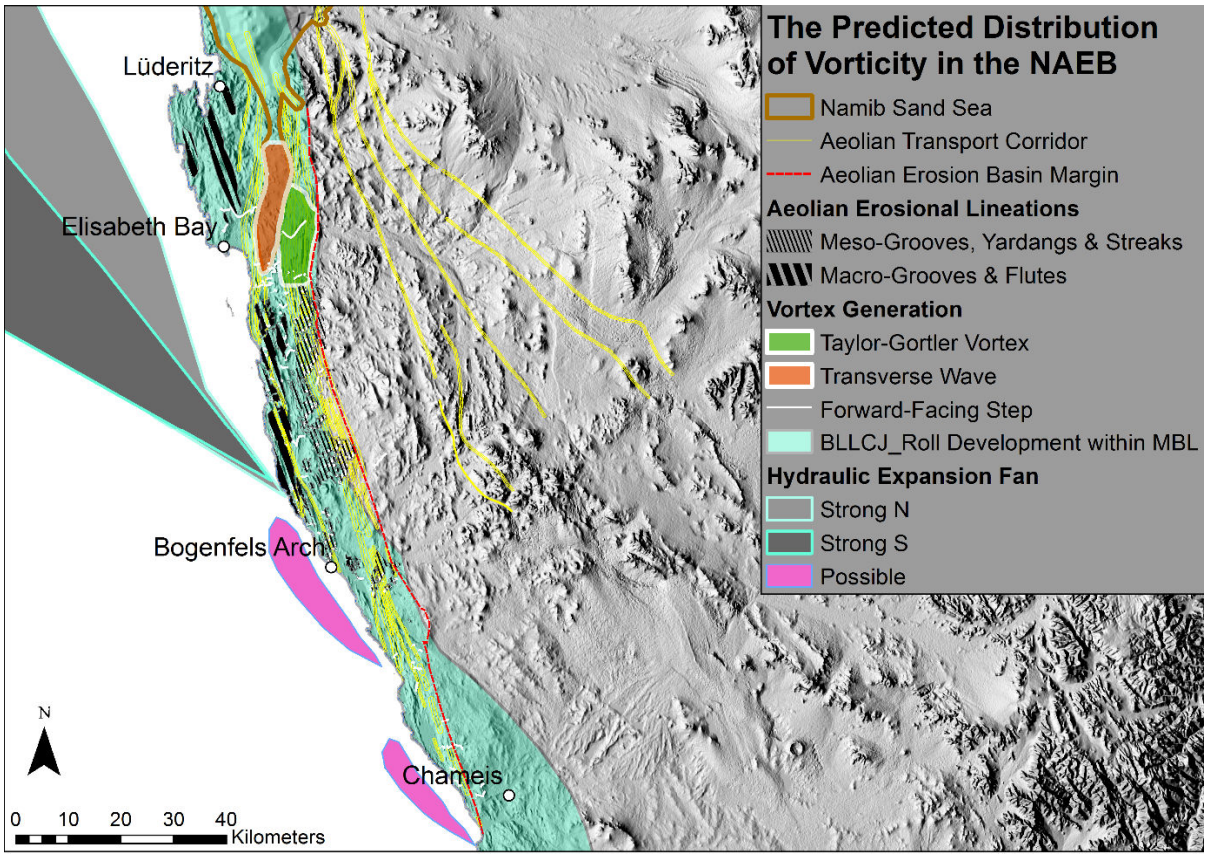

Figure 22. The predicted distribution of different types of vorticity which are likely to influence the development of Aeolian Transport Corridors, aeolian erosional features and depositional bedforms at varying scales throughout the Namib Aeolian Erosion Basin.

The realisation that the hydraulic behaviour of the BLLCJ flow is controlled by changes in coastline orientation has significant implications for understanding the response of the aeolian system to changes in coastal geometry driven by sea-level change. While climatic forcing of wind-energy has been noted previously, changes in coastline orientation could also result in marked shifts in the location and energy of surface wind maxima due to modification of hydraulic behaviour of the BLLCJ. In the case of the Namibian Aeolian System, sand supply is intimately linked to the Orange River. Changes in coastal orientation are likely to be driven by variation in shelf geometry and/or by the deposition of large sediment bodies on the shelf during lowstands. The development of large fan-delta systems (Corbett & Burrell, 2001) during lowstands are known to have created large convexities in the coastline and would also increase sand supply. Such changes could explain major sand sea expansions, such as that represented by the Miocene Tsondab Sandstone Formation.

This study underpins the need to observe sedimentary systems and the processes occurring within them across a large spectrum of scale in order to contextualise local empirical measurement. Platforms such as Google Earth Engine are providing an exciting way to begin to do this. It opens up a wonderful opportunity to understand better the dynamics of large-scale aeolian systems and unravel the dynamics of complex systems in ways not previously possible. Full appreciation of this opportunity is most likely going to come through multi-discipline teams which are able to apply fundamentally different perspectives and skills to take full advantage of the opportunity.

Conclusion

The discovery of the Benguela Low-Level Coastal Jet has significant implications for understanding the architecture and dynamics of the Namibian Aeolian System which extends along the entire continental margin.

For the first time the hydraulic behaviour of flow within the Benguela Low-Level Coastal Jet is shown to influence fundamentally the architecture of both erosion and accumulation zones within the large-scale Namibian Aeolian System. The hydraulic behaviour of the jet flow exerts a strong influence on the development and pattern of sandflow pathways both within erosional and accumulation zones. These patterns are reflected in the aeolian erosion features as well as the pattern of dune forms produced.

The landfall of the BLLCJ flow makes the southern Namib one of the highest-energy unimodal wind systems on earth. Jet flow through this part of the system is constrained to the MBL which is <200 m deep, creating a thin, fast flow which may well be supercritical at times. Horizontal rolls generated beneath the capping inversion enclosing the MBL probably control the initial development and maintenance of ATCs. However with increasing distance downwind other types of horizontal vortex come in to play, shaping the flow pathways through the NAEB.

The development of erosional features such as large-scale aeolian lineations reveal the presence of topographically fixed counter-rotating horizontal vortices. The identification of Aeolian Transport Corridors downwind of planar sand sheet repositories within the Namib Aeolian Erosion Basin strongly suggests that within the thin BLLCJ, helical counter-rotating vortices develop and that they play a role in creating fixed linear pathways termed Aeolian Transport Corridors for sandflow through the system. These pathways are characterised by marked coarse-grained aeolian bedload transport which creates distinctive sedimentary textures and fabrics on a large scale.

Forward-facing topographic steps are important sites of localised vortex generation and play a key role in the evolution of the aeolian erosional landscape. Clear differences in the scale of aeolian erosional grooves/flutes are associated with different lithologies.

Whilst the effect of horizontal rolls in aeolian sediment transport is likely to remain a controversial subject this study provides evidence of their existence at a variety of scales in a system that is remarkably tuned to generate them. In the case of the Namib, this led to the genesis of aeolian diamond placers, the mining of which led to this research being possible.

Acknowledgements

I would like to thank Derek Jackson for encouraging me to explore further the possibility that ATCs are related to the development of large-scale turbulent structures in the ASL and for introducing me to the remarkable Earth Engine time-lapse video. This research benefitted greatly from interaction with Chris Patricola and John Shaw who generously shared their knowledge and experience. Chris helped me to develop an understanding of low-level jets and John introduced me to the distinctive effects of longitudinal and horseshoe vortices in sculpting erosional landscapes. I would also like to thank Ricardo Mejia-Alvarez for reading the manuscript.

Finally this research would never have been possible without the ongoing support of Jürgen Jacob at Namdeb (Pty) Ltd, who generously provided access to their amazing ALS dataset which took mapping to a new level that was previously not dreamt of.

References

Adrian, R.J. 2007. Hairpin vortex organization in wall turbulence. *Physics of Fluids*, **19**, 041301-141301-16.

Adrian, R.J., Balachandar, S. & Liu, Z.C. 2001. Spanwise growth of vortex structure in wall turbulence. *International Journal of the Korean Society of Mechanical Science and Technology*, **15**, 1741-1749.

Adrian, R.J., Meinhart, C.D. & Tomkins, C.D. 2000. Vortex organization in the outer region of the turbulent boundary layer. *Journal of Fluid Mechanics*. **422**, 1-54.

Anderson, R.S. & Haff, P.K. 1988. Simulation of eolian saltation. *Science* (New York, N.Y.), **241**, 820-823.

Andreotti, B., Fourrière, A., Ould-Kaddour, F.,

Murray, B. & Claudin, P. 2009. Giant aeolian dune size determined by the average depth of the atmospheric boundary layer. *Nature*, **457**, 1120-1123.

Baddock, M.C., Wiggs, G.F.S. & Livingstone, I. 2011. A field study of mean and turbulent flow characteristics upwind, over and downwind of barchan dunes. *Earth Surface Processes and Landforms*, **36**, 1435-1448.

Bagnold, R.A. 1941. *The Physics of Blown Sand and Desert Dunes*. London, Methuen, 265 pp.

Balakumar, B. & Adrian, R. 2007. Large- and very-large-scale motions in channel and boundary-layer flows. *Philosophical Transactions of the Royal Society, A: Mathematical, Physical and Engineering Sciences*, **365**, 665–681.

Biswas, A., Zimbelman, J. & Hargitai, H. 2015. Zibar. *In*: Hargitai, H. & Keresturi, A. (Eds) *Encyclopedia of Planetary Landforms*. New York, Springer-Verlag, pp. 2383-2386.

Bluck, B.J., Ward, J.D., Cartwright, J. & Swart, R. 2007. The Orange River, southern Africa: an extreme example of a wave-dominated sediment dispersal system in the South Atlantic Ocean. *Journal of the Geological Society*, **164**, 341-351.

Bluck, B.J., Ward, J.D. & de Wit, M.C.J. 2005. Diamond mega-placers: southern Africa and the Kaapvaal craton in a global context. *In*: McDonald, I., Boyce, A.J., Butler, I.B., Herrington, R.J. & Polya, D.A. (Eds) *Mineral Deposits and Earth Evolution*. Geological Society of London, pp. 213-245.

Bourke, M.C. & Goudie, A.S. 2009. Varieties of barchan form in the Namib Desert and on Mars. *Aeolian Research*, **1**, 45-54.

Brookes, I.A. 2001. Aeolian erosional lineations in the Libyan Desert, Dakhla Region, Egypt. *Geomorphology*, **39**, 189-209.

Bristow, N.R., Blois, G., Best, J.L. & Christensen, K.T. 2018. Turbulent flow structure associated with collision between laterally offset, fixed-bed barchan dunes. *Journal of Geophysicl Research: Earth Surfce*, **123**, 2157-2188.

Brown, R.A. 1970. A secondary flow model for the planetary boundary layer. *Journal of the Atmospheric Sciences*, **27**, 742-757.

Brown, R.A. 2000. Serendipity in the use of satellite scatterometer, SAR, and other sensor data. *Johns Hopkins APL Technical Digest* (Applied Physics Laboratory), **21**, 21-26.

Burger, U. 2015. The Geology of the Elizabeth Bay aeolian diamond placer in the Sperrgebiet, Namibia. *In*: *Abstracts of 31st IAS Meeting of Sedimentology. Kraków, International Association of Sedimentologists*, p. 99.

Burk, S.D. & Thompson, W.T. 1995. The summertime low-level jet and marine boundary layer structure along the California coast. *Monthly Weather Review*, **124**, 668-686.

Cantwell, B.J. 1981. Organised motion in turbulent flow. *Annual Review of Fluid Mechanics*, **13**, 457-515.

Charru, F. & Laval, V. 2013. Sand transport over a barchan dune. *In*: *Marine and River Dune Dynamics – MARID IV*. Madrid, Open Archive, Toulouse, pp. 67-71.

Cooke, R.U. 1970. Stone pavements in deserts. *Annals of the Association of American Geographers*, **60**, 560-577.

Cooke, R.U. & Warren, A. 1973. *Geomorphology in Deserts*. Berkeley & Los Angeles, University of California Press, 374 pp.

Corbett, I.B. 1989. *The Sedimentology of the Diamondiferous Deflation Deposits Within the Sperrgebiet, Namibia*. Thesis, University of Cape Town, 430 pp.

Corbett, I.B. 1993. The modern and ancient patten of sandflow through the southern Namib deflation basin. *In*: Pye, K. & Lancaster, N. (Eds) *Aeolian Sediments Ancient and Modern.* International Association of Sedimentologists, pp. 45-60.

Corbett, I.B. 1996. A review of diamondiferous marine deposits of western southern Africa. *Africa Geoscience Review*, **3**, 157-174.

Corbett, I.B. 2016. Sediment dynamics of the Namib aeolian erosion basin and the arid zone diamond placers of the Northern Sperrgebiet, Namibia. *Memoir Geological Survey Namibia*, **22**, 6-171.

Corbett, I. & Burrell, B. 2001. The earliest Pleistocene (?) Orange River fan-delta : an example of successful exploration delivery aided by applied Quaternary research in diamond placer sedimentology and palaeontology. *Quaternary International*, **82**, 63-73.

Dennis, D.J.C. 2015. Coherent structures in wall-bounded turbulence. *Anais da Academia Brasileira de Ciências*, **87**, 1161-1193.

Durán, O., Schwämmle, V., Lind, P.G. & Herrmann, H.J. 2009. The dune size distribution and scaling relations of barchan dune fields. *Granular Matter*, **11**, 7-11.

Edwards, K.A., Rogerson, A.M., Winant, C.D. & Rodgers, D.P. 2001. Adjustment of the marine atmospheric boundary layer to a

coastal cape. *Journal of Atmospheric Sciences*, **58**, 1511-1528.

Embabi, N.S. 1999. Playas of the Western Desert, Egypt. *Annales Academiae Scientiarum Fennicae, Geologica-Geographica*, **160**, 5-47.

Endo, N., Taniguchi, K. & Katsuki, A. 2004. Observation of the whole process of interaction between barchans by flume experiments. *Geophysical Research Letters*, **31**, 1-3.

Garzanti, E., Andò, S., Vezzoli, G., Lustrino, M., Boni, M. & Vermeesch, P. 2012. Petrology of the Namib Sand Sea : Long-distance transport and compositional variability in the wind-displaced Orange Delta. *Earth-Science Reviews*, **112**, 173-189.

Garzanti, E., Resentini, A., Andò, S., Vezzoli, G., Pereira, A. & Vermeesch, P. 2015. Physical controls on sand composition and relative durability of detrital minerals during ultra-long distance littoral and aeolian transport (Namibia and Southern Angola). *Sedimentology*, **62**, 971-996.

Goudie, A.S. 2007. Mega-Yardangs : A Global Analysis. *Geography Compass*, **1**, 65-81.

Haack, T., Burk, S.D., Dorman, C. & Rogers, D. 2000. Supercritical flow interaction within the Cape Blanco – Cape Mendocino Orographic Complex. *Monthly Weather Review*, **129**, 688-708.

Hallam, C.D. 1964. The geology of the coastal diamond deposits of Southern Africa (1959). *In*: S.H. Haughton (Ed.) *The Geology of Some Ore Deposits in Southern Africa*. Johannesburg, Geological Society of South Africa, pp. 671-728.

Hanna, S.R. 1969. The formation of longitudinal sand dunes by large helical eddies in the atmosphere. *Journal of Applied Meteorology*, **8**, 874-883.

Head, H.V. 2014. How far can the influence of a local marine diamondiferous signature be traced through an aeolian depositional environment? *In*: Kimberley Diamond Symposium. Poster.

Hersen, P., Andersen, K.H., Elbelrhiti, H., Andreotti, B., Claudin, P. & Douady, S. 2004. Corridors of barchan dunes: Stability and size selection. Physical review. *E, Statistical, Nonlinear, and Soft Matter Physics*, **69**, 011304.

Hersen, P. & Douady, S. 2005. Collision of barchan dunes as a mechanism of size regulation. *Geophysical Research Letters*, **32**, 1-5.

Hesp, P.A., Smyth, T.A.G., Nielsen, P., Walker, I.J., Bauer, B.O. & Davidson-Arnott, R. 2015. Flow deflection over a foredune. *Geomorphology*, **230**, 51-63.

Hunt, J.C.R., Snyder, W.H. & Lawson Jr, R.E. 1978. *Flow Structure and Turbulent Diffusion around a Three-dimensional Hill: Fluid Modeling Study on Effects of Stratification - Part 1. Flow Structure*. EPA-600/4-78-041. Research Triangle Park, 83 pp.

Hussein, H. & Martinuzzi, R.J. 1996. Energy balance for turbulent flow around a surface mounted cube placed in a channel. *Physics of Fluids*, **8**, 764-780.

Hutchins, N., Chauhan, K., Marusic, I., Monty, J. & Klewicki, J. 2012. Towards reconciling the large-scale structure of turbulent boundary layers in the atmosphere and laboratory. *Boundary-Layer Meteorology*, **145**, 273-306.

Hutchins, N. & Marusic, I. 2007a. Large-scale influences in near-wall turbulence. *Philosophical Transactions of the Royal Society, A: Mathematical, Physical and Engineering Sciences*, **365**, 647-664.

Hutchins, N. & Marusic, I. 2007b. Evidence of very long meandering features in the logarithmic region of turbulent boundary layers. *Journal of Fluid Mechanics*, **579**, 1-28.

Jackson, S.P. 1954. Sea-breezes in South Africa. *South African Geographical Journal*, **36**, 13-23.

Kaimal, J.C. & Finnigan, J.J. 1994. *Atmospheric Boundary Layer Flows: Their Structure and Meaurement*. Oxford, Oxford University Press, 289 pp.

Kaiser, E. 1926. Die jungen sedimentären neubildungen om extrem-ariden klima der Namibwüste. *In*: Kaiser, E. (Ed.) *Die Diamantenwuste Südwestafrikas*, Volume 2, Berlin, Reimer, pp. 317-380.

Katsuki, A. & Kikuchi, M. 2011. Simulation of barchan dynamics with inter-dune sand streams. *New Journal of Physics*, **13**, 8 pp.

Knott, P. 1979. *The Structure and Pattern of Dune-forming Winds*. Thesis, University of London, 2 volumes, 403 pp. and 249 pp.

Kocurek, G. & Nielson, J. 1986. Conditions favourable for the formation of warm-climate aeolian sand sheets. *Sedimentology*, **33**, 795-816.

Kuettner, J.P. 1959. The band structure of the atmosphere – Observations and theory. *Tellus*, **11**, 267-294.

Lancaster, N. 1985. Winds and sand movements in the Namib Sand Sea. *Earth*

Surface Processes and Landforms, **10**, 607-619.

Lancaster, N. 1995. *Geomorphology of Desert Dunes*. London, Routledge, 290 pp.

Lancaster, N. 2014. Dune systems of the Namib Desert – a spatial and temporal perspective. *Transactions of the Royal Society of South Africa*, **69**, 133-137.

Lindesay, J.A. & Tyson, P.D. 1990. Climate and near-surface airflow over the Central Namib. *In*: Seely, M.K. (Ed.) *Namib Ecology: 25 Years of Namib Research*. Pretoria, Transvaal Museum, pp. 27-37.

Martinuzzi, R. & Tropea, C. 1993. The flow around surface-mounted prismatic obstacles placed in a fully developed channel flow. *Journal of Fluids Engineering*, **115**, 85-91.

Marusic, I. & Hutchins, N. 2008. Study of the log-layer structure in wall turbulence over a very large range of Reynolds number. *Flow, Turbulence and Combustion*, **81**, 115-130.

Mathis, R., Hutchins, N. & Marusic, I. 2009. Large-scale amplitude modulation of the small-scale structures in turbulent boundary layers. *Journal of Fluid Mechanics*, **628**, 311-337.

Maxwell, T. & Haynes, C.V. 1989. Large-scale, low-amplitude bedforms (chevrons) in the selima sand sheet, Egypt. *Science* (New York, N.Y.), **243**, 1179-1182.

Maxwell, T.A. & Haynes, C.V. 1992. Remote sensing of sand transport in the Western Desert of Egypt. *In*: Sadek, A. (Ed.) *Proceedings of the First International Conference on the Geology of the Arab World*. Cairo, Dar Al-Madina Al-Monawera Press, pp. 19-31.

Maxwell, T. & Haynes, C.V. 2001. Sand sheet dynamics and Quaternary landscape evolution of the Selima Sand Sheet, southern Egypt. *Quaternary Science Reviews*, **20**, 1623-1647.

McCuaig, T.C., Beresford, S. & Hronsky, J. 2010. Translating the mineral systems approach into an effective exploration targeting system. *Ore Geology Reviews*, **38**, 128-138.

Mejia-Alvarez, R., Barros, J.M. & Christensen, K.T. 2013. Structural attributes of turbulent flow over a complex topography. *In*: Venditti, J.G., Best, J.L., Church M. & Hardy R.J. (Eds) *Coherent Flow Structures at Earth's Surface*. London, John Wiley & Sons Ltd, pp. 25-41.

Michelsen, B., Strobl, S., Parteli, E.J.R. & Pöschel, T. 2015. Two-dimensional airflow modeling underpredicts the wind velocity over dunes. *Scientific Reports* **5**, 16572; doi: 10.1038/srep16572.

Morrison, I., Businger, S., Marks, F., Dodge, P. & Businger, J.A. 2005. An observational case for the prevalence of roll vortices in the hurricane boundary layer*. *Journal of Atmospheric Sciences*, **62**, 2662-2673.

Munoz, R.C. & Garreaud, R.D. 2005. Dynamics of the low-level jet off the west coast of subtropical South America. *Monthly Weather Review*, **133**, 3661-3677.

Nicholson, S.E. 2010. A low-level jet along the Benguela coast, an integral part of the Benguela current ecosystem. *Climatic Change*, **99**, 613-624.

Omidyeganeh, M. 2011. Large-eddy simulation of three-dimensional dunes in a steady, unidirectional flow. *Journal of Turbulence*, **12**, 509-534.

Omidyeganeh, M. 2013. *Large-eddy Simulation of Unidirectional Turbulent Flow over Dunes*. Thesis, Queen's University, Ontario, 237 pp.

Omidyeganeh, M. & Piomelli, U. 2013. Large-eddy simulation of three-dimensional dunes in a steady, unidirectional flow. Part 2. Flow structures. *Journal of Fluid Mechanics*, **734**, 509-534.

Omidyeganeh, M., Piomelli, U., Christensen, K.T. & Best, J.L. 2013. Large-eddy simulation of flow over barchan dunes. *In*: Van Lancker, V. & Garlan, T. (Eds) Fourth International Conference on Marine and River Dune Dynamics. Bruges, Belgium 15-17 April, 2013, Royal Belgian Institute of Natural Sciences and SHOM. *VLIZ Special Publication* **65** - Flanders Marine Institute (VLIZ) Oostende, Belgium, 191-198.

Paik, J., Escauriaza, C. & Sotiropoulos, F. 2007. On the bimodal dynamics of the turbulent horseshoe vortex system in a wing-body junction. *Physics of Fluids*, **19**, 1-20.

Palmer, J. 2010. *The Flow Structure of Interacting Barchan Dunes*. Thesis, University of Illinois at Urbana-Champaign, 270 pp.

Palmer, J.A., Best, J.L., Christensen, K.T. & Wu, Y. 2010. The flow structure of interacting barchan dunes. *In*: Parsons, D., Garlan, T. & Best, J. (Eds) *Proceedings of Marine and River Dune Dynamics III*. Leeds, UK, pp. 265-266.

Palmer, J.A., Mejia-Alvarez, R., Best, J.L. & Christensen, K.T. 2012. Particle-image velocimetry measurements of flow over interacting barchan dunes. *Experiments in Fluids*, **52**, 809-829.

Patricola, C.M. & Chang, P. 2016. Structure and dynamics of the Benguela low-level coastal jet. *Climate Dynamics*, **49**, 2765-2788.

Pollard, A., Wakarani, N. & Shaw, J. 1996. Genesis and morphology of erosional shapes associated with turbulent flow over a forward-facing step. *In*: Ashworth, P.J., Bennett, S.J. Best, J.L. & McLelland S.J. (Eds) *Coherent Flow Structures in Open Channels*. Chichester, Wiley, pp. 249-265.

Ranjha, R., Svensson, G., Tjernström, M. & Semedo, A. 2013. Global distribution and seasonal variability of coastal low-level jets derived from ERA-interim reanalysis. *Tellus, Series A: Dynamic Meteorology and Oceanography*, **65**, 1-21.

Rogers, J. 1977. Sedimentation on the continental margin off the Orange River and the Namib Desert. *Bulletin Joint Geological Survey/University of Cape Town Marine Geoscience Group*, **7**, 162p.

Salesky, S.T., Chamecki, M. & Bou-Zeid, E. 2017. On the nature of the transition between roll and cellular organization in the convective boundary layer. *Boundary-Layer Meteorology*, **163**, 41-68.

Samelson, R.M. 1992. Supercritical Marine-Layer Flow along a smoothly varying coastline. *Journal of the Atmospheric Sciences*, **49**, 1571-1584.

Sauermann, G., Rognon, P., Poliakov, A. & Herrmann, H.J. 2000. The shape of the barchan dunes of Southern Morocco. *Geomorphology*, **36**, 47-62.

Scheidt, S.P. 2012. Sand transport pathways of dark dunes in the Sperrgebiet: Sand composition and dune migration rates from ASTER data. *In*: *Third International Planetary Dunes Workshop: Remote Sensing and Image Analysis of Planetary Dunes*. Flagstaff, Arizona, Abstract #7051.

Scheidt, S.P. & Lancaster, N. 2013. The application of COSI-Corr to determine dune system dynamics in the southern Namib Desert using ASTER data. *Earth Surface Processes and Landforms*, **38**, 1004-1019.

Sharp, R.P. 1964. Wind-driven sand in Coachella Valley, California. *Bulletin of the Geological Society of America*, **75**, 785-804.

Shaw, J. 1994. Hairpin erosional marks, horseshoe vortices and subglacial erosion. *Sedimentary Geology*, **91**, 269-283.

Shaw, J. 1996. A meltwater model for Laurentide subglacial landscapes. *In*: McCann, S.B. & Ford, D.C. (Eds) *Geomorphology Sans Frontières*. Chichester, Wiley, 236 pp.

Spaggiari, R.I. 2011. *Sedimentology of Plio-Pleistocene Gravel Barrier Deposits in the Palaeo-Orange River Mouth, Namibia: Depositional History and Diamond Mineralisation*. Thesis, Rhodes University, 389 pp.

Svensson, N., Sahlée, E., Bergström, H., Nilsson, E., Badger, M. & Rutgersson, A. 2017. A case study of offshore advection of boundary layer rolls over a stably stratified sea surface. *Hindawi*: *Advances in Meteorology*, **2017**, 15 pp.

Swart, A. 2016. *Assessment of the Baseline Meteorological and Air Quality Conditions over Uubvlei, Oranjemund, Namibia*. Thesis, Master of Science in the Faculty of Natural and Agricultural Sciences University.

Tomkins, C.D. & Adrian, R.J. 2003. Spanwise structure and scale growth in turbulent boundary layers. *Journal of Fluid Mechanics*, **490**, S0022112003005251.

Tsoar, H. 2001. Types of aeolian sand dunes and their formation. *In*: Balmforth, N.J. & Provenzale, A. (Eds) *Geomorphological Fluid Mechanics*. Springer, Berlin, Heidelberg, pp. 403-429.

Van Heerden, J. 1999. Africa and surrounding waters. *In*: Karoly D. (Ed.) *Meteorology of the Southern Hemisphere*. Springer & American Meteorological Society, 410 pp.

Wakimoto, R.M. & Black, P.G. 1994. Damage survey of Hurricane Andrew and its relationship to the eyewall. *Bulletin of the American Meteorological Society*, **75**, 189-200.

Walker, I.J., Davidson-Arnott, R.G.D., Bauer, B.O., Hesp, P.A., Delgado-Fernandez, I., Ollerhead, J. & Smyth, T.A.G. 2017. Scale-dependent perspectives on the geomorphology and evolution of beach-dune systems. *Earth-Science Reviews*, **171**, 220-253.

Wang, G., Zheng, X. & Tao, J. 2017. Very large scale motions and PM10 concentration in a high-Re boundary layer. *Physics of Fluids*, **29**, 1-5.

Wark, C.E. & Nagib, H.M. 1991. Experimental investigation of coherent structures in turbulent boundary layers. *Journal of Fluid Mechanics*, **230**, 183-208.

Washington, R., Todd, M.C., Lizcano, G., Tegen, I., Flamant, C., Koren, I., Ginoux, P., Engelstaedter, S., Bristow, C.S., Zender, C.S., Goudie, A.S., Warren, A. & Prospero, J.M. 2006. Links between topography, wind, deflation, lakes and dust : The case of the Bodele Depression, Chad. *Geophysical Research Letters*, **33**, 1-4.

Wiggs, G.F.S., Bullard, J.E., Garvey, B. & Castro, I. 2002. Interactions between airflow and valley topography with implications for aeolian sediment transport. *Physical Geography*, **23**, 366-380.

Wilson, I. 1972. Aeolian bedforms - their development and origins. *Sedimentology*, **19**, 173-210.

Winant, C.D., Dorman, C.E., Friehe, C.A. & Beardsley, R.C. 1988. The marine layer off Northern California: An example of supercritical channel flow. *Journal of Atmospheric Sciences*, **45**, 3588-3605.

Worman, S.L., Murray, A.B., Littlewood, R., Andreotti, B. & Claudin, P. 2013. Modeling emergent large-scale structures of barchan dune fields. *Geology*, **41**, 1059-1062.

Wurman, J. & Winslow, J. 1998. Intense sub-kilometer-scale boundary layer rolls observed in Hurricane Fran. *Science*, **280**, 555-557.

Zeng, Q., Cheng, X., Hu, F. & Peng, Z. 2010. Gustiness and coherent structure of strong winds and their role in dust emission and entrainment. *Advances in Atmospheric Sciences*, **27**, 1-13.

Annex I. List of Abbreviations used in text

ABL - Atmospheric Boundary Layer
ALS - Airborne Laser Scanner
ASL - Atmospheric Surface Layer
ATC - Aeolian Transport Corridor
BLLCJ - Benguela Low-Level Coastal Jet
CFD - Computational Fluid Dynamics
GEE - Google Earth Engine
HMP - High-Momentum Pathway
HMR - High-Momentum Region
LLCJ - Low-Level Coastal Jet
LMP - Low-Momentum Pathway
LMR - Low-Momentum Region
LSM - Large-Scale Motions
MBL - Marine Boundary Layer
NAEB - Namib Aeolian Erosion Basin
NAS - Namibian Aeolian System
PBL - Planetary Boundary Layer
SRTM - Shuttle Radar Topography Mission
TIBL - Thermal Internal Boundary Layer
TKE - Turbulent Kinetic Energy
VLSM - Very Large-Scale Motions